(12) INTERNATIONAL APPLICATION PUBLISHED UNDER THE PATENT COOPERATION TREATY (PCT)

(19) World Intellectual Property Organization
International Bureau

(43) International Publication Date
24 November 2016 (24.11.2016)

WIPO | PCT

(10) International Publication Number
WO 2016/187225 A1

(51) International Patent Classification:
A61L 27/20 (2006.01) *A61L 27/52* (2006.01)
A61L 27/38 (2006.01) *A61L 27/54* (2006.01)

(21) International Application Number:
PCT/US2016/032920

(22) International Filing Date:
17 May 2016 (17.05.2016)

(25) Filing Language: English

(26) Publication Language: English

(30) Priority Data:
62/162,803 17 May 2015 (17.05.2015) US

(71) Applicants: **MASSACHUSETTS INSTITUTE OF TECHNOLOGY** [US/US]; 77 Massachusetts Avenue, Cambridge, MA 02139 (US). **THE CHILDREN'S MEDICAL CENTER CORPORATION** [US/US]; 55 Shattuck Street, Boston, MA 02115 (US).

(72) Inventors: **MA, Minglin**; 117 Concord Place, Ithaca, NY 14850 (US). **ANDERSON, Daniel, G.**; 78 Carter Drive, Framingham, MA 01701 (US). **LANGER, Robert, S.**; 98 Montvale Road, Newton, MA 02459 (US). **VEISEH, Omid**; 1105 Massachusetts Avenue, Apartment 10E, Cambrige, MA 02138 (US). **VEGAS, Arturo, Jose**; 129 Franklin Street, Apartment 328, Cambridge, MA 02139 (US). **DOLOFF, Joshua, Charles**; 2 Hancock Street, Apartment 208, Quincy, MA 02171 (US). **CHEN, Delai**; 3 Hawthorne Street, Woburn, MA 01801 (US). **KASTRUP, Christian, J.**; 2137 West 10th Avenue, Vancouver, British Columbia V6K 4W4 (CA).

(74) Agents: **PABST, Patrea, L.** et al.; Pabst Patent Group LLP, 1545 Peachtree Street, N.E., Suite 320, Atlanta, GA 30309 (US).

(81) Designated States *(unless otherwise indicated, for every kind of national protection available)*: AE, AG, AL, AM, AO, AT, AU, AZ, BA, BB, BG, BH, BN, BR, BW, BY, BZ, CA, CH, CL, CN, CO, CR, CU, CZ, DE, DK, DM, DO, DZ, EC, EE, EG, ES, FI, GB, GD, GE, GH, GM, GT, HN, HR, HU, ID, IL, IN, IR, IS, JP, KE, KG, KN, KP, KR, KZ, LA, LC, LK, LR, LS, LU, LY, MA, MD, ME, MG, MK, MN, MW, MX, MY, MZ, NA, NG, NI, NO, NZ, OM, PA, PE, PG, PH, PL, PT, QA, RO, RS, RU, RW, SA, SC, SD, SE, SG, SK, SL, SM, ST, SV, SY, TH, TJ, TM, TN, TR, TT, TZ, UA, UG, US, UZ, VC, VN, ZA, ZM, ZW.

(84) Designated States *(unless otherwise indicated, for every kind of regional protection available)*: ARIPO (BW, GH, GM, KE, LR, LS, MW, MZ, NA, RW, SD, SL, ST, SZ, TZ, UG, ZM, ZW), Eurasian (AM, AZ, BY, KG, KZ, RU, TJ, TM), European (AL, AT, BE, BG, CH, CY, CZ, DE, DK, EE, ES, FI, FR, GB, GR, HR, HU, IE, IS, IT, LT, LU, LV, MC, MK, MT, NL, NO, PL, PT, RO, RS, SE, SI, SK, SM, TR), OAPI (BF, BJ, CF, CG, CI, CM, GA, GN, GQ, GW, KM, ML, MR, NE, SN, TD, TG).

Declarations under Rule 4.17:

— *of inventorship (Rule 4.17(iv))*

Published:

— *with international search report (Art. 21(3))*

— *before the expiration of the time limit for amending the claims and to be republished in the event of receipt of amendments (Rule 48.2(h))*

(54) Title: MULTI-LAYER HYDROGEL CAPSULES FOR ENCAPSULATION OF CELLS AND CELL AGGREGATES

(57) Abstract: Biomedical devices for implantation with decreased pericapsular fibrotic overgrowth are disclosed. The device includes biocompatible materials and has specific characteristics that allow the device to elicit less of a fibrotic reaction after implantation than the same device lacking one or more of these characteristic that are present on the device. Biocompatible hydrogel capsules encapsulating mammalian cells having a diameter of greater than 1 mm, and optionally a cell free core, are disclosed which have reduced fibrotic overgrowth after implantation in a subject. Methods of treating a disease in a subject are also disclosed that involve administering a therapeutically effective amount of the disclosed encapsulated cells to the subject.

WO 2016/187225 A1

MULTI-LAYER HYDROGEL CAPSULES FOR ENCAPSULATION OF CELLS AND CELL AGGREGATES

CROSS-REFERENCE TO RELATED APPLICATIONS

This application claims benefit of U.S. Provisional Application No. 62/162,803, filed May 17, 2016. Application No. 62/162,803, filed May 17, 2016, is hereby incorporated herein by reference in its entirety.

STATEMENT REGARDING FEDERALLY SPONSORED RESEARCH OR DEVELOPMENT

This invention was made with Government support under Grant No. R01 DE016516 awarded by the National Institutes of Health. The Government has certain rights in the invention.

FIELD OF THE INVENTION

The invention is generally related to the field of fabrication and use of biomedical devices, including structural, therapeutic-containing, and cell-encapsulating devices. More specifically, some aspects of the invention relate to improved physical parameters to ensure improved biocompatibility of implanted biomedical devices, including biocompatible hydrogel encapsulating mammalian cells and polymeric particles loaded with anti-inflammatory drugs.

BACKGROUND OF THE INVENTION

Biomaterials and devices transplanted in the body are being used for a broad spectrum of clinical applications such as cell transplantation, controlled drug release, continuous sensing and monitoring of physiological conditions, electronic pacing, and tissue regeneration. For these applications, the longevity and fidelity of the device is highly dependent on its ability to ward off recognition by the host immune system. Immune recognition initiates a cascade of host orchestrated cellular processes leading to foreign body reactions, which include persistent inflammation, fibrosis (walling-off), and damage to the surrounding tissue. These unwanted effects are both deleterious to the function of the device and a significant cause of pain and discomfort for the patient.

In 1980, Lim and Sun introduced an alginate microcapsule coated with an alginate/polylysine complex for encapsulation of pancreatic islets. Hydrogel microcapsules have since been extensively investigated for encapsulation of living cells or cell aggregates for tissue engineering and regenerative medicine (Orive et al., Nat. Medicine 9:104 (2003); Paul, et al., Regen. Med. 4:733 (2009); Read et al., Biotechnol. 19:29 (2001)) In general, capsules are designed to allow facile diffusion of oxygen and nutrients to the encapsulated cells, while releasing the therapeutic proteins secreted by the cells, and to protect the cells from attack by the immune system. These have been developed as potential therapeutics for a range of diseases including type I diabetes, cancer, and neurodegenerative disorders such as Parkinson's (Wilson et al., Adv. Drug. Deliv. Rev. 60:124 (2008); Joki et al., Nat. Biotech. 19:35 (2001); Kishima et al., Neurobiol. Dis. 16:428 (2004)). One of the most common capsule formulations is based on alginate hydrogels, which can be formed through ionic crosslinking. In a typical process, the cells are first blended with a viscous alginate solution. The cell suspension is then processed into micro-droplets using different methods such as air shear, acoustic vibration or electrostatic droplet formation (Rabanelet al., Biotechnol. Prog. 25:946 (2009)). The alginate droplet is gelled upon contact with a solution of divalent ions, such as Ca2+ or Ba2+.

One challenge associated with alginate microcapsules for cell encapsulation, however, is the lack of control of the relative positions of the cells within the capsules. The cells can become trapped and exposed on the capsule surface, leading to inadequate immune-protection (Wong et al., Biomat. Artific. Cells Immobiol. Biotechnol. 19:675 (1991)). It has been recognized that incomplete coverage would not only cause the rejection of exposed cells but may also allow the infiltration of macrophages and fibroblasts into the capsules through the exposed areas (Chang, Nat, Rev. Drug Discovery 4:221 (2005)). Alginate hydrogel microcapsules have been broadly investigated for their utility with pancreatic islets to treat Type I diabetes (Calafiore, Expert Opin. Biol. Ther. 3:201 (2003)). Numerous promising results have been reported in several animal models including

rodents (Lim, Science 210:908 (1980); Qi et al., Artifi. Cells, Blood Substitutes, Biotechnol. 36:403 (2008)), dogs (Soon-Shiong et al., Proc. Natl. Acad. Sci. USA 90:5843 (1993)), and nonhuman primates (El, X. Ma, D. Zhou, I. Vacek , A. M. Sun. J. Clin. Invest. 98:417 (1996)). Clinical trials have also been performed by Soon-Shiong et al., Lancet 343:950 (1994); Elliott et al., Xenotransplantation 14:157 (2007); Calafiore et al.,. Diabetes Care 29:137 (2006), Basta et al., Diabetes Care 34:2406 (2011); and Tuch et al., Diabetes Care 32:1887 (2009). In general, these clinical trials have reported insulin secretion, but without long term correction of blood sugar control, and additional challenges remain to advance these systems (Tam et al., J. Biomed. Mater. Res. Part A 98A:40 (2011); deVos et al., Biomaterials 27:5603 (2006)).

One challenge is the biocompatibility of the capsules. Upon transplantation, the foreign body responses cause fibrotic cellular overgrowth on the capsules that cut off the diffusion of oxygen and nutrients, and lead to necrosis of encapsulated islets. To this end, research groups have developed polymers to reduce the fibrotic reactions. (Ma et al., Adv. Mater. 23:H189 (2011)). Another challenge is the incomplete coverage of the islets within the capsules (deVos et al., Transplantation 62:888 (1996); deVos et al., Transplantation 62:893 (1996)). Islets protruding outside the capsules are more frequently observed when the islet number density in alginate solution increases or the capsule size decreases, both of which are desirable to minimize the transplantation volume (Leung, et al, Biochem. Eng. J. 48:337 (2010)). It has been hypothesized that if even a small fragment of islet is exposed, immune effector cells may destroy the entire islet (King et al., Graft 4:491 (2001); Weber et al., Ann. NY Acad. Sci. 875:233 (1999)). Furthermore, exposure of a small number of islets may start a cascade of events that leads to enhanced antigen-specific cellular immunity and transplant failure.

A double-encapsulation process (Elliot, 2007; Wong et al., Biomat. Artific. Cells Immobiol. Biotechnol. 19:687 (1991)) has been used to improve the encapsulation and xenograft survival where very small capsules containing cells were first formed and then several small capsules were enclosed in each larger capsule. This approach required two process steps and

the large size of the final capsules inevitably limited the mass transport that was essential to cell viability and functionality. As reported by Schneider et al. (Biomaterials 22(14):1961-1970 (2001)), islet containing alginate beads were coated with alternating layers of polyethyleneimine, polyacrylacid or carboxymethylcellulose and alginate to address some of these problems. Thin conformal coating of islets reduces the diffusion distance and total transplantation volume (Teramura et al., Adv. Drug Deliv. Rev. 62:827 (2010); Wilson et al., J. Am. Chem. Soc. 131:18228 (2009)). However, the process often involves multiple steps which cause damage to islets and it is not clear whether the coatings are sufficiently robust for clinical use (Califiore, 2003; Basta et al., Curr. Diab. Rep. 11:384 (2011)). Previous data by Basta et al. (Transpl. Immunol. 13:289 (2004)) has suggested conformal coatings may have reduced immune-protective capacity compared with the hydrogel capsules.

In summary, despite promising studies in various animal models over many years, encapsulated human islets so far have not made an impact in the clinical setting. Many non-immunological and immunological factors such as biocompatibility, reduced immunoprotection, hypoxia, pericapsular fibrotic overgrowth, effects of the encapsulation process, and post-transplant inflammation hamper the successful application of this promising technology (Vaithilinga et al., Diabet Stud 8(1):51-67 (2011)). Currently used alginate microcapsules often have islets protruding outside capsules, leading to inadequate immunoprotection. Improved encapsulation using a two-fluid co-axial electro-jetting method to confine islets in the core region of the capsules has been reported by Ma et al., Adv. Healthcare Materials 2(5):667-672 (2013).

One major challenge to clinical application of encapsulated cells and other biomaterials and medical devices is their potential to induce a non-specific host response (Williams, Biomaterials 29(20):2941-53 (2008); Park et al., Pharm Res 13(12):1770-6 (1996); Kvist et al., Diabetes Technol 8(4):463-75 (2006); Wisniewski et al., J Anal Chem 366(6):611-21 (2000); Van der Giessen et al., Circulation 94(7):1690-7 (1996); Granchi et al., J

Biomed Mater Res 29(2):197-202 (1995); Ward et al., Obstet Gynecol 86(5):848-50 (1995); Remes et al., Biomaterials 13(11):731-43 (1992)). This reaction involves the recruitment of early innate immune cells such as neutrophils and macrophages, followed by fibroblasts which deposit collagen to form a fibrous capsule surrounding the implanted object (Williams, Biomaterials 29(20):2941-53 (2008); Remes et al., Biomaterials 13(11):731-43 (1992); Anderson et al., Semin Immunol 20(2):86-100 (2008); Anderson et al., Adv Drug Deliver Rev 28(1):5-24 (1997); Abbas et al., Pathologic Basis of Disease. 7th ed. Philadelphia : W.B Saunders (2009)). Fibrotic cell layers can hinder electrical (Singarayar et al., PACE 28(4):311-5 (2005)) or chemical communications and prevent transport of analytes (Sharkawy et al., J Biomed Mater Res 37(3):401-12 (1997); Sharkawy et al., J Biomed Mater Res 40(4):598-605 (1998); Sharkawy et al., J Biomed Mater Res 40(4):586-97 (1998)) and nutrients, thus leading to the eventual failure of many implantable medical devices such as immunoisolated pancreatic islets (De Groot et al., J Surg Res 121(1):141-50 (2004); De Vos et al., Diabetologia 40(3):262-70 (1997); Van Schilfgaarde et al., J Mol Med 77(1):199-205 (1999)).

The fibrotic reactions to the capsules upon transplantation pose a major challenge to transplanting islets. The fibrosis eventually leads to necrosis of islets and failure of transplant.

There remains a substantial need for improved encapsulation methods and devices for transplantation of human islet cells.

It is an object of the present invention to provide a cell encapsulation system for transplanting cells with reduced pericapsular fibrotic overgrowth.

It is a further object of the invention to provide a method for transplanting cells with reduced pericapsular fibrotic overgrowth.

It is a further object of the invention to provide improved methods for treating diabetes using encapsulated islet cells.

It is a further object of the invention to provide a method and devices for general device fabrication to prevent fibrotic sequestration and prevention of function and long-term therapeutic efficacy.

SUMMARY OF THE INVENTION

It has been discovered that biomedical devices designed with certain physical characteristics exhibit reduced host rejection and fibrotic overgrowth of biomaterials and biomedical devices.

Disclosed is a preparation of biomedical devices, e.g., a preparation of hydrogel capsules, wherein, at least 60, 70, 80, 90, 95, or 98 % of the devices of the preparation (i) have a sphere-like shape or a spheroid-like shape and (ii) have a diameter of at least X mm, but no more than Y mm, provided that Y is greater than X, X is 1.0, 1.1, 1.2, 1.3, 1.4, 1.5, 1.6, 1.7, 1.8, 1.9, or 2.0, and Y is 2.0, 2.5, 3.0, 3.5, 4.0, 4.5, 5.0, 5.5, 6.0, 6.5, 7.0, 7.5, 8.0, 8.5, 9.0, 9.5, or 10.0.

In some forms, no more than 20% of the devices of the preparation have other than a sphere-like shape or a spheroid-like shape. In some forms, at least 50, 60, 70, 80, or 90 % of the devices of the preparation comprise a live cell, or a plurality of live cells, or at least 1,000, 2,000 or 5,000 live cells/device. In some forms, at least 50, 60, 70, 80, or 90 % of the devices of the preparation having sphere-like shape or a spheroid-like shape comprise a live cell, or a plurality of live cells, or at least 1,000, 2,000 or 5,000 live cells, In some forms, no more than 1, 2, 3, 4, 5, 10, 15 or 20 % of the devices of the preparation have an edge. In some forms, the cells in at least 50, 60, 70, 80, or 90 % of the devices of the preparation are distributed essentially homogenously throughout the device. In some forms, the cells in at least 50, 60, 70, 80, or 90 % of the devices of the preparation having sphere-like shape or a spheroid-like shape are distributed essentially homogenously throughout the device. In some forms, the cells in at least 50, 60, 70, 80, or 90 % of the devices of the preparation are not distributed essentially homogenously throughout the device. In some forms, the cells in at least 50, 60, 70, 80, or 90 % of the sphere-like shape or spheroid-like shape devices of the preparation are not distributed essentially homogenously throughout the device. Any and all combinations of these features can be used in a preparation of the biomedical devices.

In some forms, the biomedical devices can comprise a biocompatible material, such as alginate or an alginate derivative. In some forms, X = 1.2,

and Y = 10.0. In some forms, X = 1.2, and Y = 8.0. In some forms, X = 1.3, and Y = 10.0. In some forms, X = 1.3, and Y = 8.0.

In some forms, at least 60 % of the devices of the preparation have a sphere-like shape or a spheroid-like shape. In some forms, at least 70 % of the devices of the preparation have a sphere-like shape or a spheroid-like shape. In some forms, at least 80 % of the devices of the preparation have a sphere-like shape or a spheroid-like shape. In some forms, at least 80 % of the devices of the preparation are not sub-compartmentalized. In some forms, at least 80 % of the devices of the preparation are sub-compartmentalized, e.g., by a membrane or interface, and at least one subcompartment is essentially free of cells.

Also disclosed are methods of treating a subject, comprising: (a) administering to the subject a first administration of an effect of amount of a preparation as disclosed herein, which provides a therapeutic effect for at least Z days; and (b) administering to the subject a subsequent administration of an effective of amount of the preparation, where at least Z-10, Z-5, or Z days separate the first and subsequent administrations, and wherein no interim administration is provided.

Also disclosed are methods of treating a subject, comprising: (a) administering, at least Z days after the first administration to a subject of an effective of amount of a preparation as disclosed herein, a subsequent administration of an effective of amount of the preparation, where at least Z-10, Z-5, or Z days separate the first and subsequent administrations.

In some forms, Z is at least 14 days. In some forms, Z is at least 30 days.

A biomedical device for implantation with decreased pericapsular fibrotic overgrowth has been developed. The device includes biocompatible materials, has a diameter of at least 1 mm and less than 10 mm, has a spheroid-like shape, and has one or more of the additional characteristics: surface pores of the device are greater than 0 nm and less than 10 μm; the surface of the device is neutral or hydrophilic; the curvature of the surface of the device is at least 0.2 and is not greater than 2 on all points of the surface;

and the surface of the device does not have flat sides, sharp angles, grooves, or ridges. The device elicits less of a fibrotic reaction after implantation than the same device lacking one or more of these characteristic that are present on the device. In some embodiments, the devices can be a biocompatible sphere-like (spheroid) outer shell, encapsulating, for example, biologic cells or tissue, synthetic electrical leads, or sensors.

The biomedical device can be made from a variety of materials, including hydrogels, both chemically purified as well as endotoxin-containing food-grade alginate, semiconducting materials, such as silicon-dioxide-based ceramics like glass, and degradable and non-degradable polymers and plastics, such as PCL and polystyrene. The specific combinations of features result in or improve biocompatibility of devices (in particular, by reducing or eliminating immune reaction to and capsular fibrosis of the devices).

The biomedical device can be used for any biomedical application, including, for example, long-term implantable sensors and actuators, controlled drug releasing devices, prostheses and tissue regenerating biomaterials, and technologies pertaining to transplantation.

A biocompatible capsule encapsulating mammalian cells, optionally including anti-inflammatory drugs, for transplantation with decreased pericapsular fibrotic overgrowth has been developed. The capsule has encapsulated therein mammalian cells. The mammalian cells are not located in the core of the capsule. Preferably the capsule contains two or three layers. In tri-layer capsules, having an acellular core, a hydrogel layer, and an outer barrier layer, the cells are located in the middle layer. For two layer capsules, which contain a core and a shell, the cells are located in the shell. Alternatively, the cells can be in the core of a two layer capsule. Optionally, the capsule also contains one or more therapeutic, diagnostic and/or prophylactic agents, such as anti-inflammatory drugs or radiopaque imaging agents, encapsulated therein.

Generally, the core-shell capsules are fabricated without a membrane layer using a microfluidic or needle system to form capsules and microcapsules with two or more integrated layers. For example, two

concurrent liquid streams may be used to form two-layer droplets. The tri-layer capsules can be fabricated without a membrane layer. For example, three concurrent streams may be used to form three-layer droplets that harden to form the capsules and microcapsules.

Cells suitable for encapsulation and transplantation are generally secretory or metabolic cells (i.e., they secrete a therapeutic factor or metabolize toxins, or both) or structural cells (e.g., skin, muscle, blood vessel), or metabolic cells (i.e., they metabolize toxic substances). In some embodiments, the cells are naturally secretory, such as islet cells that naturally secrete insulin, or naturally metabolic, such as hepatocytes that naturally detoxify and secrete. In some embodiments, the cells are bioengineered to express a recombinant protein, such as a secreted protein or metabolic enzyme. Depending on the cell type, the cells may be organized as single cells, cell aggregates, spheroids, or even natural or bioengineered tissue.

The capsule is preferably a hydrogel capsule. In some embodiments the core of the capsule is a non-hydrogel polymer. Preferably the capsules have a diameter greater than 1 mm, more preferably the diameter is 1.5 mm or greater in size, but less than 8 mm. The larger capsules require an acellular core to ensure that the cells are able to receive adequate nutrients and gas exchange by diffusion throughout the hydrogel.

A population of hydrogel capsules encapsulating cells has been developed. Capsules in the population contain cells to be transplanted selected from the group consisting of mammalian secretory cells, mammalian metabolic cells, mammalian structural cells, and aggregates thereof. All of the capsules in the population of capsules have a diameter of at least 1 mm and less than 8 mm. The capsules in the population elicit less of a fibrotic reaction after implantation than the same capsules having a diameter of less than 1 mm. The capsules in the population can be selected by separating capsules having a diameter of at least 1 mm and less than 8 mm from capsules having a diameter of less than 1 mm and from capsules having a diameter of at least 8 mm.

The compositions may be fabricated into artificial organs, such as an artificial pancreas containing encapsulated islet cells. In some of these

embodiments, the cells are encapsulated in a single hydrogel compartment. In other embodiments, the composition contains a plurality of encapsulated cells dispersed or encapsulated in a biocompatible structure.

Methods for treating diseases generally involve administering to a subject a biocompatible hydrogel encapsulating mammalian cells and anti-inflammatory drugs. In some embodiments, the anti-inflammatory drugs are encapsulated in controlled release polymer. In some of these embodiments, the encapsulated cells preferably secrete a therapeutically effective amount of a substance to treat the disease for at least 30 days, preferably at least 60 days, more preferably at least 90 days. In particularly preferred embodiments, the cells are islet cells that secrete a therapeutically effective amount of insulin to treat diabetes in the subject for at least 30 days, preferably at least 60 days, more preferably at least 90 days.

BRIEF DESCRIPTION OF THE DRAWINGS

Figure 1 is an illustration of a tri-layer capsule, with the cells encapsulated in a core hydrogel and the drug-loaded particles contained in an outer (envelope) hydrogel. An optional membrane material is shown separating the core and envelope hydrogels.

Figure 2 is an illustration of a nozzle for forming tri-layer capsules via tri-fluid coaxial electrospraying.

Figures 3A and 3B are schematic depictions of a conventional cell encapsulation method in which cells are dispersed within a hydrogel matrix having an outer crosslinked shell (Figure 3A) and a two-fluid co-axial electro-jetting device for forming a hydrogel core containing cells, surrounded by a shell to prevent any of the cells from contacting the outer wall of the capsule and potentially being exposed to immune cells in the host into which the capsule is implanted.

Figures 4A and 4B are graphs comparing control, regular capsules and core–shell capsules in treating Type I diabetes. Figure 4A shows the blood glucose data of STZ-induced diabetic mice after the transplantation of 500 encapsulated rat islet equivalents. The error bars represent standard errors.

Figure 4B shows the number of normoglycemic mice as a function of time. 8 replicates were used for both types of capsules.

Figures 5A and 5B are graphs comparing blood glucose levels in STZ-induced C57BL/6 diabetic mice implanted with 500 μm hydrogel capsules containing islet cells (Figure 5A) and 1.5 mm alginate capsules encapsulating rat islets (500 IE's) (Figure 5B).

Figure 6 is a graph of immune response (percent of cell population made up of macrophages or neutrophils) in empty capsules of different sizes. Capsules of 300 μm, 500 μm, 900 μm, and 1500 μm were assessed.

Figure 7 is a graph of normalized signal intensity of smooth muscle actin and β-actin associated with capsules of 0.3 mm, 0.5 mm, 1 mm, and 1.5 mm determined by Western blot.

Figure 8 shows graphs of the fibrosis level for capsules of 300 μm, 500 μm, and 800 μm normalized for surface area of the capsules (Figure 8, top) or for volume of the capsules (Figure 8, bottom).

Figures 9A-9D are graphs of the relative expression of fibrosis markers in capsules of 500 μm and 1500 μm were made of SLG20 alginate (PRONOVA), polystyrene, glass, polycaprolactone (PCL), and LF10/60 alginate (FMC BioPolymer). Fibrosis was measured using CD68 (macrophage marker; Figure 9A), Ly6g (neutrophil marker; Figure 9B), CD11b (myeloid cell marker; Figure 9C), and Col1a1 (fibrosis marker; Figure 9D).

Figures 10A and 10B are graphs of immune response (percent of cell population made up of macrophages (Figure 10A) or neutrophils (Figure 10B)) in capsules of 500 μm and 1500 μm made of different materials. The capsules were made of SLG20 alginate (PRONOVA), polystyrene, glass, polycaprolactone (PCL), and LF10/60 alginate (FMC BioPolymer).

Figure 11 is a line graph of Measured Capsule Diameter (μm) versus Capsule size (μm).

Figures 12A, 12B, and 12C are line graphs of gene expression versus diameter (mm) for alpha-SMA, Col1a1, and Col1a2 respectively.

Figure 12D is a bar graph of a Western blot analysis of alpha-SMA expression within cellular overgrowth on spheres.

Figures 13A and 13B are bar graphs of the cell population of macrophages and neutrophil cells, respectively, from flow analysis using specific markers for responding host macrophage (A) and neutrophils (B). Medium-sized (0.5mm) and large-sized (1.5–2mm) versions of SLG20 alginate, LF10/60 alginate (endotoxin containing), glass and polystyrene, 14 days post intraperitoneal were implanted into C57BL/6 mice. Mock, surgery and PBS-only injection; SLG, SLG20 alginate; LF, LF10/60 alginate (endotoxin containing); PCL, polycaprolactone; PS, polystyrene.

Figures 14A-14D are bar graphs of relative expression determined by qPCR of CD68 (macrophage marker), Ly6g/Gr1 (neutrophil marker), CD11b (myeloid cell marker), and Col1a1 (collagen marker), respectively, for various spheres. Medium (MED, 0.4-0.6 mm) or large sized (LG, 1.5-2.5 mm) spheres were implanted into the intraperitoneal space of C57BL/6 mice. All materials were then retrieved 14 days post-implant, and levels of different innate immune and fibrosis markers were assayed by gene expression. CD68, macrophage marker; Ly6g/Gr1, neutrophil marker; CD11b, myeloid cell marker; and Col1a1, collagen marker. Materials: SLG20 (chemically purified alginate), LF10/60 (non-purified, endotoxin-containing alginate), polymers polystyrene (PS) and PCL (polycaprolactone), silica-based ceramic glass, and stainless steel (SS). The results show that the effect of increased size in reducing foreign body responses expands across a spectrum of materials including hydrogels, plastics, metals, and ceramics. Note on plots NT=No treatment, and MT= Mock Treatment (i.e. PBS injection alone). Error bars, mean ± SEM. N=5 mice per treatment. qPCR statistical analysis: one-way ANOVA with Bonferroni multiple comparison correction *: $p < 0.05$, **: $p < 0.001$, and ***: $p < 0.0001$, comparing MED vs. LG. Experiments were repeated twice.

Figure 15 is a bar graph of gene expression of fibrotic markers α-SMA, Collagen 1a1 (Col1a1), and Collagen 1a2 (Col1a2) directly on medium (0.5 mm) and large sized (0.5 mm) glass microspheres plotted normalized to

relative expression levels onto medium sized spheres. Glass microspheres implanted into the peritoneal cavity of Sprague-Dawley rats and retrieved after two 2 weeks. Error bars, mean ± SEM. N=3 rats per treatment. qPCR statistical analysis: one-way ANOVA with Bonferroni multiple comparison correction **: $p < 0.001$, comparing Med vs. Large.

Figures 16A and 16B are line graphs of blood glucose over days (A) and minutes in STZ-induced C57BL/6 diabetic mice transplanted with 0.5-mm and 1.5-mm alginate capsules encapsulating rat islets (500 IEs). Blood-glucose curves showing prolonged normoglycaemia with large (1.5-mm) hydrogel alginate capsules, but only short-lived success with standard (0.5-mm) capsules (A). In vivo glucose tolerance test (iv GTT) of healthy mice and diabetic mice seven days post-transplantation with rat islets encapsulated in standard (0.5-mm) or large (1.5-mm) capsules shows no significant delays in BG correction as a function of capsule geometry (B). All experiments were performed at least two or three times.

Figure 16C is a Kaplan–Meier plot showing percentage of mice cured over time. STZ-C57BL/6 mice were transplanted with either 0.5-mm or 1.5-mm capsules, containing 500 IEs of primary rat islets. All experiments were performed at least two or three times.

Figures 17A and 17B are a line graph and a bar graph, respectively, of Ca^{2+} concentration over time showing intracellular calcium influx in response to insulin secretagogues. Representative traces of intracellular calcium of single rat islets in response to 20 mM glucose and 30 mM KCl (potassium chloride) stimulus (A). Average AUC $[Ca2+]_i$ % of calcium influx in response to 20 mM or 2 mM glucose and 30 mM KCl. From left to right: Naked n = 59; 0.5 mm n = 49; 1.5 mm n = 43. Mean ± SEM (B).

Figures 18A-18D are line graphs (A, B) and bar graphs (C, D) of Ca^{2+} concentration over time showing intracellular calcium influx in response to insulin secretagogues. Average insulin secretion kinetics in response to 20 mM glucose (A). Average insulin secretion kinetics in response to 30 mM KCl (potassium chloride) (B). Average AUC [Insulin/10 islets] secreted in

response to 20 mM glucose (C). Average AUC [Insulin/10 islets] secreted in response to 30 mM KCl. (n = 3 groups, each group 50 islets, Mean ± SD) (D).

Figures 19A and 19B are line graphs of blood glucose over time (days) showing individual BG correction of 0.5 mm (A) and 1.5 mm (B) alginate capsules encapsulating rat islets (500 IE's) in STZ-induced C57BL/6 diabetic mice. Individual blood glucose curves showing only short-lived success with medium 0.5 mm diameter capsules (A), versus prolonged normoglycemia with large 1.5 mm diameter hydrogel alginate capsules (B). n = 5-7; repeated twice.

Figures 20A-20C are bar graphs of flow analysis of cells over time on implanted spheres to SLG20 alginate microspheres of diameter 0.5 and 1.5 mm using specific markers for responding host innate immune myeloid (A), neutrophil (B), and macrophage cells (C). For FACS analysis, N=5 mice per treatment. FACS experiments were performed twice. FACS size comparisons were performed by unpaired, two-tailed t-test. *, $p<0.05$; **, $p<0.001$; ***, $p<0.0001$.

Figures 21A-21F are NanoString-based analysis for expression of macrophage phenotype markers analyzed from deposited cell RNA extracts at 1, 4 and 7 days post-implant (A & D, B & E, and C & F, respectively), presented on a base 2 logarithmic scale, for SLG20 alginate microspheres of diameter 0.5 (A-C) and 1.5 mm (D-F). Error bars, mean±s.e.m.; for intravital imaging, N=3 mice per treatment; for NanoString analysis, N=4 per treatment. NanoString analysis was performed once.

Figure 22 is a bar graph of flow analysis of host response to SLG20 alginate microspheres of diameter 0.5 and 1.5 mm using specific markers for responding host innate immune myeloid (a), neutrophil (b), and macrophage cells (c) at 1, 4, 7, 14 and 28 days post-implantation. Error bars, mean±s.e.m. For FACS analysis, N=5 mice per treatment. FACS experiments were performed twice. FACS size comparisons were performed by unpaired, two-tailed t-test. *, $p<0.05$; **, $p<0.001$; ***, $p<0.0001$.

Figure 23 shows the preparation of mice for intravital imaging. The flow of processes involved in preparing mice for implantation with alginate

hydrogel spheres, loaded with quantum dots, for in vivo intravital fluorescence imaging of macrophage recruitment around and onto implanted spheres.

Figures 24A-24F show profiling macrophage phenotype shifts in the cells of the intraperitoneal space. NanoString-based analysis for RNA expression of macrophage phenotype markers from cells in the intraperitoneal space extracted (intraperitoneal lavaged) at 1, 4, and 7 days post-implant. Expression is normalized to intraperitoneal cells harvested from mock surgery (PBS-injected) mice, presented on a base 2 logarithmic scale. N=4 mice per treatment. For details of analysis see supplemental methods description.

Figure 25A-25F show profiling macrophage phenotype shifts in the cell of the peripheral omentum fat tissue. NanoString-based analysis for RNA expression of macrophage phenotype markers from cells in the peripheral fat tissue extracted at 1, 4, and 7 days post-implant. Expression is normalized to fat tissue harvested from mock surgery (PBS-injected) mice, presented on a base 2 logarithmic scale. N=4 mice per treatment.

DETAILED DESCRIPTION OF THE INVENTION

I. Definitions

"Hydrogel" refers to a substance formed when an organic polymer (natural or synthetic) is cross-linked via covalent, ionic, or hydrogen bonds to create a three-dimensional open-lattice structure which entraps water molecules to form a gel. Biocompatible hydrogel refers to a polymer that forms a gel which is not toxic to living cells, and allows sufficient diffusion of oxygen and nutrients to the entrapped cells to maintain viability.

"Alginate" is a collective term used to refer to linear polysaccharides formed from β-D-mannuronate and α-L-guluronate in any M/G ratio, as well as salts and derivatives thereof. The term "alginate", as used herein, encompasses any polymer having the structure shown below, as well as salts thereof.

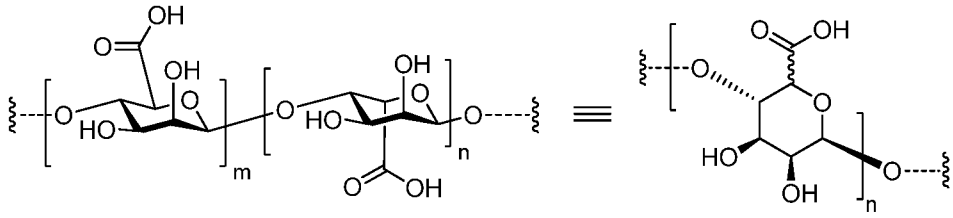

"Biocompatible" generally refers to a material and any metabolites or degradation products thereof that are generally non-toxic to the recipient and do not cause any significant adverse effects to the subject.

"Biodegradable" generally refers to a material that will degrade or erode by hydrolysis or enzymatic action under physiologic conditions to smaller units or chemical species that are capable of being metabolized, eliminated, or excreted by the subject. The degradation time is a function of polymer composition and morphology.

"Drug-loaded particle" refers to a polymeric particle having a drug dissolved, dispersed, entrapped, encapsulated, or attached thereto.

"Microparticle" and "nanoparticle" refer to a polymeric particle of microscopic and nanoscopic size, respectively, optionally containing a drug dissolved, dispersed, entrapped, encapsulated, or attached thereto.

"Anti-inflammatory drug" refers to a drug that directly or indirectly reduces inflammation in a tissue. The term includes, but is not limited to, drugs that are immunosuppressive. The term includes anti-proliferative immunosuppressive drugs, such as drugs that inhibit the proliferation of lymphocytes.

"Immunosuppressive drug" refers to a drug that inhibits or prevents an immune response to a foreign material in a subject. Immunosuppressive drugs generally act by inhibiting T-cell activation, disrupting proliferation, or suppressing inflammation. A person who is undergoing immunosuppression is said to be immunocompromised.

"Mammalian cell" refers to any cell derived from a mammalian subject suitable for transplantation into the same or a different subject. The cell may be xenogeneic, autologous, or allogeneic. The cell can be a primary cell obtained directly from a mammalian subject. The cell may also be a cell

derived from the culture and expansion of a cell obtained from a subject. For example, the cell may be a stem cell. Immortalized cells are also included within this definition. In some embodiments, the cell has been genetically engineered to express a recombinant protein and/or nucleic acid.

"Autologous" refers to a transplanted biological substance taken from the same individual.

"Allogeneic" refers to a transplanted biological substance taken from a different individual of the same species.

"Xenogeneic" refers to a transplanted biological substance taken from a different species.

"Islet cell" refers to an endocrine cell derived from a mammalian pancreas. Islet cells include alpha cells that secrete glucagon, beta cells that secrete insulin and amylin, delta cells that secrete somatostatin, PP cells that secrete pancreatic polypeptide, or epsilon cells that secrete ghrelin. The term includes homogenous and heterogenous populations of these cells. In preferred embodiments, a population of islet cells contains at least beta cells.

"Transplant" refers to the transfer of a cell, tissue, or organ to a subject from another source. The term is not limited to a particular mode of transfer. Encapsulated cells may be transplanted by any suitable method, such as by injection or surgical implantation.

"Sphere-like shape" refers to an object having a surface that roughly forms a sphere. Beyond a perfect or classical sphere shape, a sphere-like shape can have waves and undulations. Generally, a sphere-like shape is an ellipsoid (for its averaged surface) with semi-principal axes within 10% of each other. The diameter of a sphere-like shape is the average diameter, such as the average of the semi-principal axes.

"Spheroid-like shape" refers to an object having a surface that roughly forms a spheroid. Beyond a perfect or classical sphere, oblate spheroid, or prolate spheroid shape, a spheroid-like shape can have waves and undulations. Generally, a spheroid-like shape is an ellipsoid (for its averaged surface) with semi-principal axes within 100% of each other. The diameter of a

spheroid-like shape is the average diameter, such as the average of the semi-principal axes.

"Flat side" refers to a contiguous area of more than 5% of a surface that has a curvature of 0.

"Sharp angle" refers to a location on a surface across which the tangent to the surface changes by more than 10% over a distance of 2% or less of the circumference of the surface. Edges, corners, grooves, and ridges in a surface are all forms of sharp angles.

II. Biomedical Devices and Capsules

A. Biomedical Devices with Reduced Fibrosis

Biomedical devices are disclosed for implantation into a subject. The devices are formed from biocompatible materials, such as biocompatible polymers, biodegradable and non-biodegradable polymers, semiconductor materials, ceramics, and glass. In order to reduce or prevent fibrosis, the devices should include some or all of a suite of characteristics:

(1) Size: The device should have a minimum diameter of 1 mm (preferable 1.5 mm). The diameter can be increased upwards of 8 to 10 mm.

(2) Shape: The overall device should be a sphere, sphere-like, spheroid, or spheroid-like. The curvature at any point on the surface of the device should be no less than 0.2 and no more than 2. Surface pores are ignored for the purpose of calculating the curvature of the surface of the device.

(3) Hydrophobicity: The surface of the device should either be neutral or more water-loving (hydrophilic), and should not have a hydrophobic chemistry, such as with Teflon.

(4) Surface pore size: Pores on the surface of the device should be above 0 nm but should not exceed10 μm.

(5) Surface topography: The device should not have any flat sides, sharp angles, grooves, or ridges.

These characteristics have been discovered to affect the fibrosis of implanted devices. Devices having the first two characteristics and at least one of the other characteristics have been shown to exhibit reduced fibrosis.

Devices can be made with any one or combination of these characteristics. Devices having all of these characteristics are preferred. Generally, the disclosed devices will elicit less of a fibrotic reaction after implantation than the same device having any one or more of these characteristics. In some embodiments, the device will elicit less of a fibrotic reaction after implantation than the same device having the first two characteristics and at least one of the other characteristics. In some embodiments, the device will elicit less of a fibrotic reaction after implantation than the same device having all of the characteristics. In some embodiments, the biomedical devices are capsules or hydrogel capsules as described herein. Reference herein to a capsule or a hydrogel capsule is intended to also refer to a biomedical device of the same description as the referenced capsule.

The disclosed devices have advantages and improvements over existing devices and materials. For example, it has been discovered that objects with flat surfaces (curvature of zero), such as cylinders, become fibrosed even if they are large in overall size (over 1 mm). On the other extreme, objects with a high curvature (and thus having too small a diameter, i.e., less than 1 mm), are capable of high packing densities with other transplanted materials and/or surrounding tissue, which facilitates immune cell adherence and fibrotic deposition. It has been established that the specific combination of features together reduce or prevent fibrosis of many material classes, including hydrogels (both chemically purified as well as endotoxin-containing food-grade alginate), semiconducting materials (such as silicon-dioxide-based ceramics like glass), and degradable and non-degradable polymers and plastics (such as PCL and polystyrene). Thus, the disclosed devices can be made of these and a wide variety of other materials.

Hydrogel alginate spheres with the identified characteristics have been generated and demonstrated to prevent fibrosis and ensure long-term viability and functionality of transplanted mammalian cells of various origin (i.e., rat, mouse, pig, human) for treatment of disease (type 1 diabetes). Optionally, the shell of the device may also contain one or more therapeutic agents (such as

anti-inflammatories) or diagnostic agents (such as oxygen sensing or imaging chemistries).

The biomedical device can be used for any biomedical application, including, for example, long-term implantable sensors and actuators, controlled drug releasing devices, prostheses and tissue regenerating biomaterials, and technologies pertaining to implantation and transplantation. Many biomedical devices and purposes are known and the disclosed devices can be adapted for such purposes.

One embodiment provides a preparation of biomedical devices, e.g., a preparation of hydrogel capsules, wherein, at least 60, 70, 80, 90, 95, or 98 % of the devices of the preparation have a sphere-like shape or a spheroid-like shape and have a diameter of at least X mm, but no more than Y mm, provided that Y is greater than X, and X = 1.0, 1.1, 1.2, 1.3, 1.4, 1.5, 1.6, 1.7, 1.8, 1.9, or 2.0, and Y = 2.0, 2.5, 3.0, 3.5, 4.0, 4.5, 5.0, 5.5, 6.0, 6.5, 7.0, 7.5, 8.0, 8.5, 9.0, 9.5, or 10.0, and a) no more than 1, 2, 3, 4, 5, 10, 15, or 20% of the devices of the preparation have other than a sphere-like shape or a spheroid-like shape; b) at least 50, 60, 70, 80, or 90 % of the devices of the preparation comprise a live cell, or a plurality of live cells, or at least 1,000, 2,000 or 5,000 live cells/device; c) at least 50, 60, 70, 80, or 90 % of the sphere-like shape or a spheroid-like shape devices of the preparation comprise a live cell, or a plurality of live cells, or at least 1,000, 2,000 or 5,000 live cells; d) no more than 1, 2, 3, 4, 5, 10, 15 or 20% of the devices of the preparation have an edge,

e) the cells in at least 50, 60, 70, 80, or 90 % of the devices of the preparation are distributed essentially homogenously throughout the device; f) the cells in at least 50, 60, 70, 80, or 90 % of the sphere-like shape or spheroid-like shape devices of the preparation are distributed essentially homogenously throughout the device; g) the cells in at least 50, 60, 70, 80, or 90 % of the devices of the preparation are not distributed essentially homogenously throughout the device; and h) the cells in at least 50, 60, 70, 80, or 90 % of the sphere-like shape or spheroid-like shape devices of the preparation are not distributed essentially homogenously throughout the device.

B. Encapsulated Cells with Reduced Fibrosis

Capsules are disclosed for transplanting mammalian cells into a subject. The capsules are formed from a biocompatible, hydrogel-forming polymer encapsulating the cells to be transplanted. In order to inhibit capsular overgrowth (fibrosis), the structure of the capsules prevents cellular material from being located on the surface of the capsule. Additionally, the structure of the capsules ensures that adequate gas exchange occurs with the cells and nutrients are received by the cells encapsulated therein. Optionally, the capsules also contain one or more anti-inflammatory drugs encapsulated therein for controlled release.

C. Biocompatible Polymers

The disclosed compositions are formed from a biocompatible, hydrogel-forming polymer encapsulating the cells to be transplanted. Examples of materials which can be used to form a suitable hydrogel include polysaccharides such as alginate, collagen, chitosan, sodium cellulose sulfate, gelatin and agarose, water soluble polyacrylates, polyphosphazines, poly(acrylic acids), poly(methacrylic acids), poly(alkylene oxides), poly(vinyl acetate), polyvinylpyrrolidone (PVP), and copolymers and blends of each. See, for example, U.S. Patent Nos. 5,709,854, 6,129,761 and 6,858,229.

In general, these polymers are at least partially soluble in aqueous solutions, such as water, buffered salt solutions, or aqueous alcohol solutions, that have charged side groups, or a monovalent ionic salt thereof. Examples of polymers with acidic side groups that can be reacted with cations are poly(phosphazenes), poly(acrylic acids), poly(methacrylic acids), poly(vinyl acetate), and sulfonated polymers, such as sulfonated polystyrene. Copolymers having acidic side groups formed by reaction of acrylic or methacrylic acid and vinyl ether monomers or polymers can also be used. Examples of acidic groups are carboxylic acid groups and sulfonic acid groups.

Examples of polymers with basic side groups that can be reacted with anions are poly(vinyl amines), poly(vinyl pyridine), poly(vinyl imidazole), and some imino substituted polyphosphazenes. The ammonium or quaternary

salt of the polymers can also be formed from the backbone nitrogens or pendant imino groups. Examples of basic side groups are amino and imino groups.

The biocompatible, hydrogel-forming polymer is preferably a water-soluble gelling agent. In preferred embodiments, the water-soluble gelling agent is a polysaccharide gum, more preferably a polyanionic polymer.

The cells are preferably encapsulated using an anionic polymer such as alginate to provide the hydrogel layer (e.g., core), where the hydrogel layer is subsequently cross-linked with a polycationic polymer (e.g., an amino acid polymer such as polylysine) to form a shell. See e.g., U.S. Patent Nos. 4,806,355, 4,689,293 and 4,673,566 to Goosen et al.; U.S. Patent Nos. 4,409,331, 4,407,957, 4,391,909 and 4,352,883 to Lim et al.; U.S. Patent Nos. 4,749,620 and 4,744,933 to Rha et al.; and U.S. Patent No. 5,427,935 to Wang et al., Amino acid polymers that may be used to crosslink hydrogel forming polymers such as alginate include the cationic poly(amino acids) such as polylysine, polyarginine, polyornithine, and copolymers and blends thereof.

1. Polysaccharides

Several mammalian and non-mammalian polysaccharides have been explored for cell encapsulation. Exemplary polysaccharides suitable for cell encapsulation include alginate, chitosan, hyaluronan (HA), and chondroitin sulfate. Alginate and chitosan form crosslinked hydrogels under certain solution conditions, while HA and chondroitin sulfate are preferably modified to contain crosslinkable groups to form a hydrogel.

In preferred embodiments, the biocompatible, hydrogel-forming polymer encapsulating the cells is an alginate. Alginates are a family of unbranched anionic polysaccharides derived primarily from brown algae which occur extracellularly and intracellularly at approximately 20% to 40% of the dry weight. The 1,4-linked α-l-guluronate (G) and β-d-mannuronate (M) are arranged in homopolymeric (GGG blocks and MMM blocks) or heteropolymeric block structures (MGM blocks). Cell walls of brown algae also contain 5% to 20% of fucoidan, a branched polysaccharide sulphate ester with l-fucose four-sulfate blocks as the major component. Commercial

alginates are often extracted from algae washed ashore, and their properties depend on the harvesting and extraction processes.

Alginate forms a gel in the presence of divalent cations via ionic crosslinking. Although the properties of the hydrogel can be controlled to some degree through changes in the alginate precursor (molecular weight, composition, and macromer concentration), alginate does not degrade, but rather dissolves when the divalent cations are replaced by monovalent ions. In addition, alginate does not promote cell interactions.

A particularly preferred composition is a capsule or microcapsule containing cells immobilized in a core of alginate with a polylysine shell. Preferred capsules and microcapsules may also contain an additional external alginate layer (e.g., envelope) to form a multi-layer alginate/polylysine-alginate/alginate-cells capsule or microcapsule. See U.S. Patent No. 4,391,909 to Lim et al., for description of alginate hydrogel crosslinked with polylysine. Other cationic polymers suitable for use as a cross-linker in place of polylysine include poly(β-amino alcohols) (PBAAs) (Ma M et al., Adv. Mater. 23:H189-94 (2011).

Chitosan is made by partially deacetylating chitin, a natural nonmammalian polysaccharide, which exhibits a close resemblance to mammalian polysaccharides, making it attractive for cell encapsulation. Chitosan degrades predominantly by lysozyme through hydrolysis of the acetylated residues. Higher degrees of deacetylation lead to slower degradation times, but better cell adhesion due to increased hydrophobicity. Under dilute acid conditions (pH < 6), chitosan is positively charged and water soluble, while at physiological pH, chitosan is neutral and hydrophobic, leading to the formation of a solid physically crosslinked hydrogel. The addition of polyol salts enables encapsulation of cells at neutral pH, where gelation becomes temperature dependent.

Chitosan has many amine and hydroxyl groups that can be modified. For example, chitosan has been modified by grafting methacrylic acid to create a crosslinkable macromer while also grafting lactic acid to enhance its water solubility at physiological pH. This crosslinked chitosan hydrogel

degrades in the presence of lysozyme and chondrocytes. Photopolymerizable chitosan macromer can be synthesized by modifying chitosan with photoreactive azidobenzoic acid groups. Upon exposure to UV in the absence of any initiator, reactive nitrene groups are formed that react with each other or other amine groups on the chitosan to form an azo crosslink.

Hyaluronan (HA) is a glycosaminoglycan present in many tissues throughout the body that plays an important role in embryonic development, wound healing, and angiogenesis. In addition, HA interacts with cells through cell-surface receptors to influence intracellular signaling pathways. Together, these qualities make HA attractive for tissue engineering scaffolds. HA can be modified with crosslinkable moieties, such as methacrylates and thiols, for cell encapsulation. Crosslinked HA gels remain susceptible to degradation by hyaluronidase, which breaks HA into oligosaccharide fragments of varying molecular weights. Cells can be encapsulated in photopolymerized HA hydrogels where the gel structure is controlled by the macromer concentration and macromer molecular weight. In addition, photopolymerized HA and dextran hydrogels maintain long-term culture of undifferentiated human embryonic stem cells. HA hydrogels have also been fabricated through Michael-type addition reaction mechanisms where either acrylated HA is reacted with PEG-tetrathiol, or thiol-modified HA is reacted with PEG diacrylate.

Chondroitin sulfate makes up a large percentage of structural proteoglycans found in many tissues, including skin, cartilage, tendons, and heart valves, making it an attractive biopolymer for a range of tissue engineering applications. Photocrosslinked chondroitin sulfate hydrogels can be been prepared by modifying chondroitin sulfate with methacrylate groups. The hydrogel properties were readily controlled by the degree of methacrylate substitution and macromer concentration in solution prior to polymerization. Further, the negatively charged polymer creates increased swelling pressures allowing the gel to imbibe more water without sacrificing its mechanical properties. Copolymer hydrogels of chondroitin sulfate and an inert polymer, such as PEG or PVA, may also be used.

2. Synthetic polymers

Polyethylene glycol (PEG) has been the most widely used synthetic polymer to create macromers for cell encapsulation. A number of studies have used poly(ethylene glycol) di(meth)acrylate to encapsulate a variety of cells. Biodegradable PEG hydrogels can be been prepared from triblock copolymers of poly(α-hydroxy esters)-b-poly (ethylene glycol)-b-poly(α-hydroxy esters) endcapped with (meth)acrylate functional groups to enable crosslinking. PLA and poly(8-caprolactone) (PCL) have been the most commonly used poly(α-hydroxy esters) in creating biodegradable PEG macromers for cell encapsulation. The degradation profile and rate are controlled through the length of the degradable block and the chemistry. The ester bonds may also degrade by esterases present in serum, which accelerates degradation. Biodegradable PEG hydrogels can also be fabricated from precursors of PEG-*bis*-[2-acryloyloxy propanoate]. As an alternative to linear PEG macromers, PEG-based dendrimers of poly(glycerol-succinic acid)-PEG, which contain multiple reactive vinyl groups per PEG molecule, can be used. An attractive feature of these materials is the ability to control the degree of branching, which consequently affects the overall structural properties of the hydrogel and its degradation. Degradation will occur through the ester linkages present in the dendrimer backbone.

The biocompatible, hydrogel-forming polymer can contain polyphosphoesters or polyphosphates where the phosphoester linkage is susceptible to hydrolytic degradation resulting in the release of phosphate. For example, a phosphoester can be incorporated into the backbone of a crosslinkable PEG macromer, poly(ethylene glycol)-di-[ethylphosphatidyl (ethylene glycol) methacrylate] (PhosPEG-dMA), to form a biodegradable hydrogel. The addition of alkaline phosphatase, an ECM component synthesized by bone cells, enhances degradation. The degradation product, phosphoric acid, reacts with calcium ions in the medium to produce insoluble calcium phosphate inducing autocalcification within the hydrogel. Poly(6-aminoethyl propylene phosphate), a polyphosphoester, can be modified with methacrylates to create multivinyl macromers where the

degradation rate was controlled by the degree of derivitization of the polyphosphoester polymer.

Polyphosphazenes are polymers with backbones consisting of nitrogen and phosphorous separated by alternating single and double bonds. Each phosphorous atom is covalently bonded to two side chains. The polyphosphazenes suitable for cross-linking have a majority of side chain groups which are acidic and capable of forming salt bridges with di- or trivalent cations. Examples of preferred acidic side groups are carboxylic acid groups and sulfonic acid groups. Hydrolytically stable polyphosphazenes are formed of monomers having carboxylic acid side groups that are crosslinked by divalent or trivalent cations such as Ca^{2+} or Al^{3+}. Polymers can be synthesized that degrade by hydrolysis by incorporating monomers having imidazole, amino acid ester, or glycerol side groups. Bioerodible polyphosphazines have at least two differing types of side chains, acidic side groups capable of forming salt bridges with multivalent cations, and side groups that hydrolyze under *in vivo* conditions, e.g., imidazole groups, amino acid esters, glycerol and glucosyl. Hydrolysis of the side chain results in erosion of the polymer. Examples of hydrolyzing side chains are unsubstituted and substituted imidizoles and amino acid esters in which the group is bonded to the phosphorous atom through an amino linkage (polyphosphazene polymers in which both R groups are attached in this manner are known as polyaminophosphazenes). For polyimidazolephosphazenes, some of the "R" groups on the polyphosphazene backbone are imidazole rings, attached to phosphorous in the backbone through a ring nitrogen atom.

D. Conjugation of Drugs to Hydrogel-Forming Polymer

In some embodiments, one or more anti-inflammatory drugs are covalently attached to the hydrogel forming polymer. In these cases, the anti-inflammatory drugs are attached to the hydrogel forming polymer via a linking moiety that is designed to be cleaved *in vivo*. The linking moiety can be designed to be cleaved hydrolytically, enzymatically, or combinations thereof, so as to provide for the sustained release of the anti-inflammatory drug *in vivo*. Both the composition of the linking moiety and its point of

attachment to the anti-inflammatory agent, are selected so that cleavage of the linking moiety releases either an anti-inflammatory agent, or a suitable prodrug thereof. The composition of the linking moiety can also be selected in view of the desired release rate of the anti-inflammatory agents.

Linking moieties generally include one or more organic functional groups. Examples of suitable organic functional groups include secondary amides (-CONH-), tertiary amides (-CONR-), secondary carbamates (-OCONH-; -NHCOO-), tertiary carbamates (-OCONR-; -NRCOO-), ureas (-NHCONH-; -NRCONH-; -NHCONR-, -NRCONR-), carbinols (-CHOH-, -CROH-), disulfide groups, hydrazones, hydrazides, ethers (-O-), and esters (-COO-, $-CH_2O_2C-$, $CHRO_2C-$), wherein R is an alkyl group, an aryl group, or a heterocyclic group. In general, the identity of the one or more organic functional groups within the linking moiety can be chosen in view of the desired release rate of the anti-inflammatory agents. In addition, the one or more organic functional groups can be chosen to facilitate the covalent attachment of the anti-inflammatory agents to the hydrogel forming polymer. In preferred embodiments, the linking moiety contains one or more ester linkages which can be cleaved by simple hydrolysis *in vivo* to release the anti-inflammatory agents.

In certain embodiments, the linking moiety includes one or more of the organic functional groups described above in combination with a spacer group. The spacer group can be composed of any assembly of atoms, including oligomeric and polymeric chains; however, the total number of atoms in the spacer group is preferably between 3 and 200 atoms, more preferably between 3 and 150 atoms, more preferably between 3 and 100 atoms, most preferably between 3 and 50 atoms. Examples of suitable spacer groups include alkyl groups, heteroalkyl groups, alkylaryl groups, oligo- and polyethylene glycol chains, and oligo- and poly(amino acid) chains. Variation of the spacer group provides additional control over the release of the anti-inflammatory agents *in vivo*. In embodiments where the linking moiety includes a spacer group, one or more organic functional groups will generally

be used to connect the spacer group to both the anti-inflammatory agent and the hydrogel forming polymer.

In certain embodiments, the one or more anti-inflammatory agents are covalently attached to the hydrogel forming polymer via a linking moiety which contains an alkyl group, an ester group, and a hydrazide group. By way of example, conjugation of the anti-inflammatory agent dexamethasone to alginate can be via a linking moiety containing an alkyl group, an ester group connecting the alkyl group to the anti-inflammatory agent, and a hydrazide group connecting the alkyl group to carboxylic acid groups located on the alginate. In this embodiment, hydrolysis of the ester group *in vivo* releases dexamethasone at a low dose over an extended period of time.

Reactions and strategies useful for the covalent attachment of anti-inflammatory agents to hydrogel forming polymers are known in the art. See, for example, March, "Advanced Organic Chemistry," 5th Edition, 2001, Wiley-Interscience Publication, New York) and Hermanson, "Bioconjugate Techniques," 1996, Elsevier Academic Press, U.S.A. Appropriate methods for the covalent attachment of a given anti-inflammatory agent can be selected in view of the linking moiety desired, as well as the structure of the anti-inflammatory agents and hydrogel forming polymers as a whole as it relates to compatibility of functional groups, protecting group strategies, and the presence of labile bonds.

E. Anti-inflammatory and Anti-Proliferative Drugs

Drugs suitable for use in the disclosed compositions are described and can be identified using disclosed methods. Representative drugs include glucocorticoids, phenolic antioxidants, anti-proliferative drugs, or combinations thereof. These are collectively referred to herein as "anti-inflammatory drugs" unless stated otherwise.

Non-limiting examples include steroidal anti-inflammatories. Particularly preferred steroidal anti-inflammatory drugs include dexamethasone, 5-FU, daunomycin, and mitomycin. Anti-angiogenic or anti-proliferative drugs are also useful. Examples include curcumins including monoesters and tetrahydrocurcumin, and drugs such as sirolimus (rapamycin),

ciclosporin, tacrolimus, doxorubicin, mycophenolic acid and paclitaxel and derivatives thereof. In some embodiments, the anti-inflammatory drug is an mTOR inhibitor (e.g., sirolimus and everolimus). A new antiproliferative drug is biolimus A9, a highly lipophilic, semisynthetic sirolimus analogue with an alkoxy-alkyl group replacing hydrogen at position 42- O. Lisofylline is a synthetic small molecule with anti-inflammatory properties. In some embodiments, the anti-inflammatory drug is a calcineurin inhibitor (e.g., cyclosporine, pimecrolimus and tacrolimus).

In some embodiments, the anti-inflammatory drug is a synthetic or natural anti-inflammatory protein. Antibodies specific to select immune components can be added to immunosuppressive therapy. In some embodiments, the anti-inflammatory drug is an anti-T cell antibody (e.g., anti-thymocyte globulin or Anti-lymphocyte globulin), anti-IL-2Rα receptor antibody (e.g., basiliximab or daclizumab), or anti-CD20 antibody (e.g.., rituximab).

In preferred embodiments, the one or more anti-inflammatory drugs are released from the capsules after administration to a mammalian subject in an amount effective to inhibit fibrosis of the composition for at least 30 days, preferably at least 60 days, more preferably at least 90 days. In some embodiments, the anti-inflammatory drugs provide spatially localized inhibition of inflammation in the subject without systemic immunosuppression for at least 10 days, preferably at least 14 days, more preferably at least 30 days. In some embodiments, spatially localized inflammation is detected by measuring cathepsin activity at the injection sites in the subject. In other embodiments, spatially localized inflammation is detected by measuring reactive oxygen species (ROS) at the injection site in the subject. In some embodiments, systemic immunosuppression is detected by measuring no cathepsin activity or ROS at control sites in the subject, e.g., sites injected with drug-free polymeric particle or hydrogel. Methods for identifying, selecting, and optimizing anti-inflammatory drugs for use in the disclosed compositions are described below.

The release rate and amounts can be selected in part by modifying drug loading of the polymeric particle. As disclosed herein, higher drug loading can cause a significant initial burst release. This can also result in systemic immunosuppression rather than spatially localized inhibition of inflammation. In contrast, drug loading levels that are too low will not release therapeutically effective amounts of anti-inflammatory drug.

The optimal drug loading will necessarily depend on many factors, including the choice of drug, polymer, hydrogel, cell, and site of implantation. In some embodiments, the one or more anti-inflammatory drugs are loaded in the polymeric particle at a concentration of about 0.01% to about 15%, preferably about 0.1% to about 5%, more preferably about 1% to about 3% by weight. In some embodiments, the one or more anti-inflammatory drugs are encapsulated in the hydrogel at a concentration of 0.01 to 10.0 mg/ml of hydrogel, preferably 0.1 to 4.0 mg/ml of hydrogel, more preferably 0.3 to 2.0 mg/ml of hydrogel. However, optimal drug loading for any given drug, polymer, hydrogel, cell, and site of transplantation can be identified by routine methods, such as those described herein.

F. Biodegradable Polymers for Drug Delivery

The drug-loaded particles containing anti-inflammatory drugs are preferably formed from a biocompatible, biodegradable polymer suitable for drug delivery. In general, synthetic polymers are preferred, although natural polymers may be used and have equivalent or even better properties, especially some of the natural biopolymers which degrade by hydrolysis, such as some of the polyhydroxyalkanoates.

Representative synthetic polymers include poly(hydroxy acids) such as poly(lactic acid), poly(glycolic acid), and poly(lactic acid-co-glycolic acid), poly(lactide), poly(glycolide), poly(lactide-co-glycolide), polyanhydrides, polyorthoesters, polyamides, polycarbonates, polyalkylenes such as polyethylene and polypropylene, polyalkylene glycols such as poly(ethylene glycol), polyalkylene oxides such as poly(ethylene oxide), polyalkylene terepthalates such as poly(ethylene terephthalate), polyvinyl alcohols, polyvinyl ethers, polyvinyl esters, polyvinyl halides such as poly(vinyl

chloride), polyvinylpyrrolidone, polysiloxanes, poly(vinyl alcohols), poly(vinyl acetate), polystyrene, polyurethanes and co-polymers thereof, derivativized celluloses such as alkyl cellulose, hydroxyalkyl celluloses, cellulose ethers, cellulose esters, nitro celluloses, methyl cellulose, ethyl cellulose, hydroxypropyl cellulose, hydroxy-propyl methyl cellulose, hydroxybutyl methyl cellulose, cellulose acetate, cellulose propionate, cellulose acetate butyrate, cellulose acetate phthalate, carboxylethyl cellulose, cellulose triacetate, and cellulose sulfate sodium salt (jointly referred to herein as "synthetic celluloses"), polymers of acrylic acid, methacrylic acid or copolymers or derivatives thereof including esters, poly(methyl methacrylate), poly(ethyl methacrylate), poly(butylmethacrylate), poly(isobutyl methacrylate), poly(hexylmethacrylate), poly(isodecyl methacrylate), poly(lauryl methacrylate), poly(phenyl methacrylate), poly(methyl acrylate), poly(isopropyl acrylate), poly(isobutyl acrylate), and poly(octadecyl acrylate) (jointly referred to herein as "polyacrylic acids"), poly(butyric acid), poly(valeric acid), and poly(lactide-co-caprolactone), copolymers and blends thereof. As used herein, "derivatives" include polymers having substitutions, additions of chemical groups and other modifications routinely made by those skilled in the art.

Examples of preferred biodegradable polymers include polymers of hydroxy acids such as lactic acid and glycolic acid, and copolymers with PEG, polyanhydrides, poly(ortho)esters, polyurethanes, poly(butyric acid), poly(valeric acid), poly(lactide-co-caprolactone), blends and copolymers thereof.

Examples of preferred natural polymers include proteins such as albumin, collagen, gelatin and prolamines, for example, zein, and polysaccharides such as alginate, cellulose derivatives and polyhydroxyalkanoates, for example, polyhydroxybutyrate. The *in vivo* stability of the particles and microparticles can be adjusted during the production by using polymers such as poly(lactide-co-glycolide) copolymerized with PEG.

In the most preferred embodiment, PLGA is used as the biodegradable polymer. PLGA particles and microparticles are designed to release molecules to be encapsulated or attached over a period of days to weeks. Factors that affect the duration of release include pH of the surrounding medium (higher rate of release at pH 5 and below due to acid catalyzed hydrolysis of PLGA) and polymer composition. Aliphatic polyesters differ in hydrophobicity and that in turn affects the degradation rate. For example, the hydrophobic poly (lactic acid) (PLA), more hydrophilic poly (glycolic acid) PGA and their copolymers, poly (lactide-co-glycolide) (PLGA) have various release rates. The degradation rate of these polymers, and often the corresponding drug release rate, can vary from days (PGA) to months (PLA) and is easily manipulated by varying the ratio of PLA to PGA.

The diameter and porosity of the drug-loaded particle can be optimized based on the drug to be delivered and the desired dosage and rate of release. In preferred embodiments, the drug-loaded particle is a microparticle or a nanoparticle. In more preferred embodiments, the drug-loaded particle is a particle. The mean diameter of the particle may be selected and optimized based on the particular drug, dosage, and release rate needed. In preferred embodiments, the drug loaded polymeric particles are microparticles having a mean diameter of about 1μm to about 100μm, preferably about 1μm to about 50μm, more preferably about 1μm to about 10μm. In other embodiments, drug loaded polymeric particles are nanoparticles having a mean diameter of about 10nm to about 999nm, including at least about 50nm, preferably at least about 100nm, more preferably at least about 200nm. In more preferred embodiments, the drug-loaded polymeric particles have a mean diameter that is greater than 1 mm, preferably 1.5 mm or greater. In some embodiments, the drug-loaded polymeric particles can be as large at 8 mm in diameter.

G. Capsules

The capsules are two or three layer capsules. Preferably the capsules have a mean diameter that is greater than 1 mm, preferably 1.5 mm or greater. In some embodiments, the capsules can be as large at 8 mm in diameter. For example, the capsule can be in a size range of 1 mm to 8 mm, 1 mm to 6 mm,

1 mm to 5 mm, 1 mm to 4 mm, 1 mm to 3 mm, 1 mm to 2 mm, 1 mm to 1.5 mm, 1.5 mm to 8 mm, 1.5 mm to 6 mm, 1.5 mm to 5 mm, 1.5 mm to 4 mm, 1.5 mm to 3 mm, or 1.5 mm to 2 mm.

The rate of molecules entering the capsule necessary for cell viability and the rate of therapeutic products and waste material exiting the capsule membrane are selected by modulating macrocapsule permeability. Macrocapsule permeability is also modified to limit entry of immune cells, antibodies, and cytokines into the capsule or microcapsule.

It has been shown that, since different cell types have different metabolic requirements, the permeability of the membrane has to be optimized based on the cell type encapsulated in the hydrogel. The diameter of the capsules or microcapsules is an important factor that influences both the immune response towards the cell capsules as well as the mass transport across the capsule membrane.

H. Cells

The cell type chosen for encapsulation in the disclosed compositions depends on the desired therapeutic effect. The cells may be from the patient (autologous cells), from another donor of the same species (allogeneic cells), or from another species (xenogeneic). Xenogeneic cells are easily accessible, but the potential for rejection and the danger of possible transmission of viruses to the patient restricts their clinical application. Anti-inflammatory drugs combat the immune response elicited by the presence of such cells. In the case of autologous cells, the anti-inflammatory drugs reduce the immune response provoked by the presence of the foreign hydrogel materials or due to the trauma of the transplant surgery. Cells can be obtained from biopsy or excision of the patient or a donor, cell culture, or cadavers.

In some embodiments, the cells secrete a therapeutically effective substance, such as a protein or nucleic acid. In some embodiments, the cells metabolize toxic substances. In some embodiments, the cells form structural tissues, such as skin, bone, cartilage, blood vessels, or muscle. In some embodiments, the cells are natural, such as islet cells that naturally secrete insulin, or hepatocytes that naturally detoxify. In some embodiments, the cells

are genetically engineered to express a heterologous protein or nucleic acid and/or overexpress an endogenous protein or nucleic acid.

Examples of cells for encapsulation include hepatocytes, islet cells, parathyroid cells, cells of intestinal origin, cells derived from the kidney, and other cells acting primarily to synthesize and secret, or to metabolize materials. A preferred cell type is a pancreatic islet cell. Genetically engineered cells are also suitable for encapsulation according to the disclosed methods. In some embodiments, the cells are engineered to secrete blood clotting factors, e.g., for hemophilia treatment, or to secrete growth hormones for treatment of individuals who are genetically deficient. Alternatively, the cells may be engineered to produce substances that are targeted to cancers or other deleterious materials. In some embodiments, the cells are contained in natural or bioengineered tissue. In some embodiments, the cells are suitable for transplantation into the central nervous system for treatment of neurodegenerative disease.

The amount and density of cells encapsulated in the disclosed compositions, such as capsules and microcapsules, will vary depending on the choice of cell, hydrogel, and site of implantation. In some embodiments, the single cells are present in the hydrogel at a concentration of 0.1 $x10^6$ to 4 $x10^6$ cells/ml, preferably 0.5 $x10^6$ to 2 x 10^6 cells/ml. In other embodiments, the cells are present as cell aggregates. For example, islet cell aggregates (or whole islets) preferably contain about 1500-2000 cells for each aggregate of 150μm diameter, which is defined as one islet equivalent (IE). Therefore, in some embodiments, islet cells are present at a concentration of 100-10000 IE/ml, preferably 200-3,000 IE/ml, more preferably 500-1500 IE/ml.

1. Islet Cells

In preferred embodiments, the disclosed compositions contain islet cells producing insulin. Methods of isolating pancreatic islet cells are known in the art. Field et al., *Transplantation* 61:1554 (1996); Linetsky et al., *Diabetes* 46:1120 (1997). Fresh pancreatic tissue can be divided by mincing, teasing, comminution and/or collagenase digestion. The islets can then be isolated from contaminating cells and materials by washing, filtering,

centrifuging or picking procedures. Methods and apparatus for isolating and purifying islet cells are described in U.S. Patent Nos. 5,447,863 to Langley, 5,322,790 to Scharp et al., 5,273,904 to Langley, and 4,868,121 to Scharp et al., The isolated pancreatic cells may optionally be cultured prior to encapsulation or microencapsulation, using any suitable method of culturing islet cells as is known in the art. See e.g., U.S. Patent No. 5,821,121 to Brothers. Isolated cells may be cultured in a medium under conditions that helps to eliminate antigenic components.

2. Genetically Engineered Cells

In some embodiments, the disclosed compositions contain cells genetically engineered to produce a therapeutic protein or nucleic acid. In these embodiments, the cell can be a stem cell (e.g., pluripotent), a progenitor cell (e.g., multipotent or oligopotent), or a terminally differentiated cell (i.e., unipotent). The cell can be engineered to contain a nucleic acid encoding a therapeutic polynucleotide such miRNA or RNAi or a polynucleotide encoding a protein. The nucleic acid can be integrated into the cells genomic DNA for stable expression or can be in an expression vector (e.g., plasmid DNA). The therapeutic polynucleotide or protein can be selected based on the disease to be treated and the site of transplantation. In some embodiments, the therapeutic polynucleotide or protein is anti-neoplastic. In other embodiments, the therapeutic polynucleotide or protein is a hormone, growth factor, or enzyme.

III. Methods of Making Capsule

A. Method for Making Bi and Tri-layer Capsules

Triple layer capsules can be made by a tri-fluid coaxial electrospraying process.

Preferably the three layer capsules are formed in an electrospraying device with a nozzle that consists of three separate concentric tubes at its outlet. An exemplary nozzle (100) is illustrated in Figure 2. A first stream that contains a hydrogel forming material, optionally including one or more anti-inflammatory drugs or imaging reagents, is pumped into the innermost tube (110) of the nozzle. A second stream that contains hydrogel forming

material and islets is pumped into the middle tube (112) of the nozzle. A third stream that contains a hydrogel forming material is delivered to the outermost tube (114).

The three streams meet at the outlet of the nozzle. The relatively high viscosity of the alginate solution prevents any significant intermixing among the three streams and droplets with three distinct concentric layers are formed under the electric field. After the droplets fall into the gel bath which contains divalent ions such as Calcium or Barium ions, crosslinking occurs instantaneously and triple-layer capsules are formed. The triple layer capsules can be made by a tri-fluid coaxial electrospraying.

For example, a stream that contains anti-inflammatory drugs or imaging reagents is pumped into the innermost tube; a second stream that contains islets is pumped into the middle tube; and another stream is delivered to the outermost tube. The three streams meet at the outlet of the nozzle. The relatively high viscosity of the alginate solution prevents any significant intermixing among the three streams and droplets with three distinct concentric layers are formed under the electric field. After the droplets fall into the gel bath which contains divalent ions such as Calcium or Barium ions, crosslinking occurs instantaneously and triple-layer capsules are formed.

B. Methods for Making Two Layer Capsules

Two-fluid co-axial electro-jetting is used for the fabrication of core–shell capsules and encapsulation of cells or cell aggregates. In the preferred embodiment, the shell fluid consists of a cell-free alginate solution, while the core fluid contains the islets or other therapeutic cells. The relatively high viscosity of the two fluids and short interaction time between them prevent their intermixing. Under electrostatic force, microdroplets with core–shell structures are formed and converted to hydrogel capsules in a gelling bath containing divalent crosslinking ions.

C. Cell Encapsulation with Polysaccharide Hydrogel

Methods for encapsulating cells in hydrogels are known. In preferred embodiments, the hydrogel is a polysaccharide. For example, methods for

encapsulating mammalian cells in an alginate polymer are well known and briefly described below. See, for example, U.S. Patent No. 4,352,883 to Lim.

Alginate can be ionically cross-linked with divalent cations, in water, at room temperature, to form a hydrogel matrix. An aqueous solution containing the biological materials to be encapsulated is suspended in a solution of a water soluble polymer, the suspension is formed into droplets which are configured into discrete capsules or microcapsules by contact with multivalent cations, then the surface of the capsules or microcapsules is crosslinked with polyamino acids to form a semipermeable membrane around the encapsulated materials.

The water soluble polymer with charged side groups is crosslinked by reacting the polymer with an aqueous solution containing multivalent ions of the opposite charge, either multivalent cations if the polymer has acidic side groups or multivalent anions if the polymer has basic side groups. The preferred cations for cross-linking of the polymers with acidic side groups to form a hydrogel are divalent and trivalent cations such as copper, calcium, aluminum, magnesium, strontium, barium, and tin, although di-, tri- or tetra-functional organic cations such as alkylammonium salts, e.g., $R_3N+--\backslash/\backslash/--+NR_3$ can also be used. Aqueous solutions of the salts of these cations are added to the polymers to form soft, highly swollen hydrogels and membranes. The higher the concentration of cation, or the higher the valence, the greater is the degree of cross-linking of the polymer. Concentrations from as low as 0.005 M have been demonstrated to cross-link the polymer. Higher concentrations are limited by the solubility of the salt.

The preferred anions for cross-linking of polymers containing basic side chains to form a hydrogel are divalent and trivalent anions such as low molecular weight dicarboxylic acids, for example, terepthalic acid, sulfate ions and carbonate ions. Aqueous solutions of the salts of these anions are added to the polymers to form soft, highly swollen hydrogels and membranes, as described with respect to cations.

A variety of polycations can be used to complex and thereby stabilize the polymer hydrogel into a semi-permeable surface membrane. Examples of

materials that can be used include polymers having basic reactive groups such as amine or imine groups, having a preferred molecular weight between 3,000 and 100,000, such as polyethylenimine and polylysine. These are commercially available. One polycation is poly(L-lysine); examples of synthetic polyamines are: polyethyleneimine, poly(vinylamine), and poly(allyl amine). There are also natural polycations such as the polysaccharide, chitosan.

Polyanions that can be used to form a semi-permeable membrane by reaction with basic surface groups on the polymer hydrogel include polymers and copolymers of acrylic acid, methacrylic acid, and other derivatives of acrylic acid, polymers with pendant SO_3H groups such as sulfonated polystyrene, and polystyrene with carboxylic acid groups.

In a preferred embodiment, alginate capsules are fabricated from solution of alginate containing suspended cells using the encapsulator (such as an Inotech encapsulator). In some embodiments, alginates are ionically crosslinked with a polyvalent cation, such as Ca^{2+}, Ba^{2+}, or Sr^{2+}. In particularly preferred embodiments, the alginate is crosslinked using $BaCl_2$. In some embodiments, the capsules are further purified after formation. In preferred embodiments, the capsules are washed with, for example, HEPES solution, Krebs solution, and/ or RPMI-1640 medium.

Cells can be obtained directly from a donor, from cell culture of cells from a donor, or from established cell culture lines. In the preferred embodiments, cells are obtained directly from a donor, washed and implanted directly in combination with the polymeric material. The cells are cultured using techniques known to those skilled in the art of tissue culture.

Cell attachment and viability can be assessed using standard techniques, such as histology and fluorescent microscopy. The function of the implanted cells can be determined using a combination of the above-techniques and functional assays. For example, in the case of hepatocytes, *in vivo* liver function studies can be performed by placing a cannula into the recipient's common bile duct. Bile can then be collected in increments. Bile pigments can be analyzed by high pressure liquid

chromatography looking for underivatized tetrapyrroles or by thin layer chromatography after being converted to azodipyrroles by reaction with diazotized azodipyrroles ethylanthranilate either with or without treatment with P-glucuronidase. Diconjugated and monoconjugated bilirubin can also be determined by thin layer chromatography after alkalinemethanolysis of conjugated bile pigments. In general, as the number of functioning transplanted hepatocytes increases, the levels of conjugated bilirubin will increase. Simple liver function tests can also be done on blood samples, such as albumin production. Analogous organ function studies can be conducted using techniques known to those skilled in the art, as required to determine the extent of cell function after implantation. For example, islet cells of the pancreas may be delivered in a similar fashion to that specifically used to implant hepatocytes, to achieve glucose regulation by appropriate secretion of insulin to cure diabetes. Other endocrine tissues can also be implanted.

The site, or sites, where cells are to be implanted is determined based on individual need, as is the requisite number of cells. For cells having organ function, for example, hepatocytes or islet cells, the mixture can be injected into the mesentery, subcutaneous tissue, retroperitoneum, properitoneal space, and intramuscular space.

When desired, the capsules or microcapsules may be treated or incubated with a physiologically acceptable salt such as sodium sulfate or like agents, in order to increase the durability of the capsules or microcapsule, while retaining or not unduly damaging the physiological responsiveness of the cells contained in the capsules or microcapsules. By "physiologically acceptable salt" is meant a salt that is not unduly deleterious to the physiological responsiveness of the cells encapsulated in the capsules or microcapsules. In general, such salts are salts that have an anion that binds calcium ions sufficiently to stabilize the capsule, without substantially damaging the function and/or viability of the cells contained therein. Sulfate salts, such as sodium sulfate and potassium sulfate, are preferred, and sodium sulfate is most preferred. The incubation step is carried out in an aqueous solution containing the physiological salt in an amount effective to stabilize

the capsules, without substantially damaging the function and/or viability of the cells contained therein as described above. In general, the salt is included in an amount of from about 0.1 or 1 milliMolar up to about 20 or 100 millimolar, most preferably about 2 to 10 millimolar. The duration of the incubation step is not critical, and may be from about 1 or 10 minutes to about 1 or 2 hours, or more (e.g., overnight). The temperature at which the incubation step is carried out is likewise not critical, and is typically from about 4°C up to about 37°C, with room temperature (about 21°C) preferred.

IV. Treatment of Diseases or Disorders

Encapsulated cells can be administered, e.g., injected or transplanted, into a patient in need thereof to treat a disease or disorder. In some embodiments, the disease or disorder is caused by or involves the malfunction of hormone- or protein-secreting cells in a patient. In these embodiments, hormone- or protein-secreting cells are encapsulated and administered to the patient. For example, encapsulated islet cells can be administered to a patient with diabetes. In other embodiments, the cells are used to repair tissue in a subject. In these embodiments, the cells form structural tissues, such as skin, bone, cartilage, muscle, or blood vessels. In these embodiments, the cells are preferably stem cells or progenitor cells.

Also disclosed are methods of treating a subject by (a) providing a first administration of an effect of amount of a preparation as disclosed herein, which provides a therapeutic effect for at least Z days; and (b) administering a subsequent administration of an effect of amount of the preparation of claim 1, provided that wherein at least Z-10, Z-5, Z days separate the first and subsequent administration, and no interim administration is provided. In some forms, Z is at least 14, 30, 60, or 90 days.

Also disclosed are methods of treating a subject by providing a subject who has had a first administration of an effect of amount of a preparation as disclosed herein a subsequent administration of an effect of amount of the preparation of claim 1, provided that subsequent administration occurs at least Z-10, Z-5, Z days after the first administration. In some forms, Z is at least 14, 30, 60, or 90 days.

1. Diabetes

The potential of using a bioartificial pancreas for treatment of diabetes mellitus based on encapsulating islet cells within a semi permeable membrane is extensively being studied by scientists. Microencapsulation protects islet cells from immune rejection and allows the use of animal cells or genetically modified insulin-producing cells.

The Edmonton protocol involves implantation of human islets extracted from cadaveric donors and has shown improvements towards the treatment of type 1 diabetics who are prone to hypoglycemic unawareness. However, the two major hurdles faced in this technique are the limited availability of donor organs and the need for immunosuppressants to prevent an immune response in the patient's body.

Several studies have been dedicated towards the development of bioartificial pancreas involving the immobilization of islets cells inside polymeric capsules. The first attempt towards this aim was demonstrated in 1980 by Lim et al where xenograft islet cells were encapsulated inside alginate polylysine microcapsules, which resulted in significant *in vivo* results for several weeks.

The polymers typically used for islet microencapsulation are alginate, chitosan, polyethylene glycol (PEG), agarose, sodium cellulose sulfate and water insoluble polyacrylates.

2. Cancer

The use of cell encapsulated microcapsules towards the treatment of several forms of cancer has shown great potential. One approach undertaken by researchers is through the implantation of microcapsules containing genetically modified cytokine secreting cells. Genetically modified IL-2 cytokine secreting non-autologous mouse myoblasts implanted into mice delay tumor growth with an increased rate of survival of the animals. However, the efficiency of this treatment was brief due to an immune response towards the implanted microcapsules. Another approach to cancer suppression is through the use of angiogenesis inhibitors to prevent the release of growth factors that lead to the spread of tumors. Genetically modified cytochrome

P450 expressing cells encapsulated in cellulose sulfate polymers may also be useful for the treatment of solid tumors.

3. Heart Diseases

While numerous methods have been studied for cell administration to enable cardiac tissue regeneration in patients after ischemic heart disease, the efficiency of the number of cells retained in the beating heart after implantation is still very low. A promising approach to overcome this problem is through the use of cell microencapsulation therapy which has shown to enable a higher cell retention as compared to the injection of free stem cells into the heart.

Another strategy to improve the impact of cell based encapsulation technique towards cardiac regenerative applications is through the use of genetically modified stem cells capable of secreting angiogenic factors such as vascular endothelial growth factor (VEGF), which stimulate neovascularization and restore perfusion in the damaged ischemic heart.

4. Liver Diseases

Microencapsulated hepatocytes can be used in a bioartificial liver assist device (BLAD). Acute liver failure (ALF) is a medical emergency which, despite improvements in modern intensive care, still carries a substantial mortality rate. In the most severe cases, urgent orthotopic liver transplantation (OLT) currently represents the only chance for survival. However, the supply of donor organs is limited and an organ may not become available in time. An effective temporary liver support system would improve the chance of survival in this circumstance by sustaining patients until a donor liver becomes available. Furthermore, the known capacity of the native liver to regenerate following recovery from ALF raises the possibility that the use of temporary liver support for a sufficient period of time may even obviate the need for OLT in at least some cases.

In some embodiments, hepatocytes are encapsulated in capsule or microcapsule having an inner core of modified collagen and an outer shell of terpolymer of methyl methacrylate (MMA), methacrylate (MAA) and

hydroxyethyl methacrylate (HEMA) (Yin C et al., Biomaterials 24:1771–1780 (2003)).

Cell lines which have been employed or are currently undergoing investigation for use in bioartificial liver support systems include primary hepatocytes isolated from human or animal livers, and various transformed human cells, such as hepatoma, hepatoblastoma and immortalized hepatocyte lines.

The present invention will be further understood by reference to the following non-limiting examples.

The examples demonstrate the formation of core-shell alginate based capsules and microcapsules, which demonstrate that it is possible to isolate the cells within the hydrogel capsules, preventing the cells from being detected by immune cells in the body (Example 1) and that larger, greater than 1 mm in diameter, hydrogel capsules, evoke less of a fibrotic reaction than the same hydrogel capsules having a smaller diameter (Example 2).

EXAMPLES

Example 1: Preparation of Core-Shell Alginate based microcapsules.

Materials and Methods

Design of Core–Shell Nozzle and Formation of Core–Shell Capsules:

A type of alginate-based hydrogel microcapsules with core–shell structures using a two-fluid co-axial electro-jetting that is compatible with the current alginate-based cell encapsulation protocols was developed. The composition and thickness of the core and shell can be independently designed and controlled for many types of biomedical applications. Figures 3A and 3B are schematic depictions of a conventional cell encapsulation approach (Figure 3A) and a two-fluid co-axial electro-jetting for core–shell capsules and cell encapsulation (Figure 3B). Figure 3B shows a schematic of the two-fluid co-axial electro-jetting for the fabrication of core–shell capsules and encapsulation of cells or cell aggregates. This two-fluid configuration was used to make core–shell hydrogel capsules and encapsulate living cells.

The shell fluid consists of a cell-free alginate solution, while the core fluid contains the islets or other therapeutic cells. The relatively high viscosity

of the two fluids and short interaction time between them prevent their intermixing. Under electrostatic force, microdroplets with core–shell structures are formed and converted to hydrogel capsules in the gelling bath.

First, to demonstrate the formation of core–shell hydrogel capsules, a fluorescently labeled alginate was used to form the shell and a non-labeled alginate was used to form the core. The thicknesses of the core and shell can be controlled by simply tuning their respective flow rates. For cell encapsulation, the size of the core can then be designed based on the desired mass of cells per capsule, while that of the shell can be adjusted according to the requirements of mechanical strength and mass transfer. The compositions of the core and shell are also adjustable. This allows independent optimization of the material in direct contact with the encapsulating cells and the one adjacent to the host immune system when transplanted. For example, an anti-inflammatory drug or an imaging contrast reagent (e.g., iron oxide nanoparticles) can be loaded in the shell without contacting the cells in the core. It is also possible to put a different material such as Matrigel as the core inside the alginate shell. The core material, which may not be able to form mechanically robust capsules alone, can then provide a preferred local environment for the encapsulated cells.

The design of the co-axial nozzle was critical to the stable formation of uniform core–shell structures of the capsules, and complete encapsulation of islets. First, the nozzle must be concentric; any eccentricity may cause non-uniform flow of the shell fluid surrounding the core fluid, disturbing the core–shell structure. Second, the nozzle must be designed in a way that the flow of the shell fluid inside the nozzle is uniform around the core tube. Third, the inner diameter of the core tube must accommodate the sizes of islets. The co-axial nozzle has a core tube with an ID of 0.014” and an OD of 0.022” and a shell tube with an ID of 0.04” and an OD of 0.0625”. The length of the shell tube that protrudes from the nozzle body is 0.5” and was tapered at the outlet tip. The core tube was placed 100 microns inward relative to the shell tube at the outlet. The flow rates of the core and shell fluids were independently

adjusted by separate syringe pumps. The voltage was 6.2 kV and the distance between the nozzle tip and the surface of gelling solution was 1.8 cm.

To optimize encapsulation, the solution concentration of alginate with given molecular weight must be optimized. If both the concentrations of the core and shell solutions are too small, there will be significant intermixing between the core and shell solutions leading to non-uniform core–shell structures. For the PRONOVA SLG20 alginate (Mw approximately 75-220,000, FMC Biopolymer), it was found the optimal concentration ranges were from 0.8% (w/v) to 2% (w/v). All alginate solutions were at 1.4% (w/v) and the Matrigel (BD Biosciences) was used at 4 mg/mL in a 4 °C cold room to avoid gelling prior to encapsulation. Besides the properties of the core and shell solutions, optimization of operating parameters was also important to obtain ideal encapsulation. Typical flow rates were 0.005 mL/min to 0.1 mL/min for the core flow and 0.1 mL/min to 0.5 mL/min for the shell flow.

Rat Islet Isolation and Purification:

Sprague-Dawley rats from Charles River Laboratories weighting approximately 300 grams were used for harvesting islets. All rats were anesthetized by a 1:20 Xylazine (10 mg/ kg) to Ketamine (150 mg/kg) injection given intraperitoneally, and the total volume of each injection was 0.4–0.5 mL depending on the weight of rat. Isolation surgeries were performed. Briefly, the bile duct was cannulated and the pancreas was distended by an *in vivo* injection of 0.15% Liberase (Research Grade, Roche) in RPMI 1640 media solution. Rats were sacrificed by cutting the descending aorta and the distended pancreatic organs were removed and held in 50 mL conical tubes on ice until the completion of all surgeries. All tubes were placed in a 37 °C water bath for a 30 minute digestion, which was stopped by adding 10-15 mL of cold M199 media with 10% heat-inactivated fetal bovine serum and lightly shaking. Digested pancreases were washed twice in the same aforementioned M199 media, filtered through a 450 μm sieve, and then suspended in a Histopaque 1077 (Sigma)/M199 media gradient and centrifuged at 1,700 RCF at 4 °C. Depending on the thickness of the islet layer that was formed within the gradient, this step was repeated for higher purity

islets. Finally, the islets were collected from the gradient and further isolated by a series of six gravity sedimentations, in which each supernatant was discarded after four minutes of settling. Purified islets were hand-counted by aliquot under a light microscope and then washed three times in sterile 1X phosphate-buffered saline. Islets were then washed once in RPMI 1640 media with 10% heat-inactivated fetal bovine serum and 1% penicillin/streptomycin, and cultured in this media overnight for further use.

Liver Tissue Homogenization and Encapsulation:

Liver was obtained from sacrificed rats by dissecting the liver from the hepatic portal, system vessels and connective tissue. It was placed into a 0.9% NaCl solution and minced using surgical forceps and scissors in a petri dish. These pieces were washed with 0.9% saline twice to remove blood and then dissociated using a gentle MACS Dissociator (Miltenyi Biotec). After dissociation, the tissue sample was filtered through a 100 μm cell strainer and subsequently a 40 μm one. This filtration was repeated once more to obtain liver tissue cells for encapsulation. For single-fluid encapsulation, 0.06 mL dissociated liver tissue cells were dispersed in 4.5 mL 1.4% SLG20 alginate solution. For the two-fluid coaxial encapsulation, 0.06 mL dissociated liver cells were dispersed in 0.5 mL 1.4% SLG20 alginate solution that was used as the core fluid. A separate 4 mL 1.4% alginate solution was used as the shell.

Islets Encapsulation and Transplantation:

Immediately prior to encapsulation, the cultured islets were centrifuged at 1400 rpm for 1 minute and washed with Ca-Free Krebs-Henseleit (KH) Buffer (4.7 mM KCl, 25 mM HEPES, 1.2 mM KH_2PO_4, 1.2 mM $MgSO_4 \times 7H_2O$, 135 mM NaCl, pH approximately 7.4, osmotic pressure approximately 290 mOsm). After the wash, the islets were centrifuged again and all supernatant was aspirated. The islet pellet was then re-suspended in a 1.4% solution of SLG20 alginate dissolved in 0.8% NaCl solution at desired islet number density. In the case of the regular capsules, 0.27 mL alginate solution was used for every 1000 islets. For the core–shell capsules, 0.03 mL solution for every 1000 islets was used as the core fluid. Another 0.24 mL 1.4% alginate solution without islets was used as the shell

fluid. The flow rate for the shell was 0.2 mL/min and that for the core was 0.025 mL/min. For the same number of islets, the total volume of the alginate solution used in both regular encapsulation and core–shell encapsulation was therefore the same. Capsules were crosslinked using a $BaCl_2$ gelling solution (20 mM BaCl2, 250mM D-Mannitol, 25mM HEPES, pH ~ 7.4, osmotic pressure approximately 290 mOsm). Immediately after crosslinking, the encapsulated islets were washed 4 times with HEPES buffer and 2 times with RPMI Medium 1640 and cultured overnight at 37°C for transplantation. As the islets had variable sizes (50 – 400 μm) and there was an inevitable loss of islets during the encapsulation process, the total number of encapsulated islets were recounted and converted into islet equivalents (IE, normalized to 150 μm size) prior to transplantation.

Immune-competent male C57BL/6 mice were utilized for transplantation. To create insulin-dependent diabetic mice, healthy C57BL/6 mice were treated with Streptozocin (STZ) by the vendor (Jackson Laboratory, Bar Harbor, ME) prior to shipment to MIT. The blood glucose levels of all the mice were retested prior to transplantation. Only mice whose non-fasted blood glucose levels were above 300 mg/ dL for two consecutive days were considered diabetic and underwent transplantation. The mice were anesthetized using 3% isofluorane in oxygen and maintained at the same rate throughout the procedure. Preoperatively, all mice received a 0.05 mg/kg dose of buprenorphine subcutaneously as a pre-surgical analgesic, along with 0.3 mL of 0.9% saline subcutaneously to prevent dehydration. The abdomens of the mice were shaved and alternately scrubbed with betadine and isopropyl alcohol to create a sterile field before being transferred to the surgical field. A 0.5 mm incision was made along the midline of the abdomen and the peritoneum was exposed using blunt dissection. The peritoneum was then grasped with forceps and a 0.5–1 mm incision was made along the linea alba. A desired volume of capsules with predetermined number of islet equivalents were then loaded into a sterile pipette and transplanted into the peritoneal cavity through the incision. The incision was then closed using 5-0 taper

tipped polydioxanone (PDS II) absorbable sutures. The skin was then closed over the incision using a wound clip and tissue glue.

All animal protocols were approved by the MIT Committee on Animal Care and all surgical procedures and post-operative care were supervised by MIT Division of Comparative Medicine veterinary staff.

Confocal Imaging of Encapsulated Islets:

Pancreatic islets were stained with Hoechst dye (2 μg/mL) and encapsulated in fluorescent, regular capsules or core–shell capsules with a fluorescently labeled shell. The capsules were placed on chambered glass coverslips (LabTek) and allowed to settle. The encapsulated islets were then imaged under a 10X objective using a Laser Scanning Confocal Microscope 710 (LSM710). Multiple confocal slices were imaged from bottom to top of sample to construct a Z-stack. An orthogonal image and a 3D rendering were performed using LSM browser software to visualize the islet-containing capsules.

Blood Glucose Monitoring:

Blood glucose levels were monitored three times a week following the transplant surgery. A small drop of blood was collected from the tail vein using a lancet and tested using a commercial glucometer (Clarity One, Clarity Diagnostic Test Group, Boca Raton, FL). Mice with unfasted blood glucose levels below 200 mg/dL were considered normoglycemic. Monitoring continued until all mice in the experimental group had returned to a hyperglycemic state at which point they were euthanized.

Results

Better cell encapsulation using core–shell capsules was demonstrated using both homogenized rat liver tissue cells and rat pancreatic islets. Microscopic images for both regular capsules and core–shell capsules containing islets show a relatively low volume of alginate solution per islet (i.e., 0.27 mL solution for every 1000 islets) used to minimize the total volume of capsules for transplantation. This is approximately a third of the volume that is typically used (deVos et al., Transplantation 1996, 62, 888). For crosslinking, a $BaCl_2$ solution (deVos et al., Transplantation 1996, 62, 888)

was used and the average capsule sizes were both around 500 μm. For regular capsules, the islets were randomly located within the capsules and islets protruding outside were frequently observed. In contrast, the islets in the core–shell capsules were fully encapsulated. The core–shell structure of the capsules was demonstrated by using a fluorescent alginate in the shell and a non-fluorescent alginate in the core. Fluorescent images where the islets were stained blue (i.e. nuclei staining) showed that in some cases the islets were close to the core–shell interface but still completely encapsulated due to the additional shell layer. It is important to note that a confocal microscopy technique was used to confirm the full encapsulation. Conventional microscopic examination may be misleading as the relatively dense islet mass may fall at the bottom of the capsule and in line with the objective. In traditionally formed alginate capsules, the islets appeared fully encapsulated under conventional light microscope. The z-series and orthogonal views using confocal microscopy revealed however the islets were partially exposed outside the capsules. In contrast, the core–shell capsules fully enclosed the islets as viewed from all three directions. Quantitatively, based on examinations of a number of islets-containing capsules using confocal microscopy, the regular capsules had about 30% with protruding islets while the core–shell capsules had none. The hydrogel microcapsules with core–shell structures were formed with a shell of an alginate partially modified with FITC, while the core is unlabeled alginate or Matrigel. The thicknesses of the shell and the core are controlled by tuning their respective flow rates: (a) 0.1 mL/min and 0.1 mL/min; (b) 0.15 mL/min and 0.05 mL/min; (c) 0.2 mL/min and 0.02 mL/min. The compositions of the core and shell can also be independently controlled. (d) The shell alginate contains particles of an anti-inflammatory drug, curcumin. The drug particles are self-fluorescent. The shell is fluorescent alginate and the core is non-fluorescent Matrigel.

Streptozotocin (STZ) - induced diabetic mouse model (Brodsky et al., Diabetes 1969, 18, 606) was used to evaluate the functionality of the coaxially encapsulated islets and compare the efficacy with regular capsules. A comparison was conducted of islets encapsulated in regular capsules and

core–shell capsules. 3D reconstructed confocal fluorescent images of islets encapsulated in core–shell capsules showed the islets were stained blue, while the shell was labeled green.

Encapsulated rat islets were transplanted into the peritoneal cavity of the diabetic mice and their blood sugar was measured. Figure 4A shows the blood glucose level of the mice as a function of days post-transplantation for both core–shell capsules (diamonds) and regular (circles) capsules. For both types of capsules, a density of 1000 islets per 0.27 mL alginate solution was used and each mouse was transplanted with 500 islet equivalents (normalized to 150 μm size). Mice with blood glucose below 200 mg/dL are considered normoglycemic (Kim et al., Lab Chip 2011, 11, 246). A couple of days after transplantation, all diabetic mice became normoglycemic, as expected. However, differences between the two types of capsules started to appear after about 2 weeks, as demonstrated in Figure 4B. The average blood glucose level for the mice receiving regular capsules went back above 200 mg/dL by 15 days, and that of the mice receiving core–shell capsules remained below 200 mg/dL up to 50 days. Figure 4Bb shows the percentage of normoglycemic mice over days following transplantation. Regular capsules in all mice failed to control the diabetes by 20 days, while the core–shell ones in some of the mice did not fail until about 80 days after transplantation, indicating that the core–shell capsules improved the treatment significantly compared with the regular capsules.

In summary, hydrogel microcapsules with core–shell structures and their use for improved cell encapsulation and immuno-protection have been made. Better islet encapsulation using the core–shell capsules at a reduced material volume per islet was demonstrated. Improved immune-protection was achieved in a single step by simply confining the cells or cell aggregates in the core region of the capsules. Both the core–shell structure and better encapsulation were confirmed by confocal microscopy. Using a type I diabetic mouse model, it was shown that the core–shell capsules encapsulating rat islets provided a significantly better treatment than the currently used, regular capsules.

Islet microencapsulation represents a promising approach to treat Type I diabetes and has been a topic of intensive research for decades (Bratlie et al., Adv. Healthcare Mater. 2012, 1, 267). The results from different research groups were often inconsistent. Islet quality and material properties such as biocompatibility are certainly critical factors that affect the outcome of treatment. The quality of encapsulation could also influence the results and cause inconsistency. The core–shell capsules can be made in a single step using the same encapsulation protocols that have been used to make the regular capsules and do no harm to islets. In addition to providing better immuno-protection, the opportunity to control the compositions of the shell and the core provide additional opportunities in microencapsulation. Examples include the replacement of the alginate in the core with a different material that may enhance long-term islet survival. In addition, insulin-producing cells derived from stem cells (Calne et al, Nature Reviews Endocrinology 2010, 6, 173) or adult cells (Zhou, et al., Nature 2008, 455, 627) provide a great alternative to islets. The core–shell capsules allow not only improved encapsulation but also greater freedom in the designs of the encapsulating material in the shell and that in direct contact with the cells in the core.

Example 2: Preparation of Large Two-layer hydrogel capsules (> 1 mm) for encapsulation of therapeutic cells and cell aggregates

Materials and Methods

The method of encapsulation includes two general steps: (a) forming droplets of alginate solution containing islets and (b) conversion of the droplets into hydrogel capsules. Mechanical or electrostatic forces can be used to control the droplet or capsule sizes. The islets can be randomly distributed within the capsules. The islets can also be introduced in the shell region of the capsules to facilitate the mass transfer. This can be achieved by using a two-fluid encapsulation approach where one stream of alginate solutions containing islets serves as the shell fluid and a separate stream of cell-free alginate solution flows in the core. Additional components such as an anti-inflammatory drug can also be incorporated into the core.

Two types of large (D > 1 mm) alginate hydrogel capsules for islets encapsulation were prepared. In the first, islets were dispersed randomly within the capsules. In the second, islets were purposely placed in the shell region of the capsules.

1.5 mm capsules encapsulating rat islets were injected into STZ-induced diabetic mice. The 500 μm capsules were used as the control and 500 IE's were used for both sizes of capsules.

Results

The large size (D > 1 mm) capsules were much less fibrotic and provided much longer cure than conventional (0-500 μm) capsules. The 500 μm capsules were used as the control and 500 IE's were used for both sizes of capsules. All 5 mice in the 500 μm capsule group failed by 43 days (blood glucose above 200 mg/dl for 3 consecutive measurements), while the large capsules lasted much longer. One of the 5 mice failed at 43 days, one failed at 75 days, another one failed at 146 days and the remaining two remained cured at 196 days when the experiment was stopped. All the 5 mice in the 500 μm capsule group failed by 43 days (i.e. BG above 200 mg/dl for 3 consecutive measurements), while the large capsules lasted much longer. One of the 5 mice failed at 43 days, one failed at 75 days, another one failed at 146 days and the rest two remained cured at 196 days when the experiment was stopped.

In a separate follow-up study again with 500 IE's, all eight mice in the 500 μm capsule group failed by 35 days, while in the 1.5 mm capsule group, 1 out of 6 failed at 28 days, 1 failed at 105 days, 1 failed at 134 days, another failed at 137 days, and 2 remaining ones stayed cured at 175 days when the experiment was stopped.

See Figure 5A for 500 micron capsule and Figure 5B for 1.5 mm capsules.

Analysis of retrieved capsules revealed that the 500 um capsules were all fibrosed and clumped but the 1.5 mm capsules were much less fibrotic.

In summary, large hydrogel capsules, with diameter larger than 1 mm, were made by encapsulating cells or cell aggregates, such as islets using materials such as alginate hydrogel. Islets encapsulated in alginate hydrogel

capsules can be transplanted to treat Type I diabetes without the use of immunosuppressive drugs. One major challenge is the fibrotic reactions to the capsules upon transplantation, which eventually leads to necrosis of islets and failure of transplant. The typical diameter of currently used capsules is relatively small, less than 1 mm. It has been discovered that larger capsules have less fibrosis and could therefore have better disease outcomes for clinical uses.

Example 3: Comparison of Fibrotic Effects on Large (> 1 mm) and Small (< 1 mm) hydrogel capsules

The disclosed two or three layer hydrogel capsules are useful for sensor or controlled drug release applications. In some embodiments, the capsules are designed to resist foreign body responses. General characteristics of preferred capsules include: a size larger than 1mm and a spherical shape; a smooth surface with no straight edges; made from hydrophilic material; and capsule can be porous, with pores preferably be less than 1 μm in size. Capsules larger than 1mm effectively resist macrophage cell adhesion. For example, macrophage coverage can be less than 30 % of total capsule surface area. This example shows the reduced fibrotic effect on capsules larger than 1mm. Capsules larger than 1mm effectively resist macrophage and neutrophil adhesion and decrease macrophage and neutrophil recruitment (Figure 6). For example, macrophage and neutrophil levels were assayed by FACS in fibrotic tissue associated with the capsules and was reduced to less than 30% of the levels observed with smaller 300 um capsules (Figure 6). Larger core-shell (multi-layer alginate capsules) were produced using the dual nozzle electro-spray method (illustrated in Figure 1), and they also showed similar reduction in macrophage/neutrophil recruitment and adhesion. This holds true for capsules taken from completely healthy as well as STZ-induced diabetic C57BL/6 mice, throughout many timepoints post-transplantation (e.g., 7, 14, and 28 days, as well as at 1, 6 months, and 1 year). Furthermore, fibrosis was measured by visual inspection of cellular adhesion and fibrotic overgrowth upon phase contrast/brightfield imaging, as well as by confocal imaging and western blotting for F-actin (cell overgrowth marker) and alpha smooth

muscle actin (fibrosis marker). qPCR was also used to determine relative levels of collagen (1A1) deposition. These examples show the reduced fibrotic effect on capsules larger than 1mm.

Empty capsules (capsules without encapsulated cells) of different sizes were produced using SLG100 alginate (PRONOVA). The capsules were transplanted intraperitoneally in C57BL/6 mice and incubated for 2 weeks before retrieval and analysis of host rejection responses (i.e., immune inflammation and fibrosis), as determined by FACS analysis, qPCR, confocal imaging, and/or western blotting. Phase contrast images were used to assess relative levels of cellular overgrowth and fibrosis across n = 5 individuals per treatment group (i.e., capsule size). Capsules of 300 μm and 500 μm were significantly more fibrotic after 28 days than 1100 μm capsules.

Capsules of uniform sizes: small (300 μm), medium (500 μm), and large (1500 μm), were produced using the electrospray technique and incubated intraperitoneally in C57BL/6 mice and retrieved after 14 days for analysis. The capsules were examined using several measures of fibrosis (FACS analysis, qPCR, confocal imaging, and/or western blotting). Capsules of 300 μm and 500 μm showed significantly more fibrosis than 1500 μm capsules in brightfield and confocal imaging.

The immune response to capsules of different sizes was assessed by measuring the percentage of immune cell populations comprised of either macrophages or neutrophils (Figure 6). Capsules of 300 μm, 500 μm, 900 μm, and 1500 μm were incubated for 14 days intraperitoneally in immune competent C57BL/6 mice, before samples were retrieved for analysis by FACS. The percentage of macrophages was high for the 300 μm capsules and steadily declined as the capsule size increased. The percentage of neutrophils was high for the 300 μm, 500 μm and 900 μm capsules and dropped to nearly the control level for the 1500 μm capsules. Protein from retrieved capsules of 0.3 mm, 0.5 mm, 1 mm, and 1.5 mm capsules were also analyzed by western blotting. Western Blotting of smooth muscle actin (SMA) and β-actin confirmed the same trend of reduced fibrosis with increasing capsule size. The amount of smooth muscle actin and β-actin associated with the different

capsule sizes were determined by Western blot. The signal for smooth muscle actin was normalized against the signal for β-actin. The level of smooth muscle actin was low for the 1.5 mm and 1 mm capsules but was much higher for the 1.5 mm and 1.0 mm capsules (Figure 7).

The reduced fibrosis effect remains evident even when the surface area or volume of the capsules is normalized. Capsules of 300 μm, 500 μm, and 800 μm were incubated intraperitoneally in C57BL/6 mice, retrieved after 14 days, and imaged using phase contrast microscopy. The amount of fibrosis observed was normalized for surface area of the capsules (Figure 8, top) or for volume of the capsules (Figure 8, bottom). In both cases, the measure of fibrosis was greatest for the 300 μm capsules and lowest for the 800 μm capsules. Reduced fibrosis for large capsules versus small capsules was still apparent when large capsules (1000 μm) were tested at 9 times the volume of small capsules (300 μm).

The reduced fibrosis effect of large capsules remains evident across a variety of materials. Capsules of 500 μm and 1500 μm were made of SLG20 alginate (PRONOVA), polystyrene, glass, polycaprolactone (PCL), LF10/60 alginate (FMC BioPolymer), and large 2000 μm Teflon spheres. The capsules were incubated in C57BL/6 mice for 14 days, and analyzed by various techniques (i.e., qPCR and FACS). Fibrosis was measured using CD68 (macrophage marker), Ly6g (neutrophil marker), CD11b (myeloid cell marker), and Col1a1 (fibrosis marker) were assayed by qPCR. With only a couple of exceptions, the markers were expressed at or near the control levels in all 1500 μm capsules and significantly above the control level for all 500 μm capsules (Figure 9). The exceptions were Ly6g expression for polycaprolactone (PCL) capsules and LF10/60 alginate capsules and CD11b expression for LF10/60 alginate capsules. In each of these cases, expression of the marker was higher than the control for the 1500 μm capsule (but still significantly less than the expression level for the 500 μm capsule.

The immune response to capsules of 500 μm and 1500 μm made of these different materials was also assessed at the cellular level by measuring the percentage of cell population composed of macrophages and neutrophils

by FACS (Figure 10). The capsules were made of SLG20 alginate (PRONOVA), polystyrene, glass, polycaprolactone (PCL), and LF10/60 alginate (FMC BioPolymer). The capsules were incubated in C57BL/6 mice for 14 days, and analyzed by various techniques (i.e., qPCR and FACS). In every case the percentage of macrophages and the percentage of neutrophils was significantly higher for the 500 μm capsules than for the 1500 μm capsules (Figure 10).

Example 4: The Effect of Sphere Diameter on Biocompatibility

Materials and Methods

Reagents

All chemicals were obtained from Sigma-Aldrich (St. Louis, MO) and cell culture reagents from Life Technologies (Grand Island, NY), unless otherwise noted. Antibodies: Alexa Fluor 488-conjugated anti-mouse CD68 (Cat. #137012, Clone FA-11) and Alexa Fluor 647-conjugated anti-mouse Ly-6G/Ly-6C (Gr-1) (Cat. #137012, Clone RB6-8C5) were purchased from BioLegend Inc. (San Diego, CA). Alexa Fluor 647-conjugated anti-mouse TGF beta1 (Cat. #bs-0103R-A647) was purchased from Bioss antibodies. Cy3-conjugated anti-mouse alpha smooth muscle actin antibody was purchased from Sigma Aldrich (St. Louis MO). Filamentous actin (Factin)-specific Alexa Fluor 488-conjugated Phalloidin, and Newport Green were purchased from Life Technologies (Grand Island, NY). Glass spheres of medium (500 μm) and large size (2 mm) where purchased from Sigma Aldrich (St. Louis, MO). Stainless steel spheres of medium (500μm) and large (2.5mm) size were purchased from Thomas Scientific (Swedesboro, NJ). Polystyrene spheres of medium (400-500 μm) and large (2 mm) size where purchased from Phosphorex (Hopkinton, MA). A sampling of spheres used in study were submitted for endotoxin testing by a commercial vendor (Charles River, Wilmington, MA) and the results showed that spheres contained < 0.05 EU/ml of endotoxin levels.

Fabrication of alginate hydrogel spheres

Alginate hydrogel spheres were made using a custom-built, electro-jetting device, consisting of a voltage generator, a vertical syringe

pump, and a grounded autoclavable glass collector. The voltage was coupled to the syringe and needle containing the alginate solution while the gelling bath was grounded to complete the circuit. Spheres were generated using a 1.4% solution of a commercially available alginate (PRONOVA SLG20 (endotoxin levels or LF10/60 NovaMatrix, Sandvika, Norway) dissolved in 0.9% saline (pH ≈ 7.4, Osmotic pressure ≈ 290 mOsm), and crosslinked using a $BaCl_2$ gelling solution (20mM $BaCl_2$, 250mM D-Mannitol, 25mM HEPES, pH ≈ 7.4, Osmotic pressure ≈ 290 mOsm)1

Alginate hydrogel microspheres of varying sizes were generated by utilizing different needle gauges, voltages, and flow rates; 0.3 mm spheres were generated using a 30G blunt needle, a voltage of 5kV, and a 200 µl/min flow rate, 0.4 mm spheres were generated with a 25G blunt needle, a voltage of 7kV and a 200 µl/min flow rate, 0.5 mm spheres were generated with a 25G blunt needle, a voltage of 5kV and a 200 µl/min flow rate, 0.7 mm spheres were generated with a 25G blunt needle, a voltage of 4kV and a 180 µl/min flow rate, 0.9 mm spheres were generated with an 18G blunt needle, a voltage of 7kV and a 200 µl/min flow rate, 1 mm spheres were generated with an 18G blunt needle, a voltage of 6kV and a 200 µl/min flow rate, 1.5 mm spheres were generated with an 18G blunt needle, a voltage of 5kV and a 180 µl/min flow rate, and 1.9 mm spheres were generated with an 18G blunt needle with a voltage of 5 kV and a 150 µl/min flow rate. All microspheres were cross-linked in 250 mL of $BaCl_2$-gelling solution in a sterile glass container. Immediately after crosslinking, the spheres were washed with HEPES buffer (25mM HEPES, 1.2mM $MgCl_2x6H2O$, 4.7mM KCl, 132mM $NaCl_2$, pH≈7.4, ≈290 mOsm) 4 times and stored overnight at 4°C. Immediately prior to implantation into the peritoneal cavity of mice, the spheres were washed an additional 2 times with 0.9% saline. A sampling of the fabricated hydrogels was submitted for endotoxin testing by a commercial vendor (Charles River, Wilmington, MA) and the results showed that LF10/60 spheres contained 31.6 EU/mL of endotoxins while SLG20 hydrogels contained < 0.05 EU/ml of endotoxin levels.

Polycaprolactone (PCL) sphere synthesis

Polycaprolactone (PCL, Mn 70,000-90,000, Sigma) microspheres were prepared by solvent evaporation with medium (0.3-0.5 mm) and large (1.5-2.0 mm) diameters. Small diameter microspheres were fabricated by dissolving PCL in dichloromethane (Fisher) at 6.5% concentration. This solution was introduced drop-wise into a 1% polyvinylalcohol (PVA, 88 mol% hydrolyzed, Polysciences Inc.) solution stirred using a stainless steel 4-blade overhead impeller at 200 rpm. After 75 min, the dispersion was added to 400 mL of ddH_2O and stirred for an additional 105 min until all of the solvent evaporated. The microspheres were then sieved, washed several times with water, flash frozen in liquid nitrogen and lyophilized overnight. Large microspheres were prepared similarly using 9% polymer concentration, 0.5% PVA solution, and a 3-blade overhead impeller stirred at 150 rpm.

Implantation/Transplantation surgeries

All animal protocols were approved by the MIT Committee on Animal Care, and all surgical procedures and post-operative care was supervised by MIT Division of Comparative Medicine veterinary staff. Immune-competent male non-diabetic or STZ-induced diabetic C57BL/6 mice (Jackson Laboratory, Bar Harbor, ME) or male Sprague-Dawley rats (Jackson Laboratory, Bar Harbor, ME) were anesthetized with 3% isoflurane in oxygen and had their abdomens shaved and sterilized using betadine and isopropanol. Preoperatively, all mice also received a 0.05 mg/kg dose of buprenorphine subcutaneously as a pre-surgical analgesic, along with 0.3 mL of 0.9% saline subcutaneously to prevent dehydration. A 0.5 mm incision was made along the midline of the abdomen and the peritoneal lining was exposed using blunt dissection. The peritoneal wall was then grasped with forceps and a 0.5-1 mm incision was made along the linea alba. A desired volume of spheres (all materials without islets, as well as SLG20 spheres encapsulating rat islets) were then loaded into a sterile pipette and implanted into the peritoneal cavity through the incision. The incision was then closed using 5-0 taper-tipped polydioxanone (PDS II) absorbable sutures. The skin was then closed over the incision using a wound clip and tissue glue.

For non-human primate (NHP) procedures, buprenorphine (0.01-0.03 mg/kg) was administered as a pre-operative analgesic. NHPs were then sedated using an intramuscular (IM) injection of ketamine (10 mg/kg) with an addition of midazolam as dictated by DCM vet staff if needed for additional sedation. Animals were maintained on a circulating warm water blanket and covered with a towel during the procedure to maintain body temperature. Either 0.5 or 1.5 mm diameter SLG20 spheres were injected into the dorsal (back) regions of 4 non-human primates (cynomolgus macaques) using 18 and 12 gauge custom-manufactured (Harvard Apparatus) sterile stainless steel needles, with slip tip syringes in order to prevent shearing of our biomaterial upon injection. Needles were inserted tangentially to the backs of the NHPs, and were slid (tunneled) approximately 1-2 cm away from the initial injection point, in order to try to separate the injection from that of the site of eventual material response. Spheres (0.5 and 1.5 mm diameter) were injected into 4 total spots on the flank of 4 of our non-human primates: two spots on the left flank and two on the right, for 0.5 mm and 1.5 mm diameter sphere implants, respectively. Saline was injected and 4 mm diameter SLG20 alginate cylindrical discs were implanted by making a minimal 1 cm incision, also on the left and right sides of the back, respectively into 3 additional primates. Incisions were closed with either a single interrupted suture with 3-0 nylon or VetBond (tissue glue).

Retrieval of cells, tissues, and materials

At desired time points post-implantation or transplantation (with encapsulated islets), as specified in figures, mice were euthanized by CO_2 administration, followed by cervical dislocation. In certain instances, 5 ml of ice cold PBS was first injected in order perform an intraperitoneal lavage to rinse out and collect free-floating intraperitoneal immune cells. An incision was then made using the forceps and scissors along the abdomen skin and peritoneal wall, and intraperitoneal lavage volumes were pipetted out into fresh 15 ml falcon tubes (each prepared with 5 ml of RPMI cell culture media). Next, a wash bottle tip was inserted into the abdominal cavity. KREBS buffer was then used to wash out all material spheres from the abdomen and into petri

dishes for collection. After ensuring all the spheres were washed out or manually retrieved (if fibrosed directly to intraperitoneal tissues), they were transferred into 50 mL conical tubes for downstream processing and imaging. After intraperitoneal lavage and sphere retrieval, remaining fibrosed intraperitoneal tissues were also excised for downstream FACS and expression analyses.

For non-human primate subcutaneous retrievals, similar to when material was implanted, NHPs were once again given buprenorphine (0.01-0.03 mg/kg) as a pre-operative analgesic, and sedated using an IM injection of ketamine (10 mg/kg), with midazolam as dictated by DCM vet staff if needed for additional sedation. Animals were once again maintained on a circulating warm water blanket and covered with a towel during the procedure to maintain body temperature. 8 mm diameter biopsy punches were then used to sample the entire skin and subcutaneous space at 2 and later at 4 weeks post-implantation. Following biopsy punches, the retrieval site was closed with 3-0 nylon in a simple-interrupted pattern and VetBond (tissue glue).

ELISpot multiplexed cytokine analysis

Cytokine array analysis was performed using the Proteome Profiler Mouse Cytokine Array Panel A kit (Cat. #ARY006, R&D Systems). For this analysis, proteins were extracted directly from materials, as described above in the western blotting section. For each membrane, 200 µl of protein solution was mixed with 100 µl of sample buffer (array buffer 4) and 1.2 ml of block buffer (array buffer 6), then added with 15 µl of reconstituted Mouse Cytokine Array Panel A Detection Antibody Cocktail and incubated at room temperature for 1 hour. The array membrane was incubated with block buffer (array buffer 6) for 2 hours on a rocking platform shaker. The block buffer was then aspirated, and the prepared sample/antibody mixture was added onto the membrane and incubated overnight at 4°C on a rocking platform shaker. The membrane was washed three times with 20 ml of 1X wash buffer for 10 minutes on a rocking platform shaker, rinsed once with deionized water, then probed with Fluorophore-conjugated streptavidin (1:5,000 dilution, Cat.

#926-32230, Li-Cor) at room temperature for 30 minutes on a rocking platform shaker, and then washed with wash buffer three more times and with deionized water once again, as described above. Antibody-antigen complexes were visualized using Odyssey Detection (Li-Cor, Serial No. ODY-2329) at a 800 nm wavelength. The densities of the spots were analyzed using Image J software.

Statistical analysis

Data are expressed as mean ± SEM, and N = 5 mice per time point and per treatment group. For Rat studies N = 3 per treatment. These sample sizes where chosen based on previous literature. All animals were included in analyses except in instances of unforeseen sickness or morbidity. Animal cohorts where randomly selected. Investigators where not blind to performed experiments. For qPCR or FACS, data were analyzed for statistical significance either by unpaired, two-tailed t-test, or one-way ANOVA with Bonferroni multiple comparison correction, unless indicated otherwise, as implemented in GraphPad Prism 5; *: $p < 0.05$, **: $p < 0.001$, and ***: $p < 0.0001$. High throughput NanoString based gene expression analysis data was divided into sets based on macrophage subtype and compartment. Data was normalized using the geometric means of the NanoString positive controls and background levels were established using the means of the negative controls. Housekeeping genes Tubb5, Hprt1, Bact, and Cltc were used to normalize between samples. Data was then log-transformed. For each subtype, time, and compartment group, a two-way ANOVA for the effect of size blocking on genes was performed. P-values were computed from pairwise comparisons performed using Tukey's Honest Significant Difference test and the Bonferroni correction was used to control the overall error rate.

Results

To investigate the effect of sphere diameter on biocompatibility we fabricated BaC-crosslinked SLG20 alginate hydrogel spheres in eight different sizes, 0.3 mm, 0.4 mm, 0.5 mm, 0.7 mm, 0.9 mm, 1 mm, 1.5 and 1.9 mm, with very narrow size distributions (Figure 11). These spheres (350 µl/mouse) were then implanted into the intraperitoneal space of C57BL/6

mice, where they were retained for 14 days. After this period, spheres were harvested from euthanized mice and studied for cellular deposition and fibrosis (Figures 12A-12D). Dark-field phase contrast images from retrieved spheres show a marked reduction in cellular deposition onto spheres as their size is increased. Cellular deposition on spheres was examined using Z-stacked confocal imaging using DAPI (nucleus marker), F-actin (cellular cytoskeleton marker) and α- smooth muscle actin (α-SMA,myofibroblastmarker). Interestingly, the larger spheres had significantly reduced fibrotic deposition. Additional immunostaining for the host immune cell markers CD68 (macrophage), Ly6G/Ly6C- GR1 (neutrophil) and TGF-β (inflammation marker) also showed reduced immune cell deposition on larger spheres. qPCR expression analysis of additional fibrosis markers, namely collagen 1a1 (Col1a1), collagen 1a2 (Col1a2) and α-SMA, further indicated reduced cellular deposition as the sphere size was increased (Figures 12A-12C). Western blot analysis of α-SMA expression within the cellular overgrowth on spheres showed a significant decrease as sphere size is increased (Figure 12D).

To ensure that the size-modulated fibrotic response effect is not simply a function of surface area, two sizes of spheres were implanted, 0.5 mm and 1.5 mm, normalized in total surface area. In other words, 100 μl/mouse of medium-sized and 300 μl/mouse of large-sized spheres were implanted into the intraperitoneal space of C57BL/6 mice and then retrieved after 14 days. Dark-field phase contrast images of the retrieved spheres revealed only limited cellular deposition on the 1.5-mm spheres and significant cellular deposition on the 0.5-mm spheres. These findings indicate that the phenomenon is size-mediated and independent of the total surface area of implanted material.

Whether the effects of implant size on fibrosis are related to a delay in the kinetics of cellular deposition on the larger-sized spheres was investigated. To study this hypothesis, 0.3-mm and 1.5-mm SLG20 alginate hydrogel spheres were implanted into the intraperitoneal space of C57BL/6 mice for a significantly longer period of six months. After six months the implanted

hydrogel spheres were retrieved and examined for cellular deposition. Dark-field phase contrast images from retrieved capsules show that the 1.5-mm spheres are largely devoid of cellular deposition whereas the 0.3-mm spheres are covered with deposited cells and are clumped together.

Whether or not this size-modulated fibrotic deposition phenomenon would extend to other materials known to produce higher levels of fibrotic reactions on implantation was evaluated. To this end, medium-sized (0.4-0.6 mm) and larger-sized (1.5-2.5 mm) spheres composed of SLG20 alginate (sterile-grade alginate), LF10/60 alginate (pharmaceutical-grade alginate), stainless steel, glass, polycaprolactone and polystyrene were implanted into the intraperitoneal space of C57BL/6 mice. The surface roughness of the material spheres evaluated here included only relatively smooth- surfaced materials (<1 μm roughness). Bright-field images from retrieved materials 14 days post-implant revealed significant cellular deposition on the medium-sized versions of all materials tested. Interestingly, all materials tested at an increased size led to a marked reduction of the thickness of cellular overgrowth deposition. Immunofluorescence-stained z-stacked confocal images of retrieved materials show a significant decrease in macrophage (CD68) and myofibroblast (alpha-SMA) deposition across all materials tested; significantly, large SLG20 alginate, LF10/60 (endotoxin containing alginate), glass and stainless steel spheres had negligible cellular deposition.

Example 5: Evaluation of innate immune response to spheres of different sizes

Materials and Methods

qPCR analysis

Total RNA was isolated from tissue (peripheral tissue alone, spheres alone and/or with adhered cells and fibrotic overgrowth, if present, and ip lavage alone), liquid nitrogen snapfrozen immediately following excision, using TRIzol (Invitrogen; Carlsbad, CA) according to the manufacturer's instructions. In addition, to help ensure complete tissue disruption, strong mechanical disruption with a Polytron homogenizer was also employed. Thus, gene expression signatures shown throughout are proportional and

representative of the entire cell population present on and/or around retrieved materials. Before reverse transcription using the High Capacity cDNA Reverse Transcription kit (Cat. #4368814; Applied Biosystems, Foster City, CA), all samples were first normalized for comparison by loading the same input 1 μg total RNA in a volume of 20 μl for each sample. cDNA (4.8 μl; 1:20 dilution) in a total volume of 16 μl (including SYBR Green and PCR primers) was amplified by qPCR with the following primers. Primers (Table 2) were designed using Primer Express software (Applied Biosystems, Carlsbad, CA, USA) and evaluated using LaserGene software (DNAStar, Madison, WI, USA) to ensure either mouse or rat (host)-specificity. Samples were incubated at 95°C for 10 min followed by 40 cycles of 95°C for 15 sec and 60°C for 1 min in an ABI PRISM 7900HT Sequence Detection System (Applied Biosystems). Results were analyzed using the comparative C_T (DDC_T) method as described by the manufacturer. Results were analyzed using the comparative C_T ($\Delta\Delta C_T$) method and are presented as relative RNA levels compared to the RNA expression in either mock-implanted control cell samples (peripheral intraperitoneal fat tissue, or free floating intraperitoneal lavage cells) after normalization to the β-actin RNA content of each sample. For material spheres alone, everything relative to either 0.3 or 0.5 mm alginate SLG20 spheres was compared. In addition, to further ensure proper normalization and sample handling across multiple retrieval time points, RNA for all samples for each harvest condition (i.e., ip lavage, spheres with or without adhered cells and fibrosis, and peripheral tissues with infiltration, as described), were quantified, reverse transcribed, and analyzed by qPCR in parallel. Mouse-specific (host) or rat (islet)-specific forward and reverse primer sets were utilized for this study (Table 2).

Gene	Primers (5' to 3'): Sense & Antisense
Mouse Collagen 1a1 (m*Col1a1*)	Forward: 5'-CATGTTCAGCTTTGTGGACCT-3' (SEQ ID NO:1)
	Reverse: 5'-GCAGCTGACTTCAGGGATGT-3' (SEQ ID NO:2)
Mouse Collagen 1a2 (m*Col1a2*)	Forward: 5'-GCAGGTTCACCTACTCTGTCCT-3' (SEQ ID NO:3)
	Reverse: 5'-CTTGCCCCATTCATTTGTCT-3' (SEQ ID NO:4)
Mouse Alpha Smooth Muscle actin (m*Acta2*)	Forward: 5'-CGCTTCCGCTGCCCAGAGACT-3' (SEQ ID NO:5)
	Reverse: 5'-TATAGGTGGTTTCGTGGATGCCCGCT-3' (SEQ ID NO:6)
Mouse Myeloid cell marker CD11b (m*Itgam*)	Forward: 5'-CCAAGAGAATGCAAAAGGCTTT-3' (SEQ ID NO:7)
	Reverse: 5'-GGGGGGCTGCAACAACCACA-3' (SEQ ID NO:8)
Mouse Macrophage marker CD68 (m*Cd68*)	Forward: 5'-GCCCGAGTACAGTCTACCTGG-3' (SEQ ID NO:9)
	Reverse: 5'-AGAGATGAATTCTGCGCCAT-3' (SEQ ID NO:10)
Mouse neutrophil marker Gr1 (m*Ly6g*)	Forward: 5'-TGCCCCTTCTCTGATGGATT-3' (SEQ ID NO:11)
	Reverse: 5'-TGCTCTTGACTTTGCTTCTGTGA-3' (SEQ ID NO:12)
Mouse β-actin (m*ActB*)	Forward: 5'-GCTTCTTTGCAGCTCCTTCGTT-3' (SEQ ID NO:13)
	Reverse: 5'-CGGAGCCGTTGTCGACGACC-3' (SEQ ID NO:14)
Rat Collagen 1a1 (r*Col1a1*)	Forward: 5'-CATGTTCAGCTTTGTGGACCT-3' (SEQ ID NO:15)
	Reverse: 5'-GCAGCTGACTTCAGGGATGT-3' (SEQ ID NO:16)
Rat Collagen 1a2 (r*Col1a2*)	Forward: 5'-CCTGGCTCTCGAGGTGAAC-3' (SEQ ID NO:17)
	Reverse: 5'-CAATGCCCAGAGGACCAG-3' (SEQ ID NO:18)
Rat Alpha Smooth Muscle actin (r*Acta2*)	Forward: 5'-TGCCATGTATGTGGCTATTCA-3' (SEQ ID NO:19)
	Reverse: 5'-ACCAGTTGTACGTCCAGAAGC-3' (SEQ ID NO:20)
Rat Pdx1 (r*Pdx1*)	Forward: 5'-CTCTCGTGCCATGTGAACC-3' (SEQ ID NO:21)
	Reverse: 5'-TTCTCTAAATTGGTCCCAGGAA-3' (SEQ ID NO:22)
Rat β-actin (r*ActB*)	Forward: 5'-ACCTTCTTGCAGCTCCTCCGTC-3' (SEQ ID NO:23)
	Reverse: 5'-CGGAGCCGTTGTCGACGACG-3' (SEQ ID NO:24)

Table 2. Mouse (m) or rat (r)-specific (host) forward and reverse primer sets used for qPCR analysis of RNA levels. Gene names are also shown in parentheses.

Results

The omental and epididymal fat pad tissue peripheral to the implants for innate immune cell infiltration were evaluated using a combination of flow cytometry (Figures 13A and 13B) and qPCR analysis (Figures 14A-14D). These analyses revealed that across all materials tested (SLG20 alginate, LF10/60 alginate, stainless steel, glass, polycaprolactone and polystyrene)

increasing sphere size led to a significant reduction of innate immune cell accumulation in peripheral tissue. These findings were further validated through a multiplexed inflammatory mouse cytokine profile. Notably, our evaluation of a spectrum of materials with a range of mechanical stiffness properties varying from soft (alginate hydrogels, <100 kPa; Papajova et al., *Carbohydrate polymers* **90**(1)**:** 472-482 (2012)) to hard (stainless steel, 100s ofGPa) demonstrates that size and shaper other than stiffness plays a critical role in biocompatibility.

Example 6: Studies in Larger Animals

Materials and Methods

Imaging of the retrieved material spheres

For phase contrast imaging retrieved materials were gently washed using Krebs buffer and transferred into 35 mm petri dishes for phase contrast microscopy using an Evos Xl microscope (Advanced Microscopy Group). For bright-field imaging of retrieved materials, samples were gently washed using Krebs buffer and transferred into 35 mm petri dishes for bright-field imaging using a Leica Stereoscopic microscope.

Confocal Immunofluorescence

Immunofluorescence imaging was used to determine immune populations attached to spheres. Materials were retrieved from mice and fixed overnight using 4% paraformaldehyde at 4°C. Samples where then washed twice with KREBS buffer, permeabilized for 30 min using a 0.1% Triton X100 solution, and subsequently blocked for 1 hour using a 1% bovine serum albumin (BSA) solution. Next, the spheres were incubated for 1 hour in an immunostaining cocktail solution consisting of DAPI (500 nM), specific marker probes (1:200 dilution) in BSA. After staining, spheres were washed three times with a 0.1% Tween 20 solution and maintained in a 50% glycerol solution. Spheres were then transferred to glass bottom dishes and imaged using an LSM 700 point scanning confocal microscope (Carl Zeiss Microscopy, Jena Germany) equipped with 5 and 10X objectives. Obtained images where adjusted linearly for presentation using Photoshop (Adobe Inc. Seattle, WA).

Results

Whether this observed size-modulated fibrotic effect would translate to a larger rodent model was examined. To examine this, 0.5-mm and 2.0-mm glass spheres were implanted into the intraperitoneal space of Sprague-Dawley rats and then retrieved the materials after 14 days. Bright-field and Z-stacked confocal images obtained from retrieved glass microspheres show that the large spheres are devoid of any cellular deposition, whereas the smaller spheres are significantly clumped together and embedded within a thick fibrotic capsule. qPCR expression analysis of fibrosismarkers, collagen 1a1 (Col1a1), collagen 1a2 (Col1a2) and αSMA, verified that increasing sphere 3 size resulted in a significant reduction of fibrosis formation directly on spheres (Figure 15). These results suggest our size-dependent fibrotic response observations in C57BL/6 mice also translate to other larger rodent species.

Example 7: Studies in Non-Human Primates

Materials and Methods

Histological processing for H&E and Masson's Trichrome staining

Retrieved materials where fixed overnight using 4% paraformaldehyde at 4°C. After fixation, alginate sphere or retrieved tissue samples were washed using 70% alcohol. The materials where then mixed with 4 degrees calcium-cooled Histogel (VWR, CA # 60872-486). After the molds hardened, the blocks were processed for paraffin embedding, sectioning and staining according to standard histological methods.

Results

To evaluate whether these findings could trans-late to higher-order species and also to other implant sites, SLG20 alginate hydrogels, prepared as 0.5-mm and 1.5-mm spheres ($N = 4$) as well as cylinders (4 mm diameter x 1 mm height; $N = 2$), were implanted subcutaneously into the dorsal regions of non-human primates (NHPs) for either 14 or 28 days. At both 14 and 28 days post-implantation retrieval time points the 1.5-mm SLG20 alginate spheres were not embedded in host tissue and freely dissociated from the implant site on incision with a biopsy punch. The retrieved 1.5-mm overgrowth. H&E

stained sections of retrieved large spheres confirmed negligible cellular deposition and a lack of fibrosis. Conversely, at both 14- and 28-day retrieval time points, the implanted 0.5-mm spheres and cylinders were profusely embedded in host tissues. Excised tissue obtained from the implant sites of SLG20 alginate 1.5-mmspheres, 0.5-mmspheres, cylinders and saline-injected control tissue were examined through histological analysis using a combination of H&E and Masson's Trichrome staining. The obtained images confirm the lack of large sphere embedding or fibrosis. However, extensive embedding and fibrosis build-up (up to 100 μm thick) is visible, enveloping the implanted cylinders and medium-sized spheres.

To confirm that the subcutaneous dorsal NHP observations could also translate to the intraperitoneal site of NHPs, a smaller of SLG20 alginate hydrogels were separately implanted into non-human primates (n=1 per treatment) using a minimally invasive laparoscopic procedure. A laparoscopic camera was used to capture images and video of the spheres immediately after, and again at 14 days post-implantation. The obtained in situ images reveal that the 1.5-mm spheres remain translucent and are not embedded into host omentum/fat tissue after 14 days; conversely, the 0.5-mm spheres are impeded in to the omentum/fat tissue. An IP lavage with saline at 14 days post-implantation enabled retrieval of SLG20 1.5-mm spheres; however, the 0.5-mm spheres could not be retrieved because of strong adherence and embedding into the IP host tissue (omentum). The retrieved 1.5-mm spheres were examined using dark-field imaging and seem to be transparent with negligible cellular overgrowth. Z-stacked confocal imaging of the retrieved 1.5-mmspheres confirms minimal cellular deposition, a lack of immune macrophages, and fibrosis-associated activated myofibroblast coverage. To verify the embedding of the 0.5-mm spheres within the NHP omentum, a biopsy punch was used to excise a sample of this tissue for histological analysis, which confirmed their embedding, and significant fibrotic tissue build-up was observed enveloping the medium-sized spheres.

Example 8: Studies with Implanted Devices

Materials and Methods

Rat Islet Isolation, Purification, and Encapsulation

Male Sprague-Dawley rats from Jackson Laboratories (Bar Harbor, ME) weighing approximately 300 grams were used for harvesting islets. All rats were anesthetized by a 1:20 xylazine (10 mg/kg) to ketamine (150 mg/kg) injection given intraperitoneally, and the total volume of each injection was 0.4 ml – 0.5 ml depending on the weight of rat. Isolation surgeries were performed as described by Lacy and Kostianovsky2. Briefly, the bile duct was cannulated and the pancreas was distended by an in vivo injection of 0.15% Liberase (Research Grade, Roche) in RPMI 1640 media solution. Rats were sacrificed by cutting the descending aorta and the distended pancreatic organs were removed and held in 50 ml conical tubes on ice until the completion of all surgeries. All tubes were placed in a 37°C water bath for a 30 min digestion, which was stopped by adding 10-15 ml of cold M199 media with 10% heat-inactivated fetal bovine serum (HIFBS) and lightly shaking. Digested pancreases were washed twice in the same aforementioned M199 media, filtered through a 450 μm sieve, and then suspended in a Histopaque 1077 (Sigma)/M199 media gradient and centrifuged at 1,700 RCF at 4°C. Depending on the thickness of the islet layer that was formed within the gradient, this step was repeated for higher purity islets. Finally, the islets were collected from the gradient and further isolated by a series of six gravity sedimentations, in which each supernatant was discarded after four minutes of settling. Purified islets were hand-counted by aliquot under a light microscope and then washed three times in sterile 1X phosphate-buffered saline. Islets were then washed once in RPMI 1640 media with 10% HIFBS and 1% penicillin/streptomycin, and cultured in this media overnight for further use.

Immediately prior to encapsulation, the cultured islets were centrifuged at 1,400 rpm for 1 minute and washed with Ca-free Krebs-Henseleit (KH) Buffer (4.7mM KCl, 25mM HEPES, 1.2mM KH_2PO_4, 1.2mM $MgSO_4x7H_2O$, 135mM NaCl, pH≈7.4, ≈290 mOsm). After washing, islets were centrifuged again and all supernatant was aspirated. The islet pellet

was then resuspended in a 1.4% solution of SLG20 alginate dissolved in 0.9% NaCl solution at an islet density of 1,000 islets per 0.75 ml alginate solution. Spheres were crosslinked using a $BaCl_2$ gelling solution and their sizes were controlled using similar procedures as the empty spheres (described above). Immediately after crosslinking, the encapsulated islets were washed 4 times with HEPES buffer and 2 times with RPMI Medium 1640 with 10% HIFBS and cultured overnight at 37°C for transplantation. As the islets had variable sizes (50 - 400 μm) and there was an inevitable loss of islets during the encapsulation process, the total number of encapsulated islets were recounted and converted into islet equivalents (IE, normalized to 150 μm size) based on a previously published method[3] prior to transplantation.

Blood glucose monitoring

To create insulin-dependent diabetic mice, healthy C57BL/6 mice were treated with Streptozotocin (STZ) by the vendor (Jackson Laboratory, Bar Harbor, ME) prior to shipment to MIT. The blood glucose levels of all the mice were retested prior to transplantation. Only mice whose non-fasted blood glucose levels were above 300 mg/dL for two consecutive days were considered diabetic and underwent transplantation.

Blood glucose levels were monitored three times a week following transplantation of islet containing alginate capsules. A small drop of blood was collected from the tail vein using a lancet and tested using a commercial glucometer (Clarity One, Clarity Diagnostic Test Group, Boca Raton, FL). Mice with unfasted blood glucose levels below 200mg/dL were considered normoglycemic. Monitoring continued until all mice had returned to a hyperglycemic state at which point they were euthanized and the spheres were retrieved.

Western Blotting

Protein was extracted directly from materials for western blot analysis. For protein analyses, retrieved materials were prepared by immersing materials in Pierce RIPA buffer (Cat. #89901, Thermo Scientific) with protease inhibitors (Halt Protease inhibitor single-use cocktail, Cat. #78430, Thermo Scientific) on ice, and then lysed by sonication (for 30 seconds on, 30

seconds off, twice at 70% amplitude). Samples were then subjected to constant agitation for 2 hours at 4°C. Lysates were then centrifuged for 20 min at 12,000 rpm at 4°C, and protein-containing supernatants were collected in fresh tubes kept on ice. In samples from fat tissue, an excess of fat (a top layer on the supernatant) was first removed before supernatant transfer. 20 μg protein (quantified by BCA assay, Pierce BCA protein assay kit, Cat. #23225, Thermo Scientific) for each lane was boiled at 95°C for 5 min and electrophoresed on SDS-polyacrylamide gels (Any kD 15-well comb mini-gel, Biorad, Cat. #456-9036) and then blotted onto nitrocellulose membranes (Biorad, Cat. #162-0213). Blots were probed with anti-αSmooth Muscle actin antibody (1:400 dilution, Rabbit polyclonal to alpha smooth muscle actin; Cat. #ab5694, AbCam), anti-PDX1 antibody (1:1000 dilution, Rabbit polyclonal to pancreatic & duodenal homeobox 1; Cat. #06-1379, EMD Millipore), and anti-β-actin antibody (1:4000 dilution, monoclonal anti-β-actin antibody produced in mouse; Cat. #A1978, Sigma Aldrich) as a loading control followed by donkey anti-rabbit (1:15,000 dilution, Cat. #926-32213, Li-Cor) and goat anti-mouse (1:15,000 dilution, Cat. #926-68070, Li-Cor) fluorophore-conjugated secondary antibodies. Antibody-antigen complexes were visualized using Odyssey detection (Li-Cor, Serial No. ODY-2329) at 700 and 800 nm wavelengths.

Newport Green and Live/Dead Islet Staining

LIVE/DEAD® Viability/Cytotoxicity Kit (Life technologies, Carlsbad CA; CA# L-3224) was used according to the manufacturer's instructions to assess the viability of islets postencapsulation. Newport Green™ DCF Diacetate (Life technologies, Carlsbad CA; CA# N-7991), cell permeant dye combined with DAPI was used to stain encapsulated islet cells post-retrieval.

NanoString analysis

RNAs for mock-implanted/mock-treated (MT) controls, or for 0.5 or 1.5 mm alginate spherebearing mice (n = 4/group) were isolated from tissue samples taken at various time points after implantation, as described. Respective RNAs were quantified, diluted to the appropriate concentration

(100 ng/μl), and then 500 ng of each sample was processed according to NanoString manufacturer protocols for expression analysis via our customized multiplexed gene mouse macrophage subtyping panel. RNA levels (absolute copy numbers) were obtained following nCounter (NanoString Technologies Inc., Seattle, WA) quantification, and group samples were analyzed using nSolver analysis software (NanoString Technologies Inc., Seattle, WA).

Results

Material geometry was investigated to see if it could produce improved/prolong function of an implanted biomedical device. To study this effect, the survival of islets of Langerhans (islets) immunoisolated/encapsulated within conventionally sized 0.5-mm alginate microcapsules was evaluated compared against islets protected within a 1.5-mm capsule. Previously, it was shown that host recognition and fibrosis via cellular and collagen deposition on the surface of transplanted 0.5-mm alginate microcapsules results in encapsulated islet graft cell death and the failure of diabetic correction in STZ-treated C57BL/6 mice. Notably, in the context of islet encapsulation, the diameter of the hydrogel capsules is a parameter that has been largely overlooked, and based on our observations it could play an important role in improving the efficacy of the transplanted grafts. Furthermore, it has been traditionally assumed that small capsules (<350 μm) allow better diffusion and transportation of nutrients and oxygen to the encapsulated islets than medium (350-700 μm) and larger capsules (>700 μm; ref. 40). Thus, to our knowledge larger 1.5-mmspherical capsules have previously not been evaluated for islet cell encapsulation.

A xenogeneic treatment model of transplanting rat pancreatic islets into STZ-induced diabetic C57BL/6 mice was used to investigated the role of capsule size on cell survival. Rat islets (500 IEs per mouse) were separately encapsulated into SLG20 alginate hydrogels, prepared as 1.5-mm or 0.5-mm spheres. For these studies an islet density preparation of 500 IEs per 0.325ml alginate solution was used because at this density very few protrusions of islets outside of capsules were observed. Live/dead staining was used to

confirm the viability of islets after encapsulation (Figures 16A-16C). To investigate potential diffusion barriers due to using larger-sized 1.5-mm capsules, before transplantation, the kinetics of both glucose and insulin diffusion within 1.5-mm and 0.5-mm capsules loaded with islets were evaluated. No significant differences were observed in diffusion kinetics of glucose (Figures 17A and 17B) or insulin (Figures 18A-18D) as a function of capsule geometry. After transplantation, blood-glucose (BG) correction was used as an indicator to non-invasively monitor cell graft function over time, and measurements were taken at least three times a week. All mice (n=5) in the 0.5-mm capsule group failed (that is, BG above 2 mg ml^{-1} for three consecutive measurements), on average, by 30 days following transplantation, whereas in the 1.5-mm capsule group (n= 5), stayed cured, on average, even until 175 days (a greater than five times increase) post- transplantation, when the experiment was stopped (Figures 19A and 19B). The difference in both BG normalization (Figure 16A) and fraction cured (Figure 16C) was significantly different ($p < 0.0001$) between the 0.5-mm and 1.5-mm capsule groups following the initial failure in regulating BGs by the 0.5-mm group (around day 25) throughout the remainder of the experiment. At seven days post-transplantation a glucose tolerance test (GTT) was used to evaluate the kinetics of blood-glucose correction, and no significant delays were measured as a function of capsule geometry (Figure 16B).

On termination of this study, six months post-transplantation, capsules were retrieved and analysed for fibrosis and presence of viable islets. Dark-field imaging revealed that the 0.5-mm capsules were covered in cellular deposition and clumped, whereas the 1.5- mm capsules were largely clean and devoid of cellular deposition. Confocal images acquired from retrieved 0.5-mm and 1.5-staining only in the 1.5-mm capsule group. Western blot assays were also performed on extracted proteins from retrieved capsules in each group to monitor relative expression of PDX-1 (islet viability marker) and α-SMA (fibrosis marker). For this assay, approximately 50% of capsules retrieved from each mouse was digested and processed for total protein extraction. Four out of five mice in the 0.5-mm capsule group had

comparatively diminished PDX-1 expression and all five mice showed high levels of α smooth muscle expression; conversely, high levels of PDX-1 and minimal α-SMA were detected in capsules retrieved from all five mice in the 1.5-mm capsule group. PDX-1 expression results were further verified using qPCR analysis of RNA isolated from retrieved capsules, and approximately eight times higher levels of rat PDX-1 were detectable in the 1.5mm capsules compared to the 0.5-mmcapsule group. Taken in combination, our results suggest that grafts in 1.5-mm capsules survived approximately six times longer than those prepared in conventionally sized 0.5-mm capsules because the tuned geometry hydrogels were able to resists fibrosis for a longer duration. Interestingly, although no significant build-up of fibrosis on the capsules was observed on retrieval after 180 days, the mice in this treatment group lost blood-glucose control after approximately 140 days. This possibly suggests some islet viability loss after transplantation, which could be related to the long-term durability of the rat islets used in this treatment model.

Example 9: Kinetic Profiling Analysis Of Host-Mediated Innate Immune Recognition Following Implantation

Materials and Methods

Insulin secretion kinetics

Islet insulin responses were assessed by loading 50 rat islets naked or encapsulated at 0.5 mm and 1.5 mm alginate capsules into the same microfluidic device used for calcium measurements. Perifusate samples were collected every minute (500 μL/min) by an automated fraction collector (Gilson, model 203B, WI, USA). Insulin concentrations were quantified every other minute using a rodent chemiluminescent insulin ELISA (Alpco, NH, USA). The following perifusion protocol was used: 1) KRB2 (0-20 min); 2) 20 mM glucose or 30 mM KCl (20-55 min); 3) KRB2 (55-100 min). The area under the curve for each insulin curve (n=3 for naked, 0.5 mm, and 1.5 mm) was calculated in order to statistically compare groups using one-way ANOVA ($p < 0.05$ as significant).

FACS analysis

Single-cell suspensions of freshly excised tissues were prepared using a gentleMACS Dissociator (Miltenyi Biotec, Auburn, CA) according to the manufacturer's protocol. Single-cell suspensions were prepared in a passive PEB dissociation buffer (1X PBS, pH 7.2, 0.5% BSA, and 2 mM EDTA) and suspensions were passed through 70 μm filters (Cat. #22363548, Fisher Scientific, Pittsburgh, PA). This process removed the majority of cells adhered to the surface (>90%). All tissue and material sample-derived, single-cell populations were then subjected to red blood cell lysis with 5 ml of 1X RBC lysis buffer (Cat. #00-4333, eBioscience, San Diego, CA, USA) for 5 min at 4°C. The reaction was terminated by the addition of 20 ml of sterile 1X PBS. The cells remaining were centrifuged at 300-400g at 4°C and resuspended in a minimal volume (~50 μl) of eBioscience Staining Buffer (cat. #00- 4222) for antibody incubation. All samples were then co-stained in the dark for 25 min at 4°C with two of the fluorescently tagged monoclonal antibodies specific for the cell markers CD68 (1 μl (0.5 μg) per sample; CD68-Alexa647, Clone FA-11, Cat. #11-5931, BioLegend), Ly-6G (Gr-1) (1 μl (0.5 μg) per sample; Ly-6G-Alexa-647, Clone RB6-8C5, Cat. #108418, BioLegend), CD11b (1 μl (0.2 μg) per sample; or CD11b-Alexa-488, Clone M1/70, Cat. #101217, BioLegend). Two ml of eBioscience Flow Cytometry Staining Buffer (cat. #00-4222, eBioscience) was then added, and the samples were centrifuged at 400-500g for 5 min at 4°C. Supernatants were removed by aspiration, and this wash step was repeated two more times with staining buffer. Following the third wash, each sample was resuspended in 500 μl of FlowCytometry Staining Buffer and run through a 40 μm filter (Cat. #22363547, Fisher Scientific) for eventual FACS analysis using a BD FACSCalibur (cat. #342975), BD Biosciences, San Jose, CA, USA). For proper background and laser intensity settings, unstained, single antibody, and IgG (labeled with either Alexa-488 or Alexa-647, BioLegend) controls were also run.

Results

To better understand innate immune response as a function of implant size, a kinetic profiling analysis of host-mediated innate immune recognition was conducted following implantation of 0.5-mm and 1.5-mm SLG20 alginate spheres, over a 28-day period (Figures 20A-20C) in C57BL/6 mice. Flow cytometry was used to quantify the accumulation of myeloid cells 1 (Figure 20A), neutrophils (Figure 20B) and macrophages (Figure 20C) directly on spheres of 0.5-mm and 1.5-mm sizes at 1, 4, 7, 14 and 28 days post-implant. At all time points evaluated, a significant increase in the accumulation of myeloid cells was observed onto 0.5-mm spheres compared to the 1.5-mm spheres (Figure 20A). In probing macrophage and neutrophil cells, by four days post-implantation significantly increased accumulation on 0.5-mm spheres were observed, which appears to plateau by day 7 (Figures 20C and 20C). Notably, on 1.5-mm spheres negligible numbers of neutrophil cells and a limited number of myeloid and macrophage cells were observed at all time points.

Example 10: Key Drivers Of The Foreign Body Reaction To Implanted Materials

Materials and Methods

Insulin secretion kinetics

Islet insulin responses were assessed by loading 50 rat islets naked or encapsulated at 0.5 mm and 1.5 mm alginate capsules into the same microfluidic device used for calcium measurements. Perifusate samples were collected every minute (500 μL/min) by an automated fraction collector (Gilson, model 203B, WI, USA). Insulin concentrations were quantified every other minute using a rodent chemiluminescent insulin ELISA (Alpco, NH, USA). The following perifusion protocol was used: 1) KRB2 (0-20 min); 2) 20 mM glucose or 30 mM KCl (20-55 min); 3) KRB2 (55-100 min). The area under the curve for each insulin curve (n=3 for naked, 0.5 mm, and 1.5 mm) was calculated in order to statistically compare groups using one-way ANOVA ($p < 0.05$ as significant).

Real-time fluorescence imaging of islet intracellular calcium

Real-time fluorescence imaging of islet intracellular calcium $[Ca^{2+}]_i$ was performed in a microfluidic device modified for encapsulated islets[4]. In brief, fifty Sprague Dawley rat islets naked or encapsulated in alginate capsules (0.5 mm and 1.5 mm diameter) were incubated with 5 μM Fura-2/AM (a calcium indicator, Molecular Probes, CA, USA) at 37°C in Krebs-Ringer buffer (KRB) supplemented with 2 mM glucose (KRB2) and 0.5% BSA for 35 min. The islets were then loaded into the microfluidic device mounted on an inverted epifluorescence microscope (Leica DMI 400B, IL, USA). Excess dye was washed out with KRB2 for 35 min at 500 μL/min. Dual-wavelength Fura-2/AM dye were excited ratiometrically at 340 and 380 nm, and changes in the $[Ca^{2+}]_i$ levels are expressed as F340/F380 (% increase from basal 2 mM glucose). Excitation wavelengths were controlled by excitation filters (Chroma Technology, VT, USA) mounted in a Lambda DG-4 wavelength switcher. Emission of Fura-2/AM was filtered using a Fura2/FITC polychroic beamsplitter and a double band emission filter (Chroma Technology. Part number: 73.100bs). SimplePCI software (Hamamatsu Corp, IL, USA) was used for imaging acquisition and analysis. These images were collected with a high-speed, highresolution charge coupled camera (CCD, Retiga-SRV, Fast 1394, QImaging).

Individual islet intracellular calcium responses were assessed with the following perifusion protocol: 1) KRB2 (0-5 min); 2) 20 mM glucose (5-25 min); 3) KRB2 (25-45 min); 4) 30 mM KCl (45-60 min); 5) KRB2 (60-70 min). The area under the curve for each time period was calculated for each individual islet in order to statistically compare groups using one-way ANOVA ($p < 0.05$ as significant). Three separate batches of rodent isolations were used for assessments where each condition was tested from the same batch of islets (naked islets n = 59; 0.5 mm n = 49; 1.5 mm n = 43).

Intravital Imaging and MAFIA depletion

For intravital imaging, SLG20 hydrogels of 0.5 mm and 1.5 mm sizes were loaded with Qdot 605 (Life technologies, Grand Island, NY) and surgically implanted into

C57BL/6-Tg(Csf1r-EGFP-NGFR/FKBP1A/TNFRSF6)2Bck/J mice as described above. After 1, 4, or 7 days post implantation, the mice were placed under isoflurane anesthesia and a small incision was made at the site of the original surgery to expose beads. The mice were placed on an inverted microscope and imaged using a 25x, N.A. 1.05 objective on an Olympus FVB-1000 MP multiphoton microscope at an excitation wavelength of 860 nm. Z-stacks of 200 μm (10 μm steps) were acquired at 2-minute intervals for time series of 20 - 45 minutes depending on the image. The mice were kept under constant isoflurane anesthesia and monitored throughout the imaging session. Obtained images were analyzed using Velocity 3D Image Analysis Software (Perkin Elmer, Waltham, MA).

In addition, to investigate fibrosis or the lack thereof in control (non-depleted) or induced macrophage-depleted MAFIA mice, 0.5 mm SLG20 spheres were transplanted as described above. In the case of targeted macrophage depletion, an additional group of n = 5 mice were injected intravenously (tail vein) with B/B homodimerizer (Clontech). Significant macrophage depletion was achieved (~80-90%, mean group decrease = 84.36%, Figure 22) following our administering of an intravenous injection of 10 mg/kg of the homodimerizer AP20187 in these mice. Repeat depletion in the MAFIA model three days prior and then once every 3 days, starting 3 days following alginate sphere implantation up until retrieval, was able to knock down macrophage numbers far below peritoneal levels observed in the IP space of transplanted, non-depleted control MAFIA mice (~65.26% vs ~10.2%; Figure 22).

Results

Macrophages have been implicated as key drivers of the foreign body reaction to implanted materials41. To probe their role towards the fibrotic responses to the implanted materials a series of experiments were performed in which SLG20 alginate spheres were transplanted into the IP space of a transgenic mouse model, MAFIA, which enables the induction of macrophage cell depletion. In this model, a macrophage Fas-induced apoptosis transgene enables inducible/reversible apoptosis of macrophages using the mouse

colony stimulating factor 1 receptor promoter (CSF1R) to drive expression of a mutant human FK506 binding protein 1A, 12 kDa (ref. 42). Furthermore, an EGFP transgene included in this model enables the in situ fluorescent monitoring of macrophage cells.

First, to confirm the importance of macrophages in driving the fibrosis responses 0.5-mm SLG20 spheres were transplanted into the IP space of MAFIAmice treated to induce depletion of macrophages and also as a control into MAFIA mice without depletion for 14 days. Dark-field microscope images of the retrieved spheres revealed only limited cellular deposition onto spheres implanted in mice with depleted macrophages, and conversely significant cellular deposition onto spheres received from mice with macrophages (Figure 22). These results confirm that macrophages are indeed a key driver of the fibrotic responses observed in response to our transplanted materials.

Second, to monitor macrophage behaviour in real time, in vivo intravital imaging on implanted alginate spheres of 0.5mm and 1.5mm in size was performed, which were fluorescently labelled. Spherical implants were studied in the IP space of MAFIA mice (Figure 23). In vivo Z-stacked intravital images obtained from implanted medium- and large-sized spheres at 1, 4 and 7 days post-implant indicate that macrophage cells extravasate from peripheral fat pad tissue and accumulate onto 0.5-mm spheres over that one-week period, whereas very few macrophages can be observed near the 1.5-mm spheres. Z-stacked and time lapse intravital images of macrophage accumulation onto 0.5-mm and 1.5-mm spheres at 1, 4 and 7 days post-implantation confirm both a lack of macrophage activity and numbers surrounding 1.5-mmspheres, and significant macrophage activity and numbers around 0.5-mm spheres. It was hypothesized that because the 1.5-mm spheres are surrounded by only a few macrophage cells, the macrophages around the large spheres are not becoming activated, resulting in reduced recruitment and extravasation of additional macrophages.

Macrophage cells have remarkable plasticity that allows them to efficiently respond to environmental signals and change their phenotype to

address the implicated stimuli. There is a broad spectrum of macrophage activations, which can be categorized into three states: namely, classical activation (pro-inflammatory, $M_{Classic}$), alternative activation (pro-healing, M_{Wound}) and regulatory activation (M_{Reg}). These phenotypes can be characterized through gene expression analysis of specific markers that correlate with each activation state. A pro-inflammatory macrophage phenotype correlates with elevated expression of tumour necrosis factor α (TNF-α), interleukin 1 (IL1), and interferon regulatory factor 5 (IRF5; A pro-wound-healing phenotype of macrophage correlates with upregulation in expression of dendritic cell immune receptor (Dcir), stabilin 1 (Stab1), chemokine (C-C motif) ligand 22 (CCL22), chitinase-like 3 (YM1), and arginase 1 (Arg). Meanwhile, a regulatory macrophage phenotype has been characterized to correlate with elevated expression of interleukin 10 (IL10), TNF superfamily member 14 (Light) and sphingosine kinase 1 (Sphk1). To elucidate the changing activation/differentiation states of macrophages a range of implanted constructs were examined using a series of markers reflecting MClassic, MWound and MReg phenotypes. At 1, 4 and 7 days post-implantation, gene expression analysis was used to probe phenotype marker expression of cells isolated from the intraperitoneal space, omental fat pad tissue, and directly on spheres. Overall, significantly different gene expression patterns were observed for cells associated with these tissues following implantation of 0.5-mm spheres when compared to 1.5-mm spheres.

Table 1. P-values indicating level of significance for comparisons between mock surgeries and implanted SLG20 spheres innate immune responses over time classified by macrophage markers, size, and days after implantation. Nanostring data was log-transformed and a linear model consisting of time, size, gene, compartment, and macrophage type was constructed. Pairwise comparisons between the mock and implanted groups were performed using Tukey's range test. Significance level $\alpha = 0.05$. N=4 mice per treatment.

Compartment	Type	Day 1		Day 4		Day 7	
		0.5 mm	1.5 mm	0.5 mm	1.5 mm	0.5 mm	1.5 mm
Intraperitoneal Space	Classic	0.5832	1.0000	0.0168	1.0000	0.0017	0.8812
	Regulatory	1.0000	1.0000	1.0000	1.0000	1.0000	1.0000
	Wound	0.0001	0.0097	<0.0001	0.0041	<0.0001	0.1455
Fat	Classic	1.0000	1.0000	0.2175	0.2302	0.0326	0.5249
	Regulatory	1.0000	1.0000	0.8362	0.6927	1.0000	1.0000
	Wound	0.9603	1.0000	<0.0001	0.0075	0.0001	1.0000
Spheres	Classic	0.0001	1.0000	<0.0001	<0.0001	<0.0001	<0.0001
	Regulatory	1.0000	1.0000	0.0089	0.5295	<0.0001	1.0000
	Wound	<0.0001	<0.0001	<0.0001	<0.0001	<0.0001	<0.0001

Implantation of both 0.5-mm and 1.5-mm spheres resulted in an increased expression of markers associated with a wound-healing phenotype in the intraperitoneal and peripheral omentum fat compartments (Table 1). This phenotype was elevated at day 4 for both sizes of spheres implanted in mice, and decreased by day 7 for the 1.5-mm spheres. It is believed that these data are consistent with macrophage activation in these compartments--that is, reduced when the implanted material consists of 1.5- mm spheres. Fibrotic tissue obtained directly from the 0.5-mm spheres showed increasing expression of markers associated with all three macrophage phenotypes. In contrast, expression of macrophage markers associated only with classical and wound- healing phenotypes was enriched in 1.5-mm spheres (Table 1**). Regulatory macrophage markers were not significantly upregulated at any time point or in any compartment tested following implantation of 1.5-mm spheres. However, increased expression of markers associated with this macrophage phenotype was observed on days 4 and 7 in cells associated with the 0.5-mm spheres. Combined our observations suggest that a lack of regulatory macrophage cell accumulation on large-sized spheres correlates with the truncated fibrosis responses.

In summary, the data demonstrated that by tuning the geometry of implanted materials one can influence their host recognition and propagation of foreign body reactions. Spherical materials that are of 1.5 mm in diameter or greater proved to be significantly more biocompatible

than their smaller-sized or differently shaped counterparts. This effect was demonstrated to be independent of total implanted surface area and visible with all materials tested. Further, our finding suggests that simply increasing implant size is insufficient to resist foreign body responses, and that a spherical shape is also integral in resisting host fibrosis/rejection. Significantly, alginate microspheres of 1.5 mm in diameter demonstrated an ability to ward off cellular deposition for at least six months. Modulating the spherical dimensions of a broad spectrum of materials, encompassing hydrogels, ceramics, metals and plastics, also showed that spheres of 1.5 mm in diameter or greater significantly mitigated foreign reactions and fibrosis. These findings have important implications for the design of *in vivo*-implanted biomedical devices for a range of applications, trolled drug release, implantable prosthesis for tissue engineering.

Example 11: Profiling Macrophage Phenotype Shifts

Figures 24A-24F shows profiling macrophage phenotype shifts in the cells of the intraperitoneal space. NanoString-based analysis for RNA expression of macrophage phenotype markers from cells in the intraperitoneal space extracted (intraperitoneal lavaged) at 1, 4, and 7 days post-implant. Expression is normalized to intraperitoneal cells harvested from mock surgery (PBS-injected) mice, presented on a base 2 logarithmic scale. N=4 mice per treatment. For details of analysis see supplemental methods description.

Figures 25A-25F shows profiling macrophage phenotype shifts in the cell of the peripheral omentum fat tissue. NanoString-based analysis for RNA expression of macrophage phenotype markers from cells in the peripheral fat tissue extracted at 1, 4, and 7 days post-implant. Expression is normalized to fat tissue harvested from mock surgery (PBS-injected) mice, presented on a base 2 logarithmic scale. N=4 mice per treatment.

Implantation of both 0.5 mm- and 1.5 mm-sized spheres resulted in an increased expression of markers associated with a wound healing phenotype in the intraperitoneal and peripheral omentum fat compartments. This phenotype was elevated at day 4 for both sizes of spheres implanted in mice, and decreased by day 7 for the 1.5 mm-sized spheres. We believe that these

data are consistent with macrophage activation in these compartments, that is reduced when the implanted material are 1.5 mm spheres. Fibrotic tissue obtained directly from the 0.5 mm-sized s showed increasing expression of markers associated with all three macrophage phenotypes. In contrast, expression of macrophage markers associated only with classical and wound-healing phenotypes was enriched on 1.5-mm spheres. Regulatory macrophage markers were not significantly up-regulated at any time point or in any compartment tested following implantation of 1.5 mm-sized spheres. However, increased expression of markers associated with this macrophage phenotype was observed on days 4 and 7 in cells associated with the 0.5 mm spheres. Combined, the observations suggest that a lack of regulatory macrophage cell accumulation on large size spheres correlates with the truncated fibrosis responses.

Example 12: Diffusion Of Insulin And Glucose As A Function Of Capsule Geometry

In beta-cells, glucose-induced insulin secretion is a complex process involving glucose metabolism, mitochondrial energy production, potassium-dependent ATP channels (K_{ATP} channels), voltage-dependent calcium channels (VDCCs), calcium influx, and insulin secretion, which has a biphasic and oscillatory kinetic patterns. In this study, we applied a microfluidic perifusion device to dynamically measure intracellular calcium influx (a downstream and immediately proximal trigger for the fusion of insulin granules to the plasma membrane and exocytosis) and insulin concentrations in perifusate samples in order to characterize the impact of encapsulation and capsule size on insulin secretion coupling factors and insulin secretion. As shown in Figures 18A-18D, glucose-induced intracellular calcium signals were similar among the three groups with typical phase responses in all three groups. No significant differences were observed from the start time of calcium influx up to the maximal calcium peak in response to both 20 mM glucose and 30 mM KCl (potassium chloride) challenge. Additionally, the areas under the curve (AUCs) of calcium concentrations under both stimulators were not significantly different (Figures

18C and 18D). However, the time to reach the maximal calcium level for the 1.5 mm capsules was statistically delayed in response to glucose compared to the naked islets and 0.5 mm capsules ($p = 0.03$), but not statistically delayed in response to KCl stimulation.

The results suggest that small molecules, such as glucose (180.2 daltons) and KCl (74.6 daltons), diffuse very rapidly into the alginate capsules and efficiently induce calcium influx at a similar rate as naked islets. This suggests that the encapsulation process and alginate material do not acutely impede glucose metabolism or insulin stimulator-secretion coupling factors such as mitochondrial energy production and ion channels that are important for in vitro and in vivo function. Furthermore, diffusion efficiency in the capsule may depend on molecular weight of the analyte since there was a delayed time to reach a maximal calcium level in the 1.5 mm capsules in response to glucose (180.2 daltons), but not to KCl (74.6 daltons).

Next, the insulin secretion kinetics of the naked and encapsulated islets were investigated. As shown in Figure 19A, naked islets show typical biphasic insulin secretion patterns in response to glucose, while both encapsulated islet groups show loss of the biphasic pattern showing that insulin secretion gradually increases over the period of glucose stimulation without a defined phase I secretion. No significant differences were observed from the start time of insulin secretion up to the maximal peak insulin secretion in response to both 20 mM glucose and 30 mM KCl challenges. However, the times to reach maximal insulin secretion from 20 mM glucose and 30 mM KCl were significantly delayed for 0.5 mm and 1.5 mm encapsulated islets compared to naked islets ($p = 0.0002$ (20mM glucose), 0.04 (30 mM KCl)). Further analysis of insulin secretory kinetic curves showed that the total insulin secreted by naked islets in the first ten minutes of stimulation was significantly higher than for both 0.5 mm- and 1.5 mm encapsulated islets in responses to both glucose and KCl ($p = 0.02$ and 0.04, respectively), but not significantly different for later time segments during stimulation. This data further suggests that the larger molecular weight of the insulin (5,808 Da) is the determining factor resulting in longer diffusion time through the alginate

gel into the perifusate chamber for both encapsulated groups compared to naked islets.

Total insulin secreted by all groups during stimulation (20-55 min) and during the wash out period after stimulation (55-100 min) was also found not to be significantly different in response to both stimulators. This suggests that overall bulk insulin secretion is unaffected by encapsulation or capsule size. More importantly, encapsulated islets returned to basal insulin secretory levels similar to naked islets, which is a critical factor when considering future clinical application as prolonged insulin secretion after stimulation could cause dangerous hypoglycemia.

Together with normal glucose-induced calcium influx, our results indicate that the altered insulin secretion profiles of the encapsulated islets seem to be largely affected by the presence of an alginate gel due to increasing diffusion time of larger MW insulin from the capsule to the perifusate. This may explain the observed loss of phase I insulin secretion of encapsulated islets in response to glucose. However, there is no significant difference in insulin secretory kinetics between 0.5 mm- and 1.5 mm-encapsulated islets, suggesting capsule size has little effect on insulin secretion.

In summary, islet stimulation kinetics by small molecular weight secretagogues is unaffected by encapsulation or capsule size; however, initial insulin secretory kinetics are delayed similarly for encapsulated islets at both capsule sizes. Nonetheless, overall bulk insulin kinetics for both capsule sizes are well-conserved and similar to naked islets.

Modifications and variations of the present invention will be further understood by reference to the following claims. All references cited herein are specifically incorporated by reference.

We claim:

1. A preparation of biomedical devices, wherein at least 60 % of the devices of the preparation (i) have a sphere-like shape or a spheroid-like shape and (ii) have a diameter of at least X mm, but no more than Y mm, provided that Y is greater than X, X is 1.0, 1.1, 1.2, 1.3, 1.4, 1.5, 1.6, 1.7, 1.8, 1.9, or 2.0, and Y is 2.0, 2.5, 3.0, 3.5, 4.0, 4.5, 5.0, 5.5, 6.0, 6.5, 7.0, 7.5, 8.0, 8.5, 9.0, 9.5, or 10.0, and

(a) no more than 20% of the devices of the preparation have other than a sphere-like shape or a spheroid-like shape;

(b) at least 50 % of the devices of the preparation comprise a live cell, or a plurality of live cells, or at least 1,000, 2,000 or 5,000 live cells/device;

(c) at least 50 % of the devices of the preparation having sphere-like shape or a spheroid-like shape comprise a live cell, or a plurality of live cells, or at least 1,000, 2,000 or 5,000 live cells;

(d) no more than 20% of the devices of the preparation have an edge;

(e) the cells in at least 50 % of the devices of the preparation are distributed essentially homogenously throughout the device;

(f) the cells in at least 50 % of the devices of the preparation having sphere-like shape or a spheroid-like shape are distributed essentially homogenously throughout the device;

(g) the cells in at least 50 % of the devices of the preparation are not distributed essentially homogenously throughout the device; and

(h) the cells in at least 50 % of the sphere-like shape or spheroid-like shape devices of the preparation are not distributed essentially homogenously throughout the device.

2. The preparation of claim 1, wherein the biomedical devices comprise a biocompatible material, wherein the biocompatible material is alginate or an alginate derivative.

3. The preparation of any of claims 1-2, wherein X = 1.2, and Y = 10.0.

4. The preparation of any of claims 1-2, wherein X = 1.2, and Y = 8.0.

5. The preparation of any of claims 1-2, wherein X = 1.3, and Y = 10.0.

6. The preparation of any of claims 1-2, wherein X = 1.3, and Y = 8.0.

7. The preparation of any one of claims 1-6, wherein at least 60 % of the devices of the preparation have a sphere-like shape or a spheroid-like shape.

8. The preparation of any one of claims 1-7, wherein at least 70 % of the devices of the preparation have a sphere-like shape or a spheroid-like shape.

9. The preparation of any one of claims 1-8, wherein at least 80 % of the devices of the preparation have a sphere-like shape or a spheroid-like shape.

10. The preparation of any one of claims 1-9, wherein at least 80 % of the devices of the preparation are not sub-compartmentalized.

11. The preparation of any one of claims 1-10, wherein at least 80 % of the devices of the preparation are sub-compartmentalized and at least one subcompartment is essentially free of cells.

12. A method of treating a subject, comprising:

(a) administering to the subject a first administration of an effect of amount of the preparation of any one of claims 1-11, which provides a therapeutic effect for at least Z days; and

(b) administering to the subject a subsequent administration of an effective of amount of the preparation,

wherein at least Z-10, Z-5, or Z days separate the first and subsequent administrations, and wherein no interim administration is provided.

13. The method of claim 12, wherein Z is at least 14 days.

14. The method of claim 12, wherein Z is at least 30 days.

15. A method of treating a subject, comprising:

administering, at least Z days after the first administration to a subject of an effective of amount of the preparation of any one of claims 1-11, a subsequent administration of an effective of amount of the preparation,

wherein at least Z-10, Z-5, or Z days separate the first and subsequent administrations.

16. The method of claim 14, wherein in Z is at least 14 days.

17. The method of claim 15, wherein Z is at least 30 days.

18. Hydrogel capsules encapsulating cells,

wherein the capsules consist of three layers:

an inner acellular core layer;

a hydrogel layer containing cells to be transplanted selected from the group consisting of mammalian secretory cells, mammalian metabolic cells, mammalian structural cells, and aggregates thereof; and

an outer acellular barrier or structural layer.

19. The hydrogel capsules of claim 18 having a mean diameter of greater than 1 mm and less than 8 mm.

20. The hydrogel capsules of claim 18 or 19, wherein the core layer comprises a therapeutic, prophylactic, or diagnostic agent.

21. The hydrogel capsules of claim 20, wherein the core layer comprises a therapeutic agent selected from the group consisting of anti-inflammatories, phenolic antioxidants, and anti-proliferative drugs.

22. The hydrogel capsules of claim 20 or 21, wherein the core layer comprises a therapeutic agent which is released at the site of implantation.

23. Hydrogel capsules encapsulating cells,

wherein the capsules consist of two or more layers:

a hydrogel layer containing cells to be transplanted selected from the group consisting of mammalian secretory cells, mammalian metabolic cells, mammalian structural cells, and aggregates thereof; and

an outer acellular barrier or structural layer,

wherein the capsule has a diameter of at least 1 mm and less than 8 mm and elicits less of a fibrotic reaction after implantation than the same capsule having a diameter of less than 1 mm.

24. The hydrogel capsules of claim 23 having a diameter of at least 1.2 mm.

25. The hydrogel capsules of claim 23 having a diameter of at least 1.5 mm.

26. The hydrogel capsules of any one of claims 24-25, wherein the capsules consist of three layers:

an inner acellular core layer;

the hydrogel layer containing cells to be transplanted selected from the group consisting of mammalian secretory cells, mammalian metabolic cells, mammalian structural cells, and aggregates thereof; and

the outer acellular barrier or structural layer.

27. The hydrogel capsules of any one of claims 18-26, wherein the hydrogel comprises a polymer selected from the group consisting of polysaccharides, collagen, agarose, polyphosphazenes, poly(acrylic acids), poly(methacrylic acids), copolymers of acrylic acid and methacrylic acid, poly(alkylene oxides), poly(vinyl acetate), polyvinylpyrrolidone (PVP), and copolymers and blends thereof.

28. The hydrogel capsules of any one of claims 18-27, wherein the hydrogel is a polysaccharide selected from the group consisting of alginate, chitosan, hyaluronan, and chondroitin sulfate.

29. The hydrogel capsules of any one of claims 18-28, wherein the surface of the capsules is hydrophilic.

30. The hydrogel capsules of any one of claims 18-29, wherein the cells are islet cells or undifferentiated or partially differentiated precursors thereof.

31. The hydrogel capsules of any one of claims 18-30, wherein the mammalian cells are allogeneic or autologous.

32. The hydrogel capsules of any one of claims 18-31, wherein the mammalian cells are islet cells.

33. A population of hydrogel capsules encapsulating cells, wherein the capsules contain cells to be transplanted selected from the group consisting of mammalian secretory cells, mammalian metabolic cells, mammalian structural cells, and aggregates thereof , wherein all of the capsules in the population of capsules have a diameter of at least 1 mm and less than 8 mm,

and wherein the hydrogel capsules elicit less of a fibrotic reaction after implantation than the same capsules having a diameter of less than 1 mm.

34. The population of hydrogel capsules of claim 33, wherein the capsules in the population were selected by separating capsules having a diameter of at least 1 mm and less than 8 mm from capsules having a diameter of less than 1 mm and from capsules having a diameter of at least 8 mm.

35. The population of hydrogel capsules of claim 33 or 34, wherein all of the capsules in the population have a diameter of at least 1.2 mm.

36. The population of hydrogel capsules of claim 33 or 34, wherein all of the capsules in the population have a diameter of at least 1.5 mm.

37. The population of hydrogel capsules of any one of claims 33-36, wherein the hydrogel comprises a polymer selected from the group consisting of polysaccharides, collagen, agarose, polyphosphazenes, poly(acrylic acids), poly(methacrylic acids), copolymers of acrylic acid and methacrylic acid, poly(alkylene oxides), poly(vinyl acetate), polyvinylpyrrolidone (PVP), and copolymers and blends thereof.

38. The population of hydrogel capsules of any one of claims 33-37, wherein the hydrogel is a polysaccharide selected from the group consisting of alginate, chitosan, hyaluronan, and chondroitin sulfate.

39. The hydrogel capsules of any one of claims 33-38, wherein the surface of the capsules is hydrophilic.

40. The population of hydrogel capsules of any one of claims 33-39, wherein the cells are islet cells or undifferentiated or partially differentiated precursors thereof.

41. The population of hydrogel capsules of any one of claims 33-40, wherein the mammalian cells are allogeneic or autologous.

42. The population of hydrogel capsules of any one of claims 33-41, wherein the mammalian cells are islet cells.

43. A method of providing functional cells to an individual in need thereof comprising administering to the individual an effective amount of the hydrogel capsules of any one of claims 18-42.

44. A method of making hydrogel capsules encapsulating cells,

wherein the capsules consist of three layers:

an inner acellular core layer,

a hydrogel layer containing cells to be transplanted selected from the group consisting of mammalian secretory cells, mammalian metabolic cells, mammalian structural cells, and aggregates thereof, and

an outer acellular barrier or structural layer,

the method comprising:

providing an electrospraying device with a nozzle that consists of three separate concentric tubes at its outlet;

pumping a hydrogel forming material, optionally including one or more anti-inflammatory drugs or imaging reagents, into the innermost tube of the nozzle;

pumping a second stream that contains hydrogel forming material and cells to be encapsulated into the middle tube of the nozzle;

pumping a third stream that contains a hydrogel forming material into the outermost tube, wherein the three streams meet at the outlet of the nozzle, and the viscosity of the hydrogel solution prevents any significant intermixing among the three streams, so that droplets with three distinct concentric layers are formed under the electric field; and

allowing the droplets to fall into a gel bath which contains divalent ions to crosslink the hydrogel and form and triple-layer capsules.

45. A method of making hydrogel capsules encapsulating cells,

wherein the capsules consist of two or more layers:

a hydrogel layer containing cells to be transplanted selected from the group consisting of mammalian secretory cells, mammalian metabolic cells, mammalian structural cells, and aggregates thereof; and

an outer acellular barrier or structural layer,

wherein the capsule has a diameter of at least 1 mm and less than 8 mm and elicits less of a fibrotic reaction after implantation than the same capsule having a diameter of less than 1 mm,

the method comprising:

providing a first hydrogel fluid and a second hydrogel fluid, the first having cells suspended therein, to a two-fluid co-axial electro-jet, wherein the relatively high viscosity of the two fluids and short interaction time between them prevents the fluids from intermixing under electrostatic force;

forming microdroplets with core–shell structures; and

crosslinking the microdroplets to form hydrogel capsules in a gelling bath containing divalent crosslinking ions.

46. A biomedical device for implantation comprising biocompatible materials, wherein the device has a diameter of at least 1 mm and less than 10 mm, wherein surface pores of the device are greater than 0 nm and less than 10 μm, wherein the surface of the device is neutral or hydrophilic, wherein the device has a spheroid-like shape, wherein the curvature of the surface of the device is at least 0.2 and not greater than 2 on all points of the surface, wherein the surface of the device does not have flat sides, sharp angles, grooves, or ridges, and wherein the device elicits less of a fibrotic reaction after implantation than the same device having a diameter of less than 1 mm.

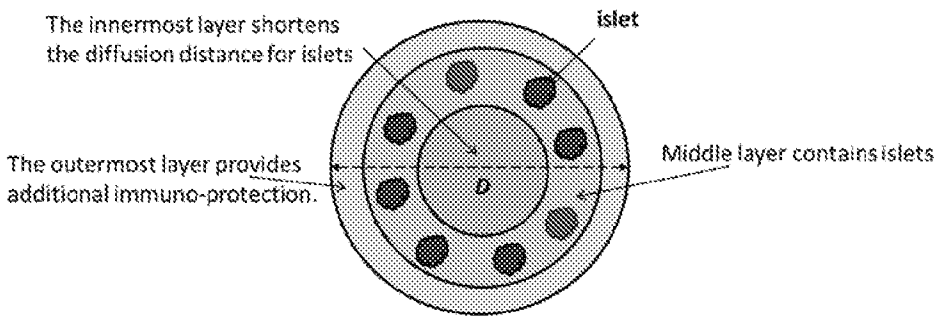
The innermost layer shortens the diffusion distance for islets
islet
The outermost layer provides additional immuno-protection.
Middle layer contains islets
D

FIG. 1

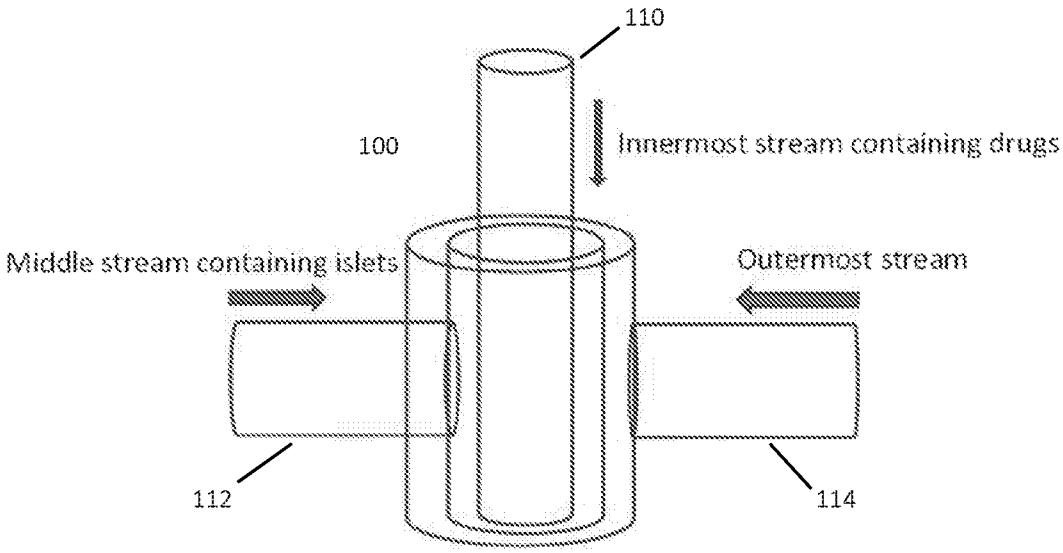
110
100
Innermost stream containing drugs
Middle stream containing islets
Outermost stream
112
114

FIG. 2

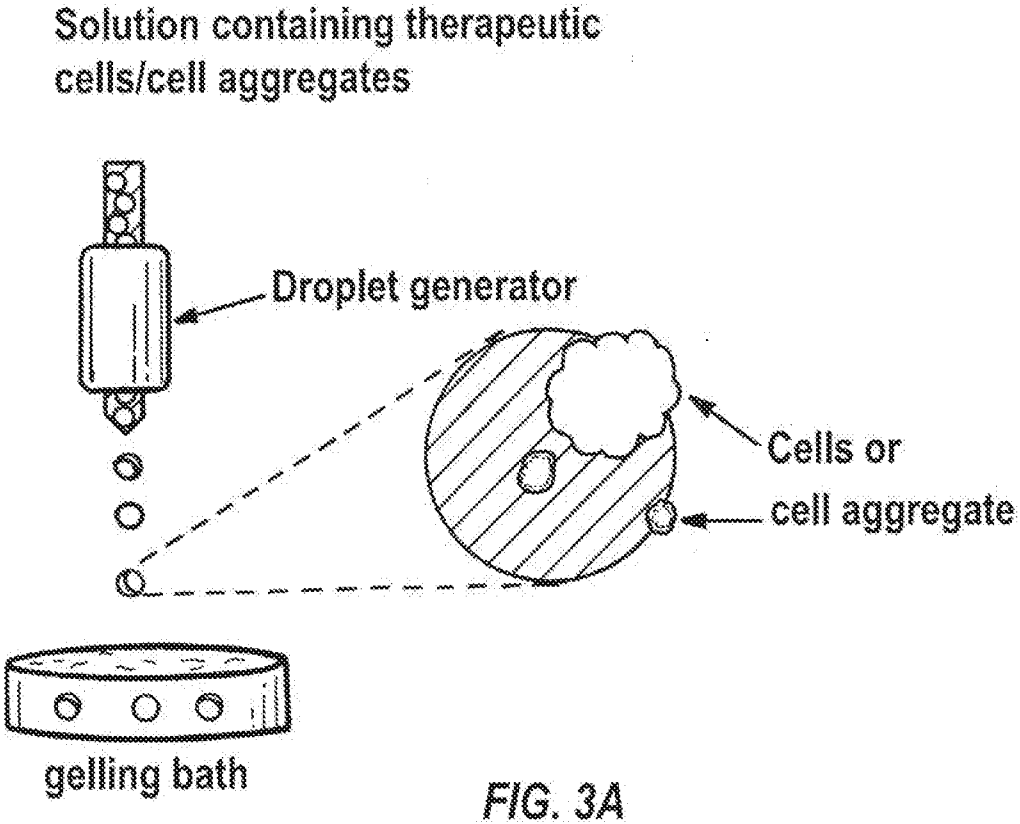
Solution containing therapeutic cells/cell aggregates
Droplet generator
Cells or
cell aggregate
gelling bath

FIG. 3A

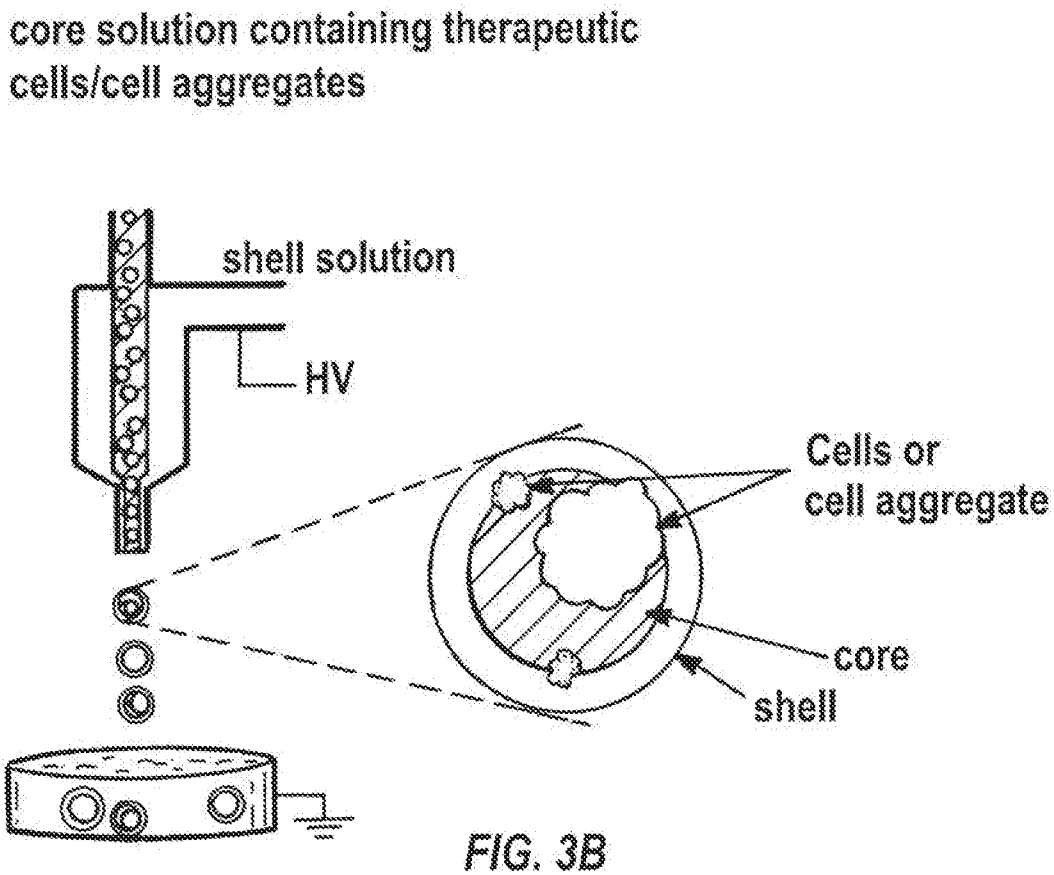
core solution containing therapeutic cells/cell aggregates
shell solution
HV
Cells or
cell aggregate
core
shell

FIG. 3B

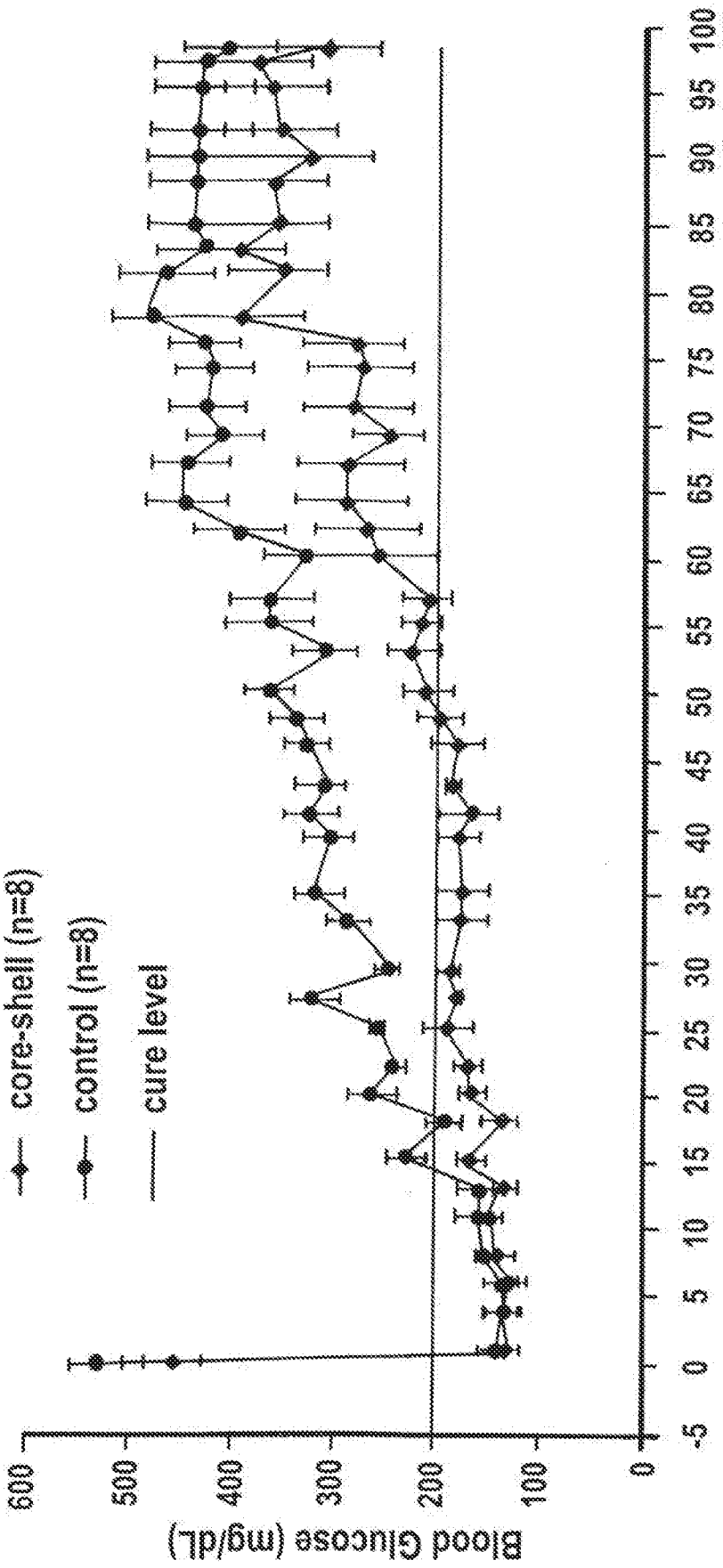
core-shell (n=8)
control (n=8)
cure level
Blood Glucose (mg/dL)
600
500
400
300
200
100
0
-5
0
5
10
15
20
25
30
35
40
45
50
55
60
65
70
75
80
85
90
95
100
Days after transplantation

FIG. 4A

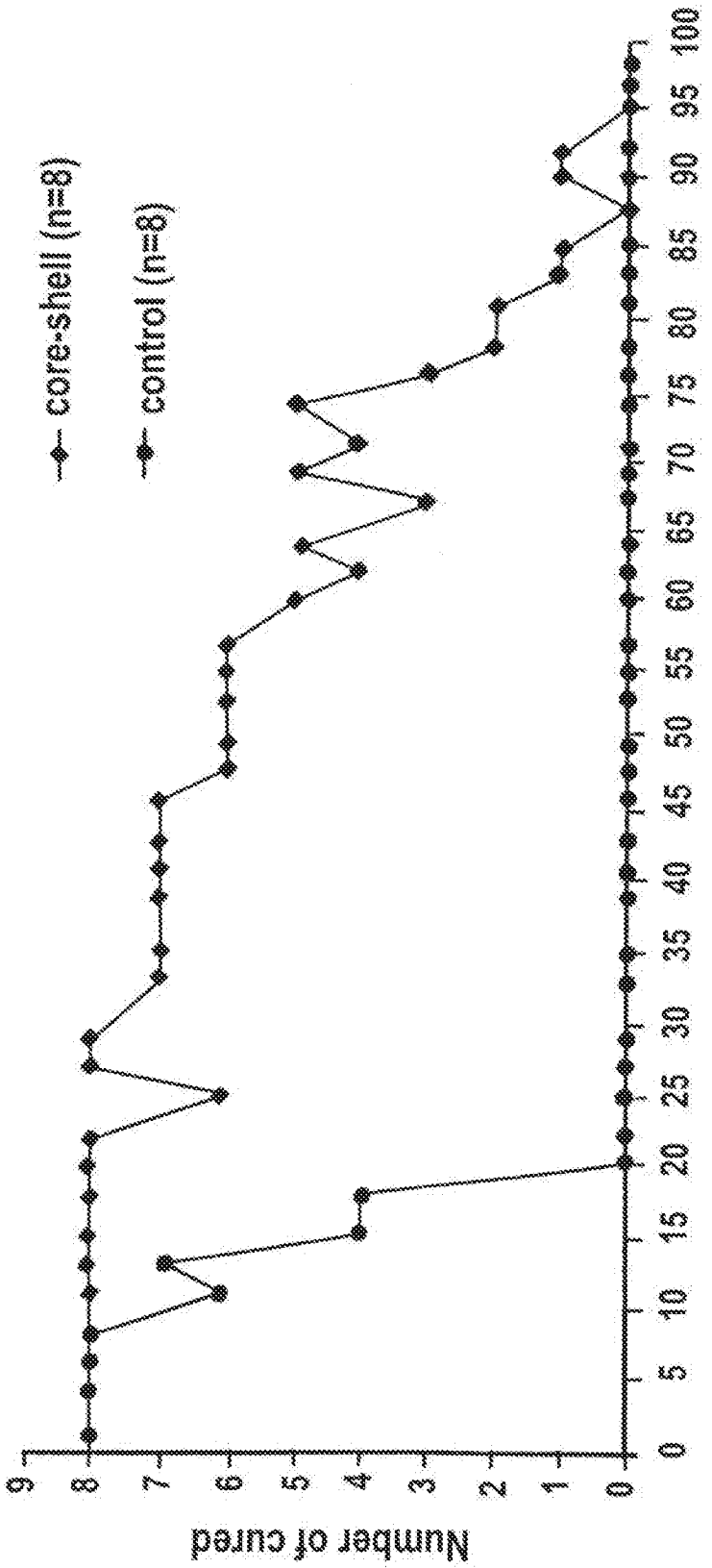
core-shell (n=8)
control (n=8)
Number of cured
Days after transplantation
0
1
2
3
4
5
6
7
8
9
0
5
10
15
20
25
30
35
40
45
50
55
60
65
70
75
80
85
90
95
100

FIG. 4B

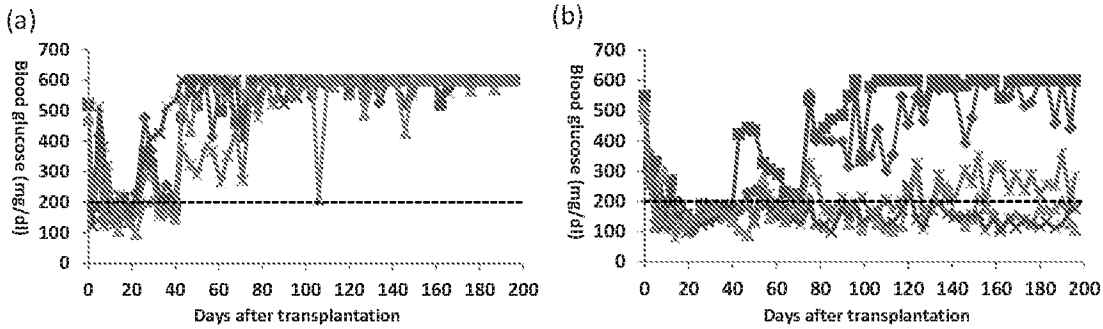

FIGS. 5A and 5B

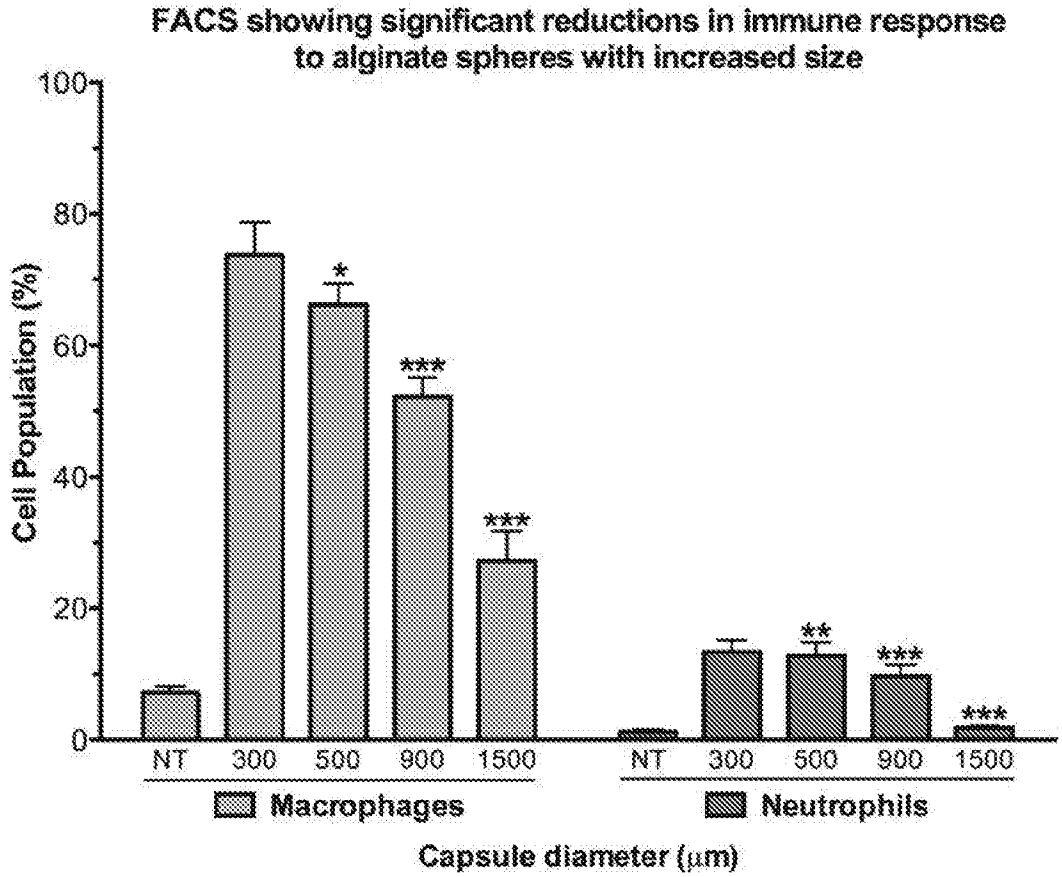

*, $p < 0.05$; **, $p < 0.01$; ***, $p < 0.001$, vs. 300 μm

FIG. 6

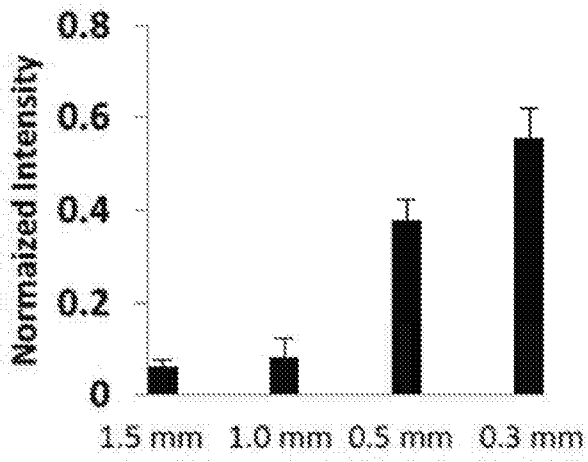
Normaized Intensity
0.8
0.6
0.4
0.2
0
1.5 mm
1.0 mm
0.5 mm
0.3 mm

FIG. 7

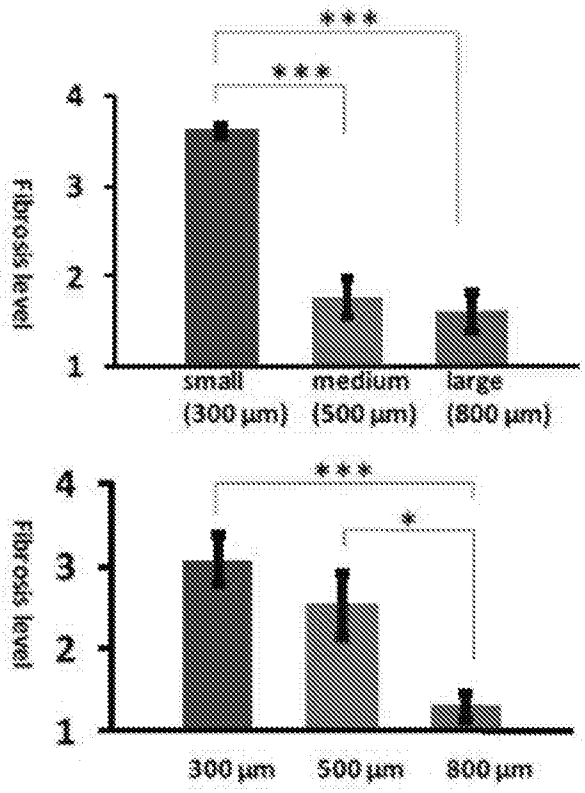
***
***
4
3
2
1
Fibrosis level
small (300 µm)
medium (500 µm)
large (800 µm)
***
*
4
3
2
1
Fibrosis level
300 µm
500 µm
800 µm

FIG. 8

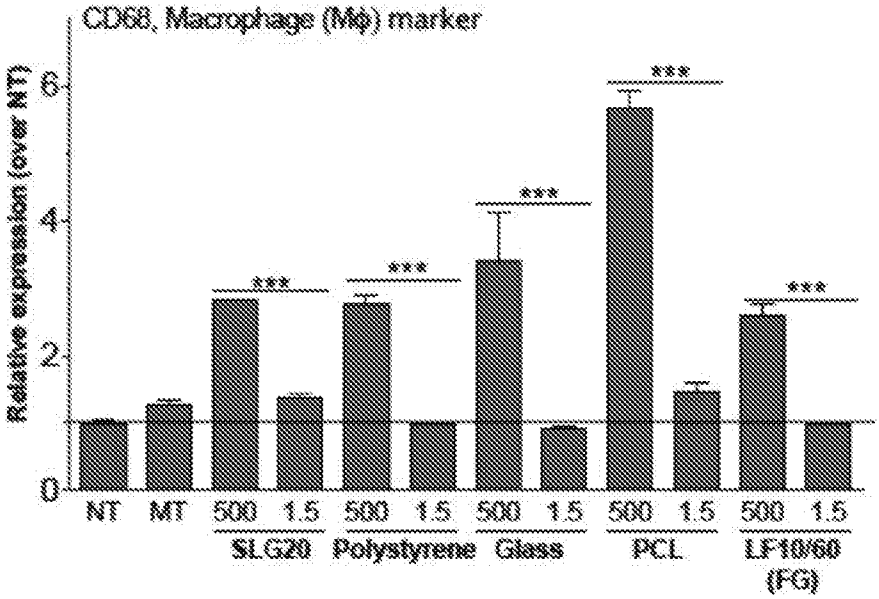
CD68, Macrophage (Mϕ) marker
Relative expression (over NT)
0
2
4
6
***
NT
MT
500
1.5
SLG20
Polystyrene
Glass
PCL
LF10/60 (FG)

FIG. 9A

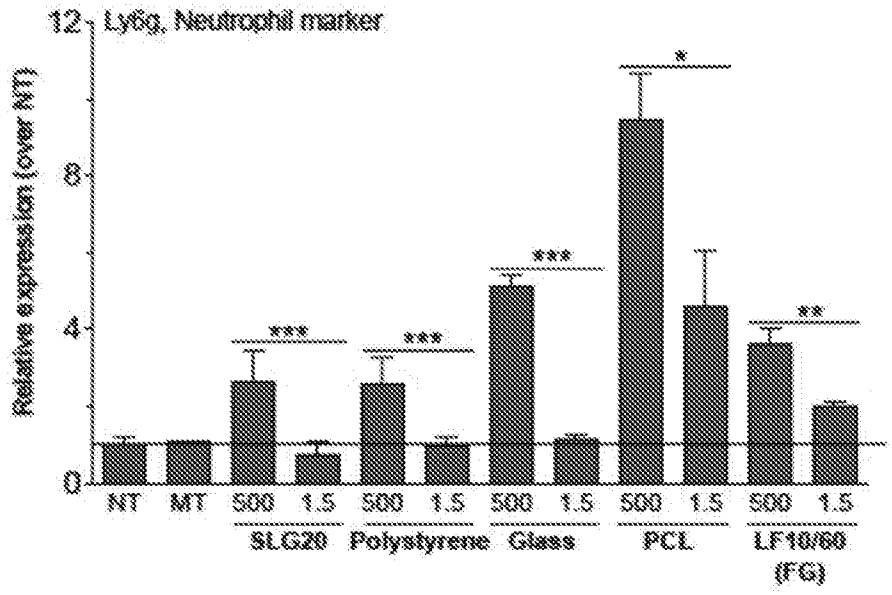
Ly6g, Neutrophil marker
Relative expression (over NT)
0
4
8
12
*
**
***
NT
MT
500
1.5
SLG20
Polystyrene
Glass
PCL
LF10/60 (FG)

FIG. 9B

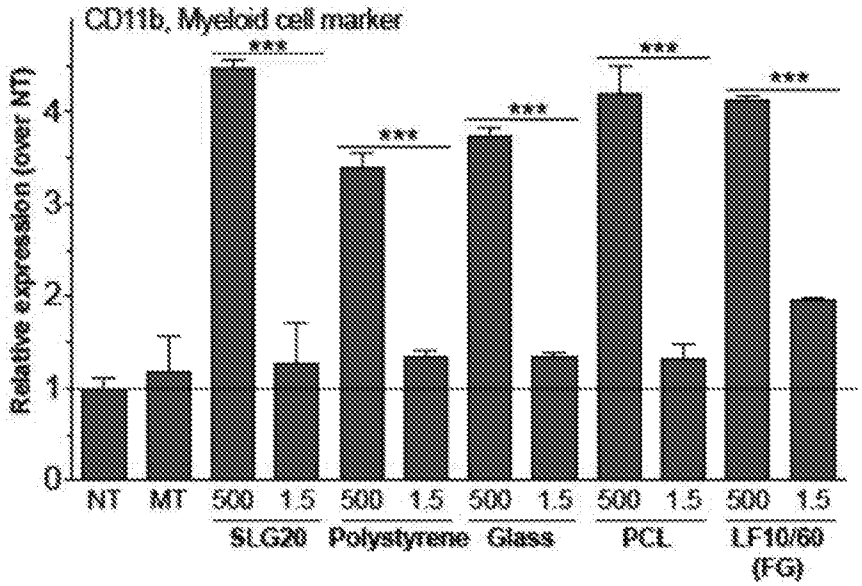
CD11b, Myeloid cell marker
Relative expression (over NT)
0
1
2
3
4
***
NT
MT
500
1.5
SLG20
Polystyrene
Glass
PCL
LF10/60
(FG)

FIG. 9C

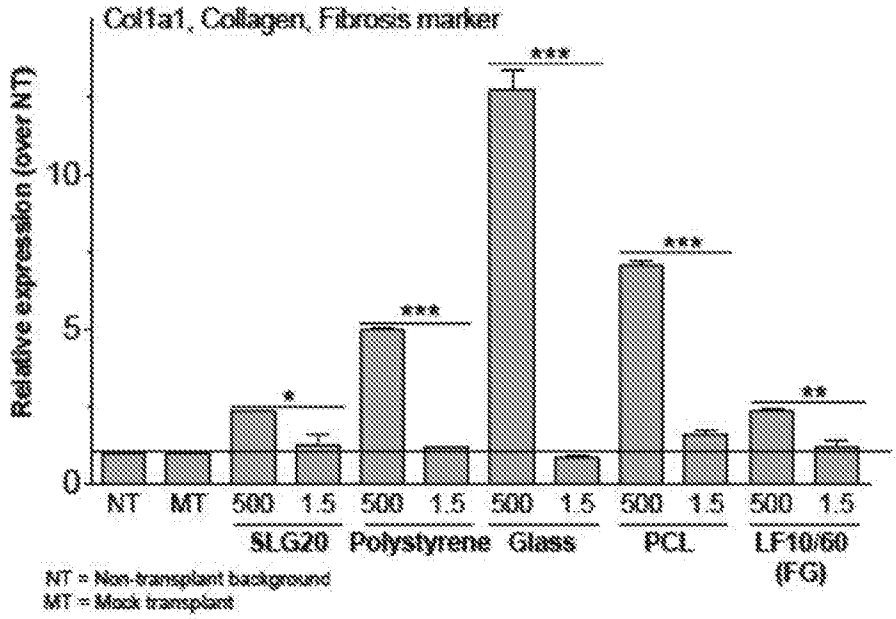
Col1a1, Collagen, Fibrosis marker
Relative expression (over NT)
0
5
10
*
**
***
NT
MT
500
1.5
SLG20
Polystyrene
Glass
PCL
LF10/60
(FG)
NT = Non-transplant background
MT = Mock transplant

FIG. 9D

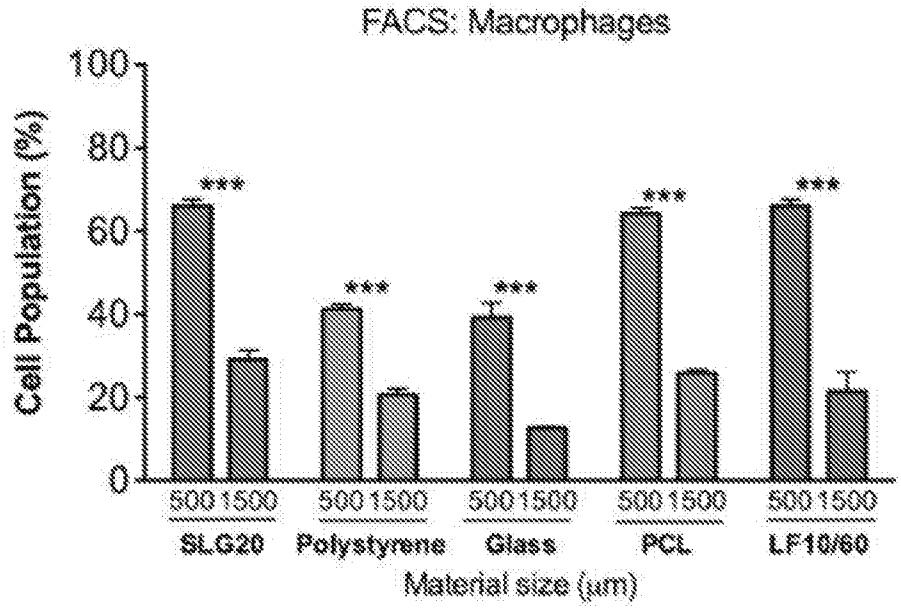

FIG. 10A

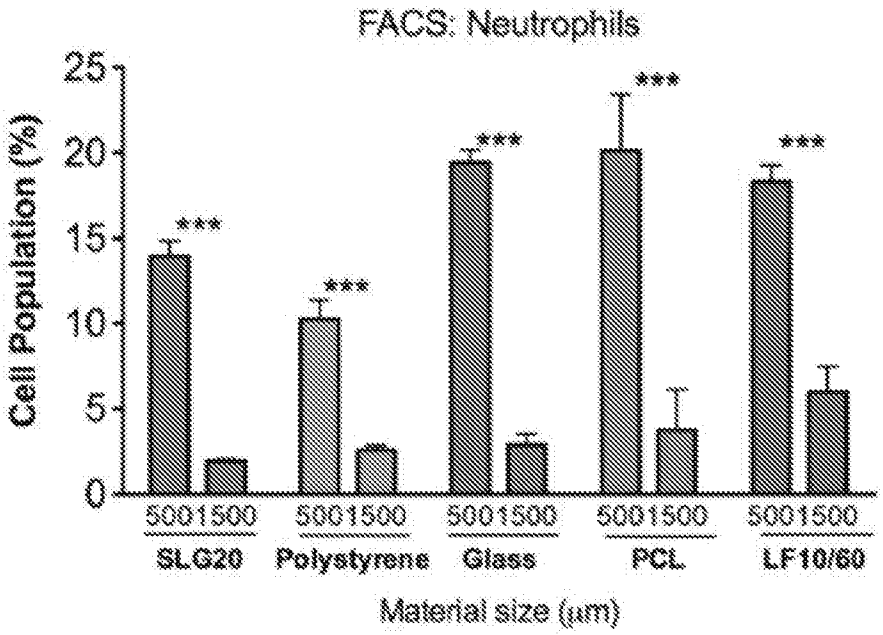

FIG. 10B

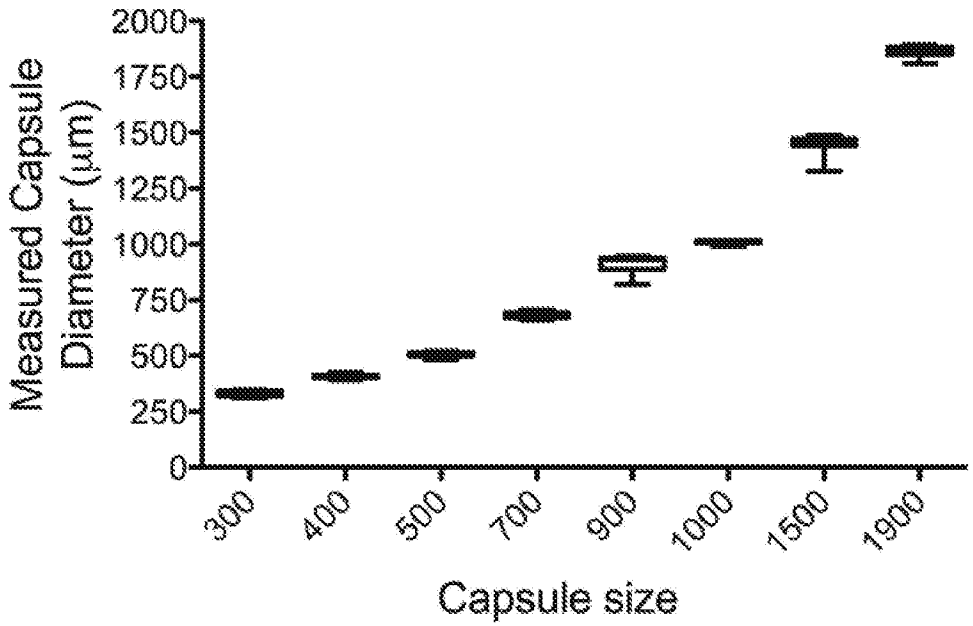
Measured Capsule Diameter (μm)
2000
1750
1500
1250
1000
750
500
250
0
300
400
500
700
900
1000
1500
1900
Capsule size

FIG. 11

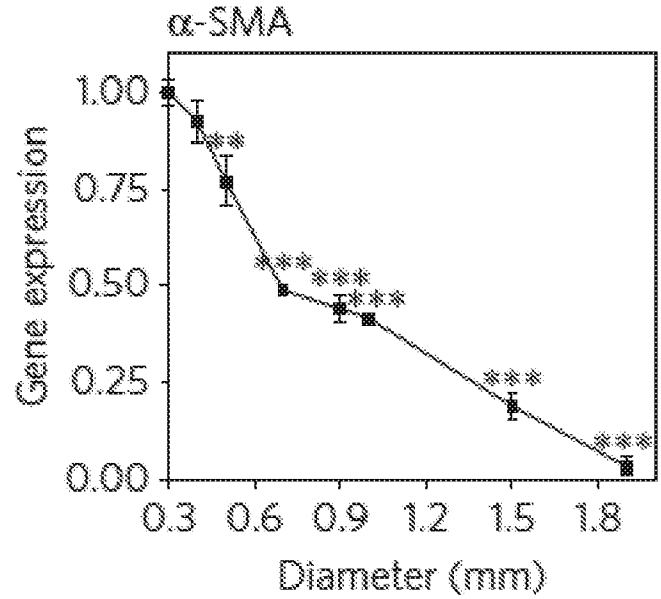

FIG. 12A

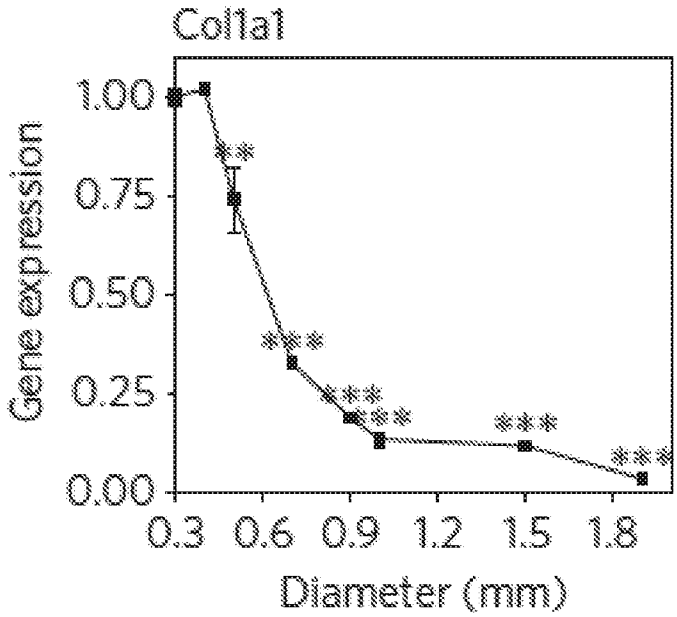

FIG. 12B

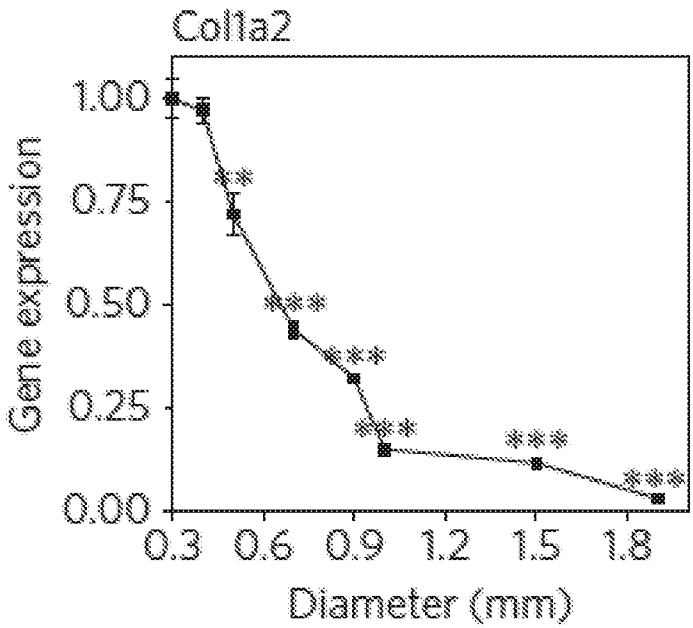

FIG. 12C

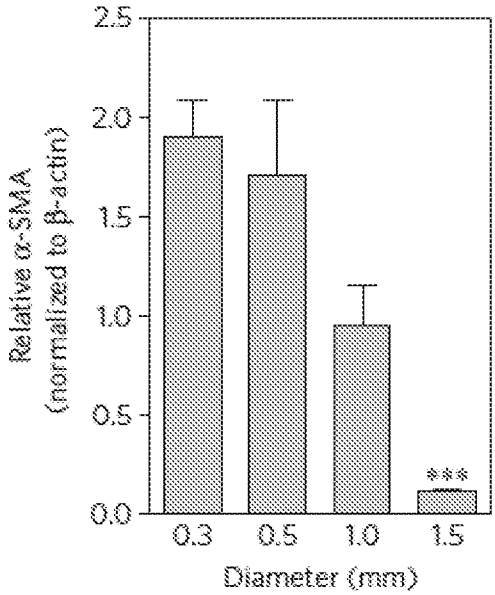

FIG. 12D

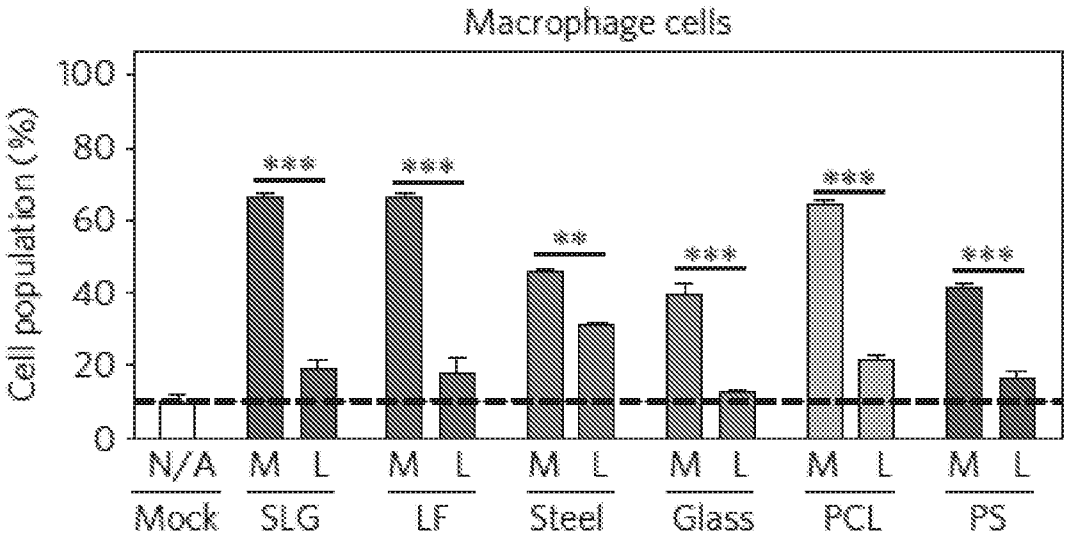

FIG. 13A

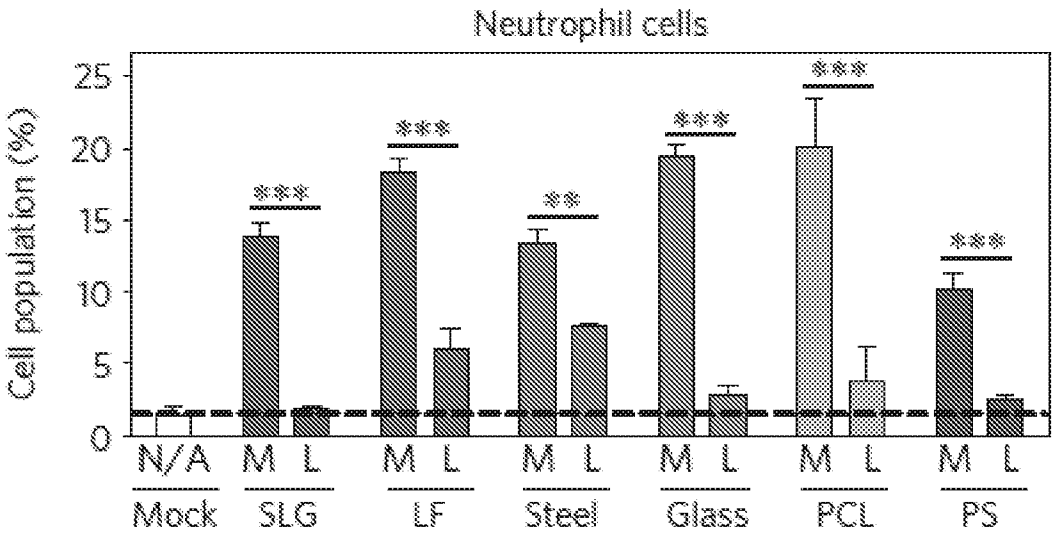

FIG. 13B

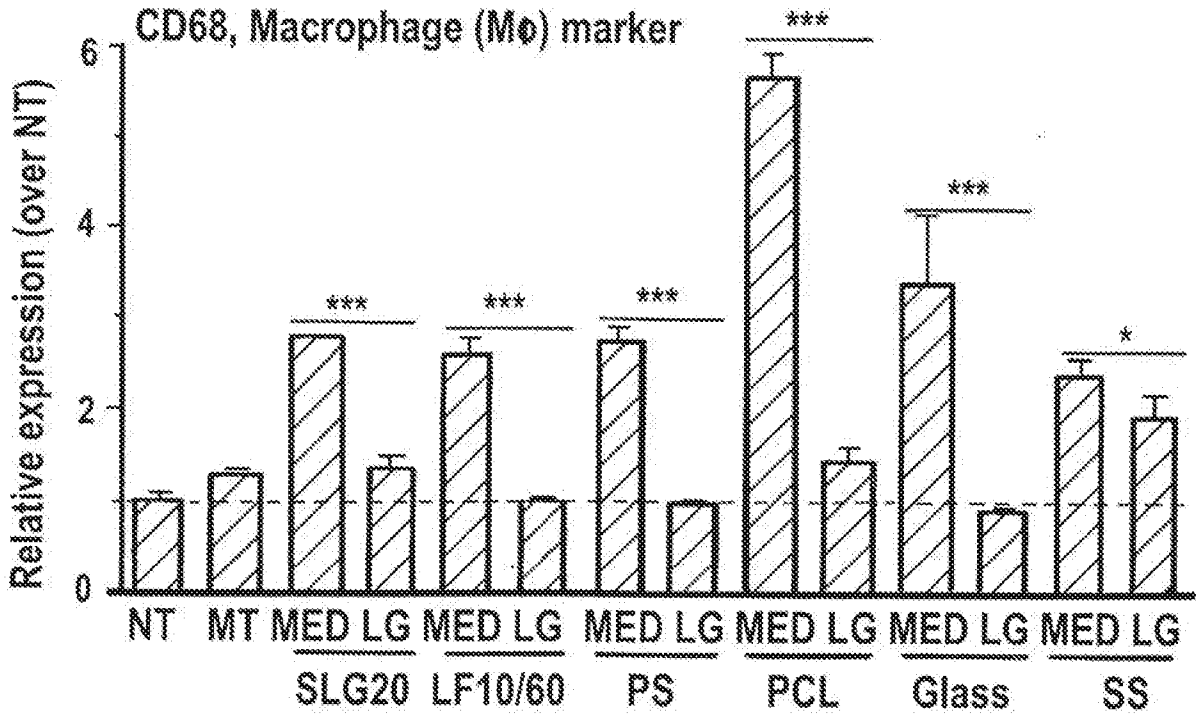

FIG. 14A

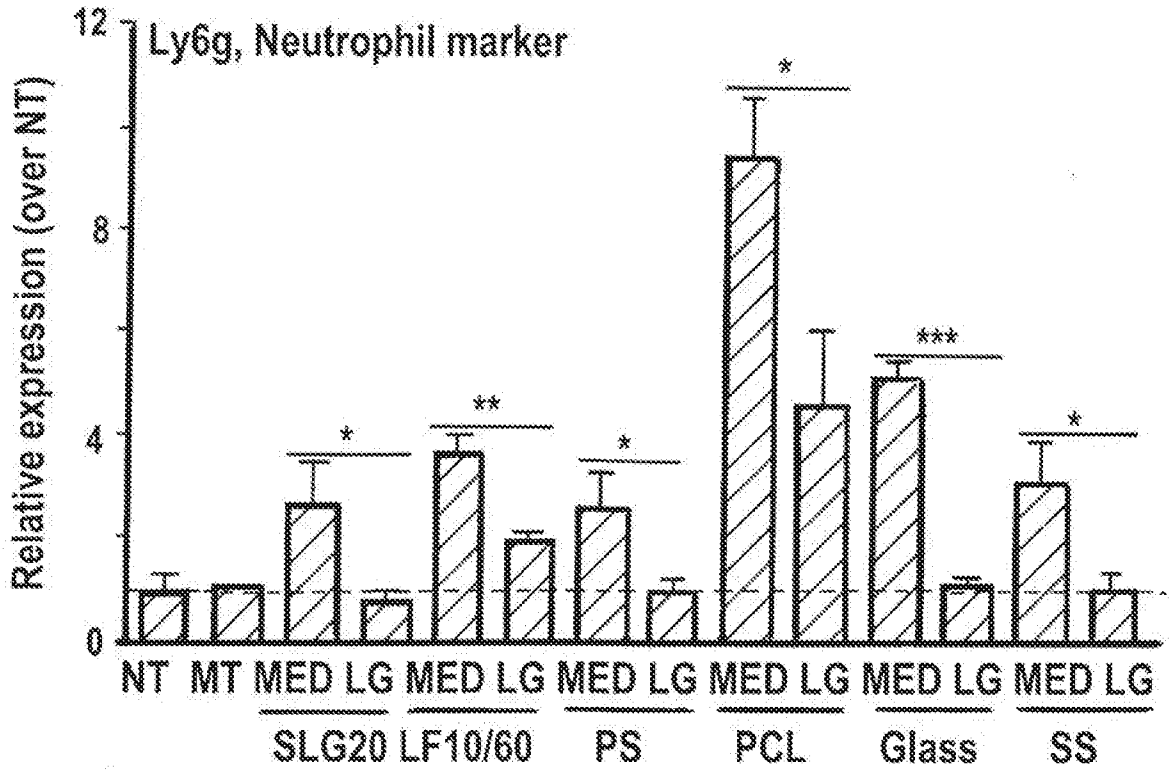

FIG. 14B

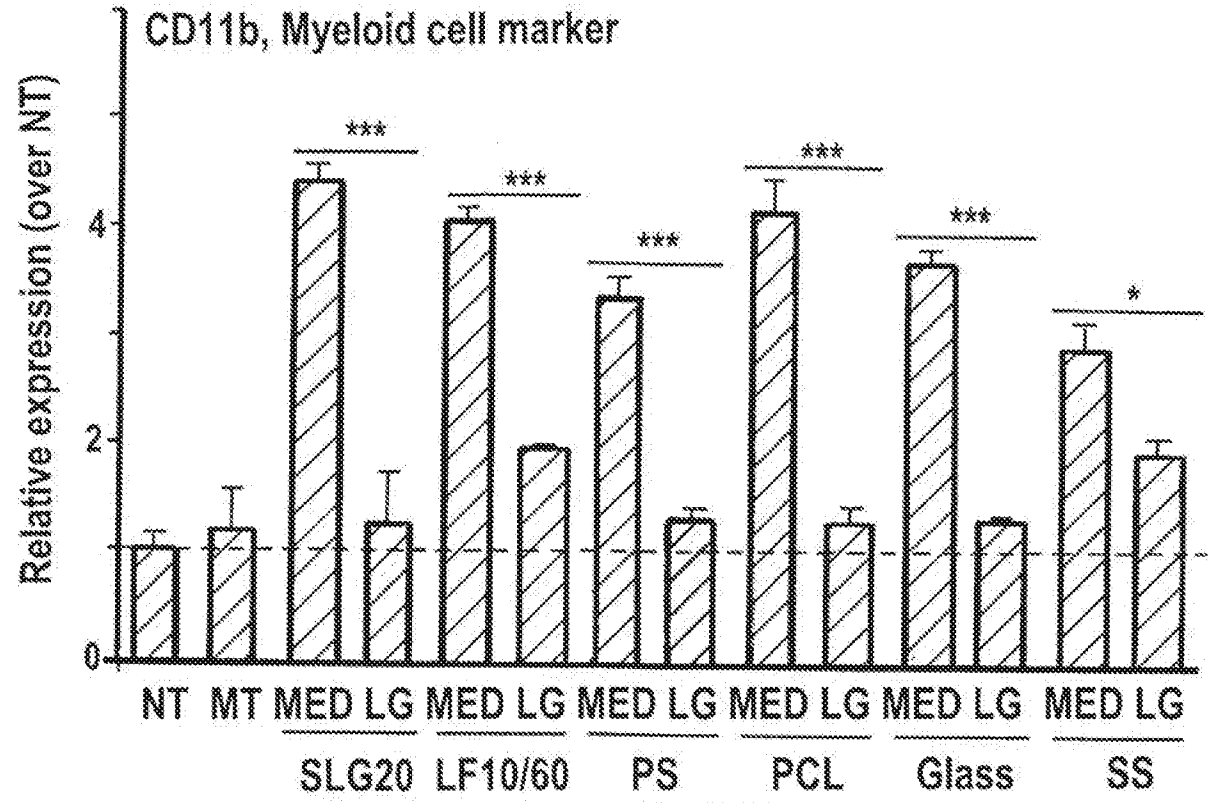

FIG. 14C

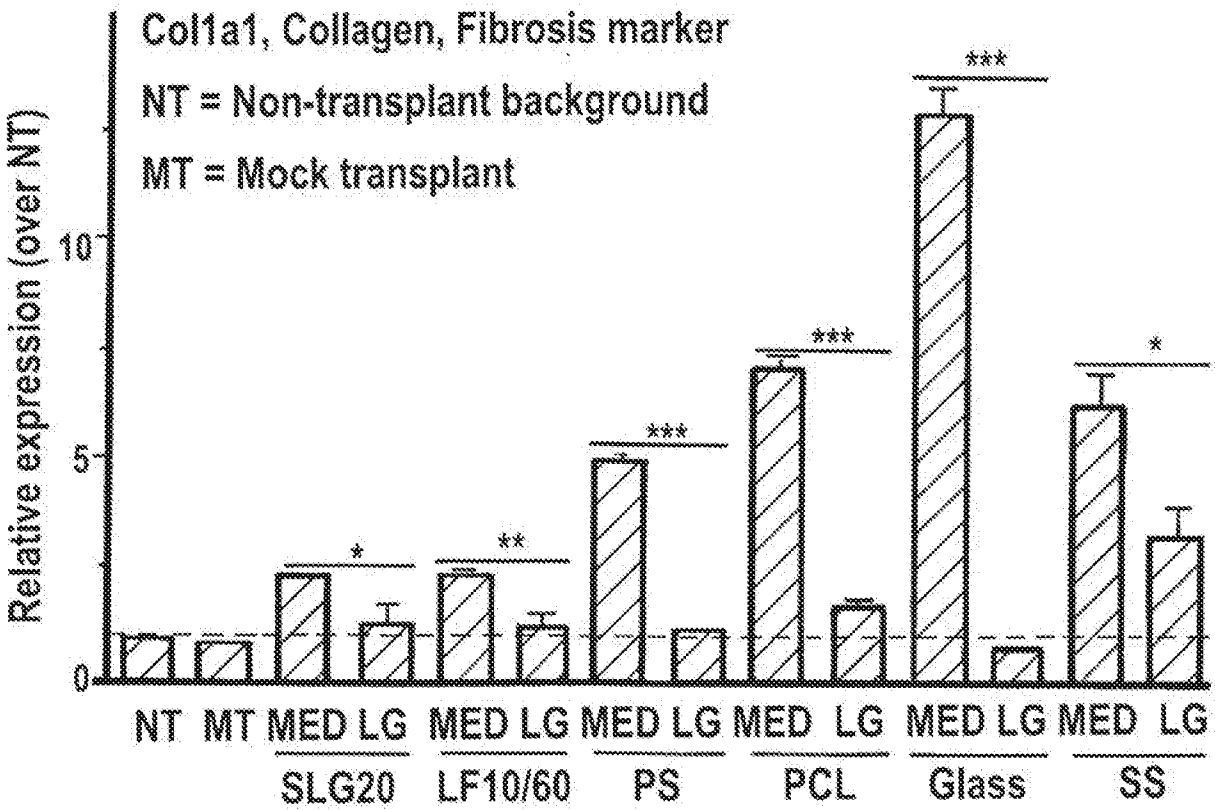

FIG. 14D

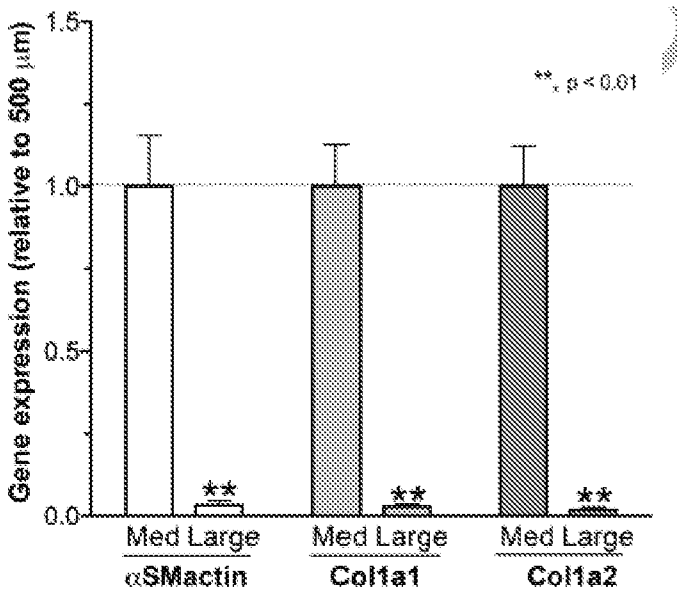
Gene expression (relative to 500 μm)
1.5
1.0
0.5
0.0
**, p < 0.01
**
**
**
Med Large
Med Large
Med Large
αSMactin
Col1a1
Col1a2

FIG. 15

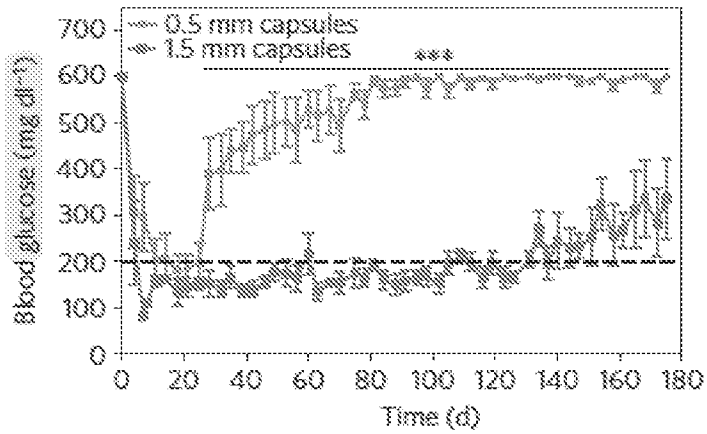

FIG. 16A

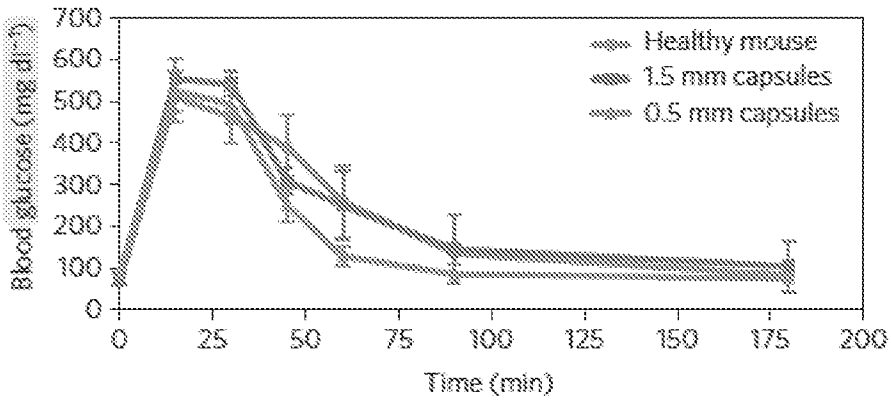

FIG. 16B

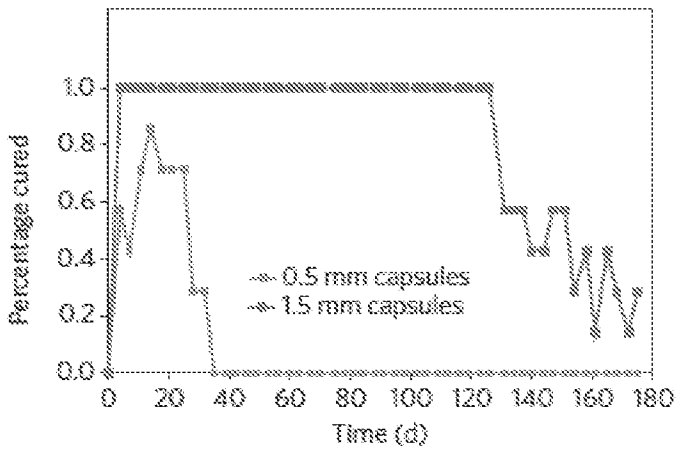

FIG. 16C

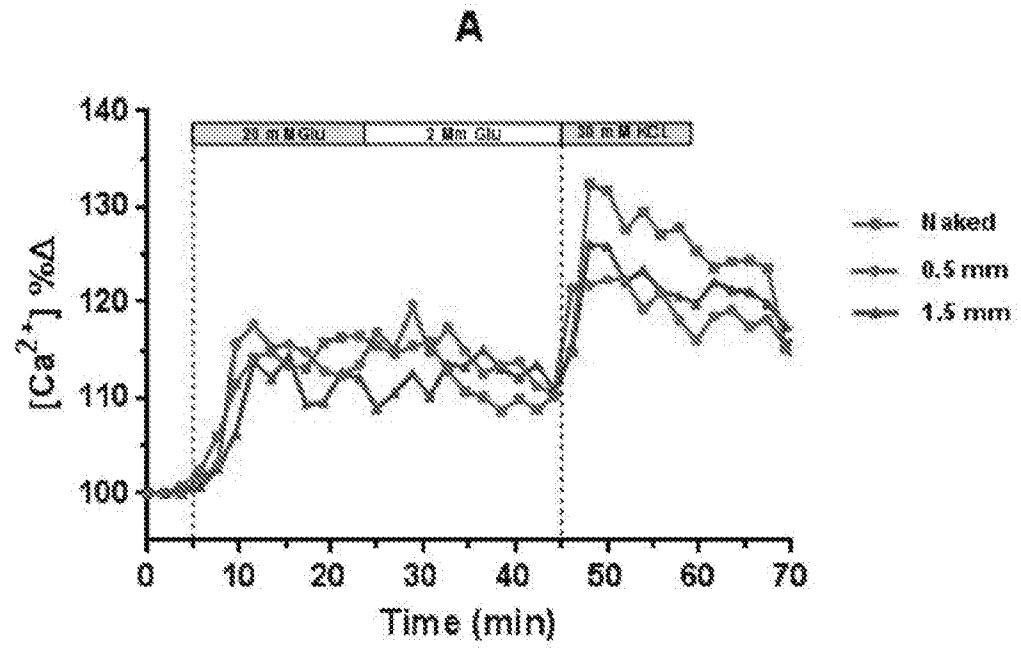

FIG. 17A

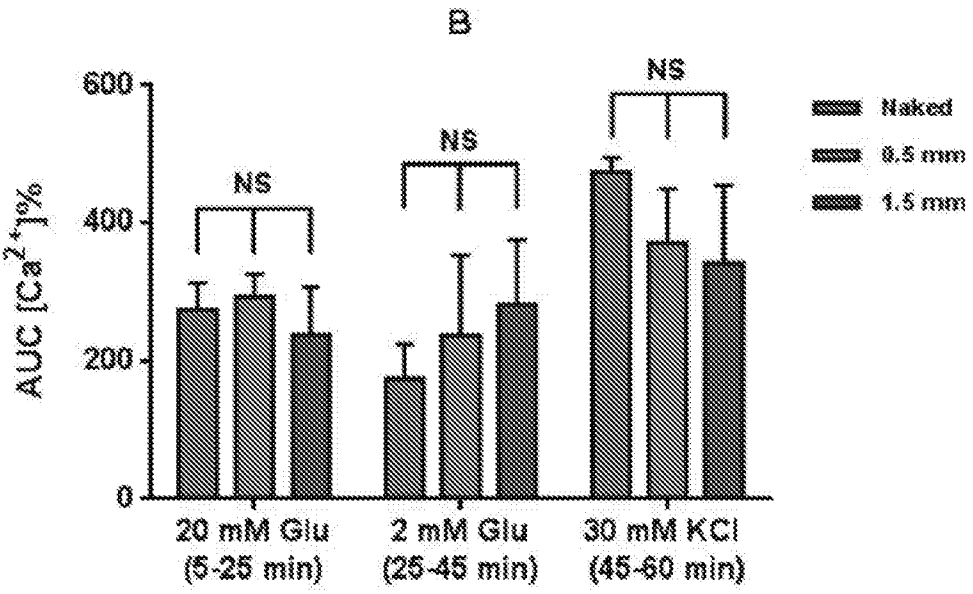

FIG. 17B

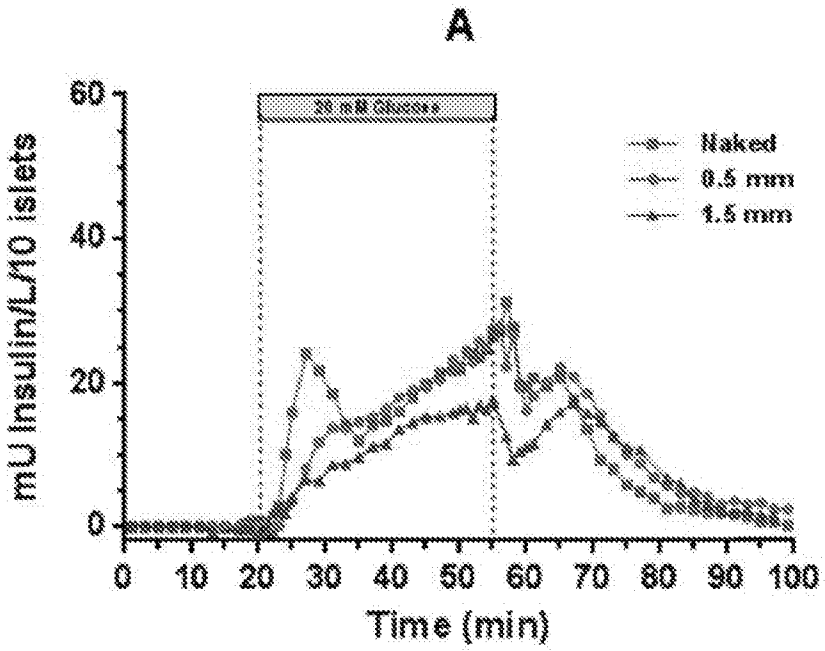

FIG. 18A

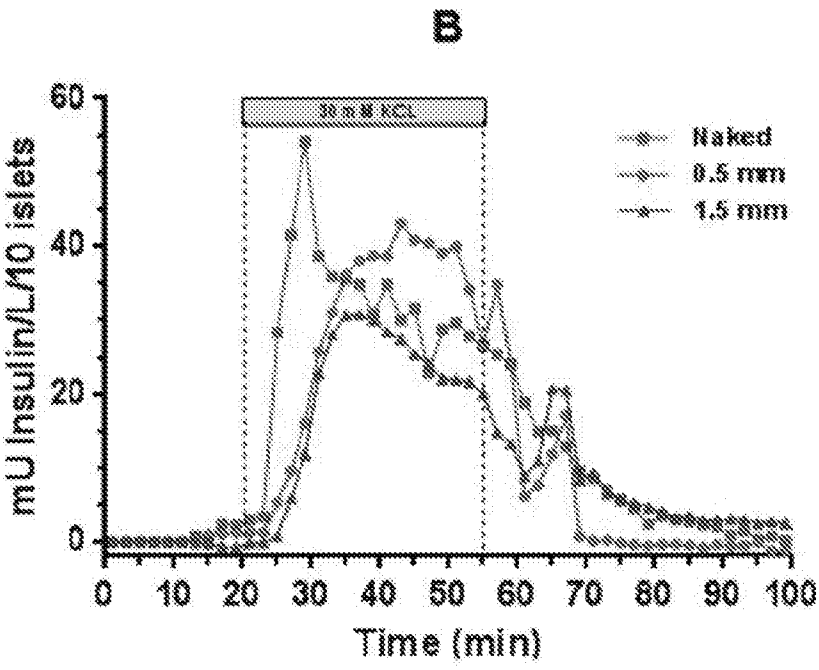

FIG. 18B

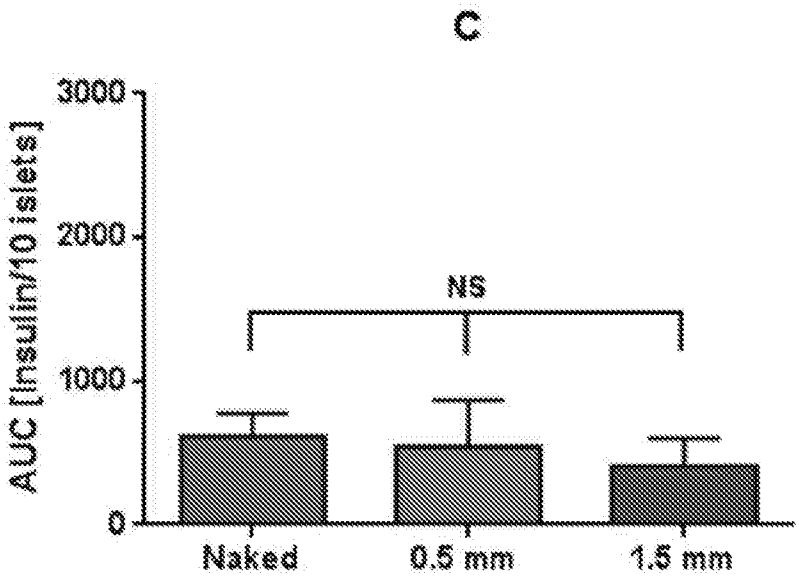

FIG. 18C

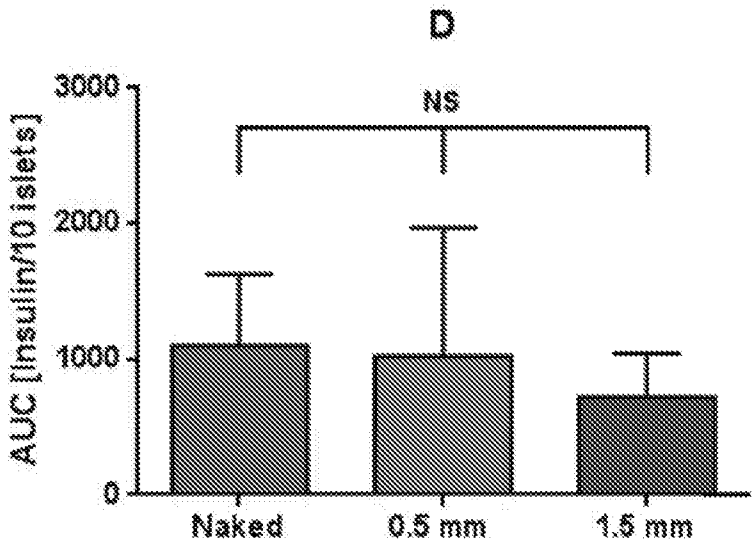

FIG. 18D

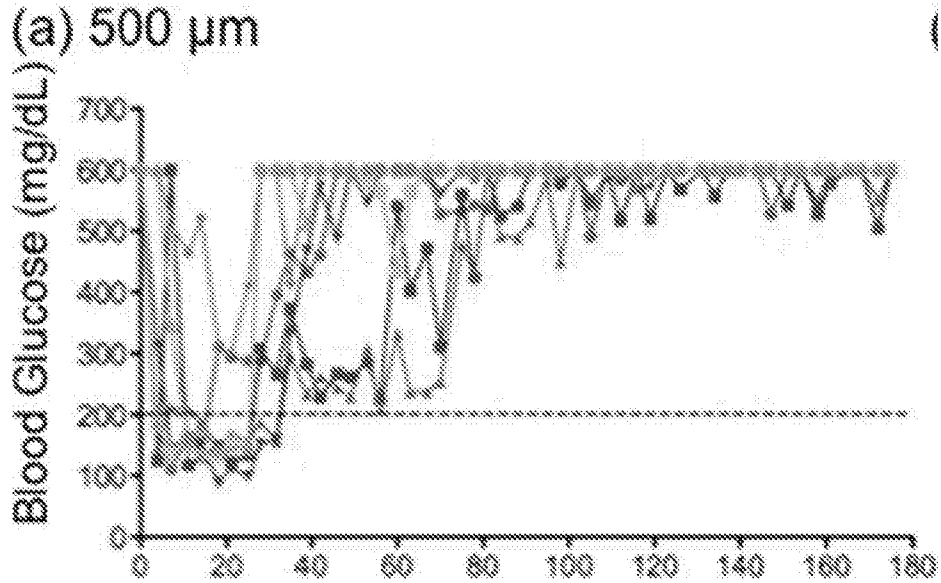

FIG. 19A

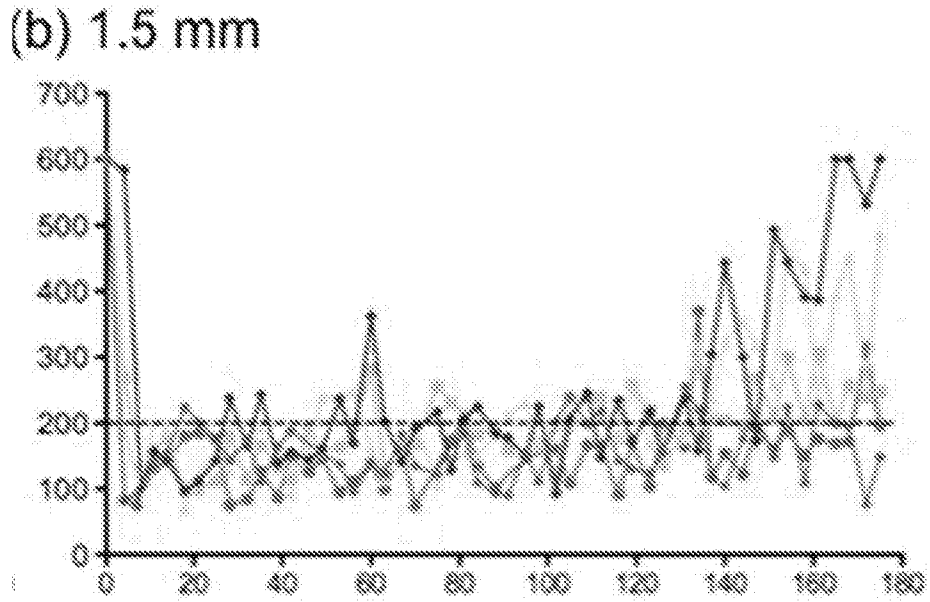

FIG. 19B

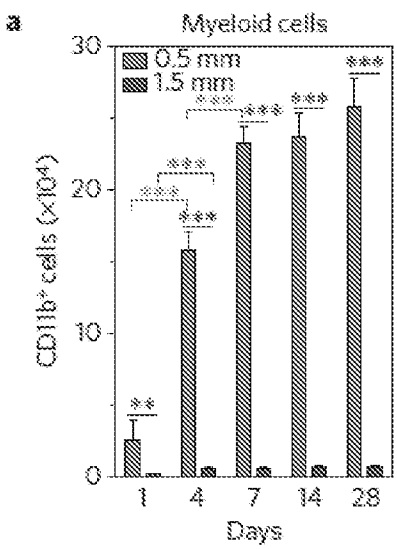

FIG. 20A

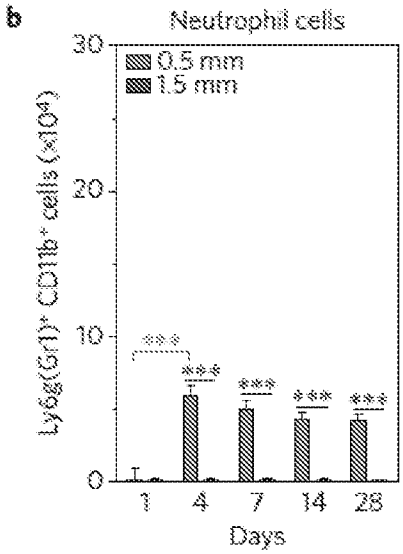

FIG 20B

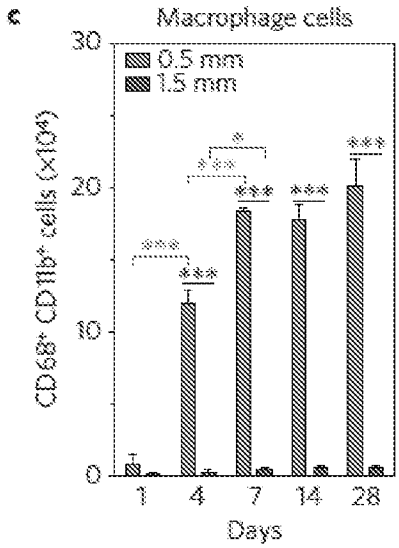

FIG. 20C

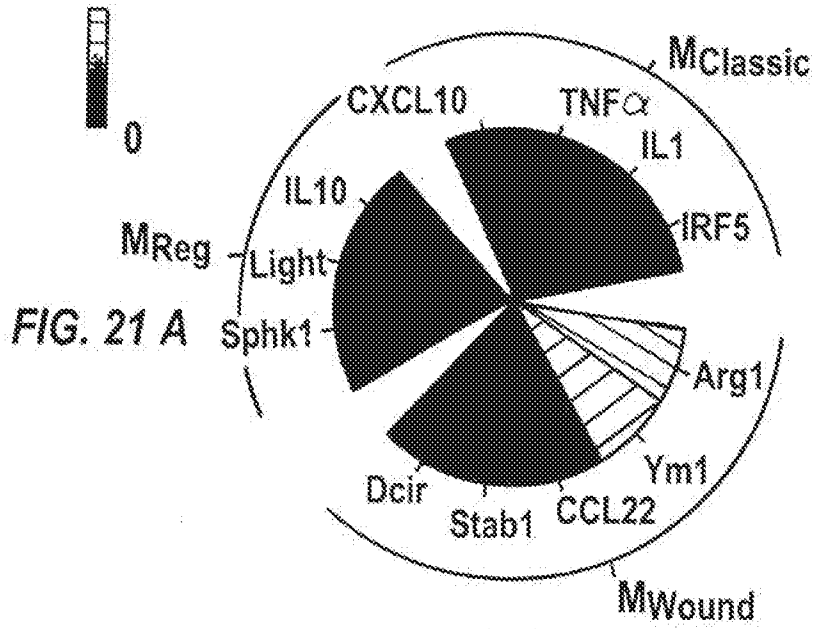

FIG. 21 A

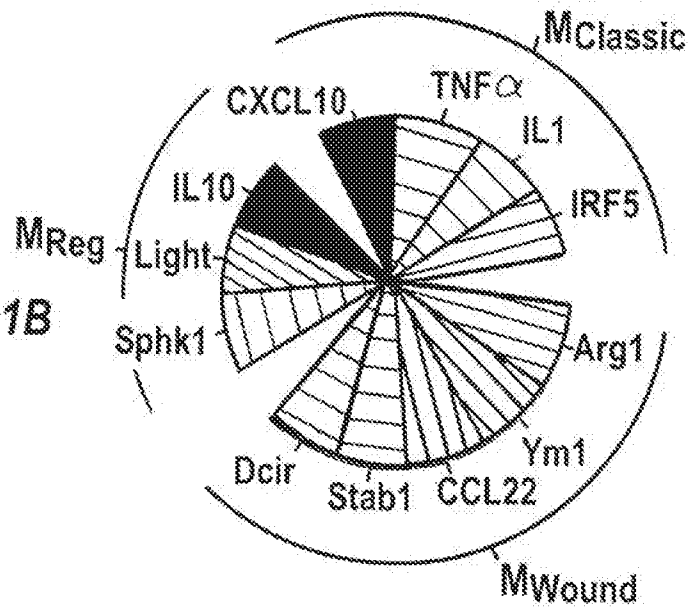

FIG. 21B

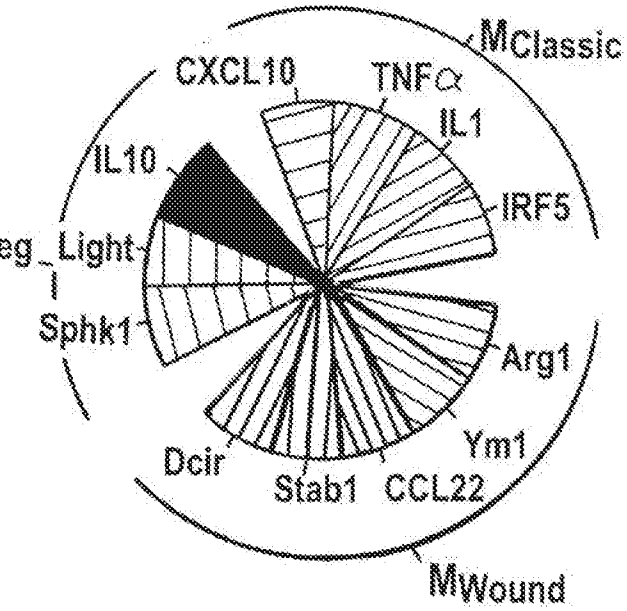

FIG. 21C

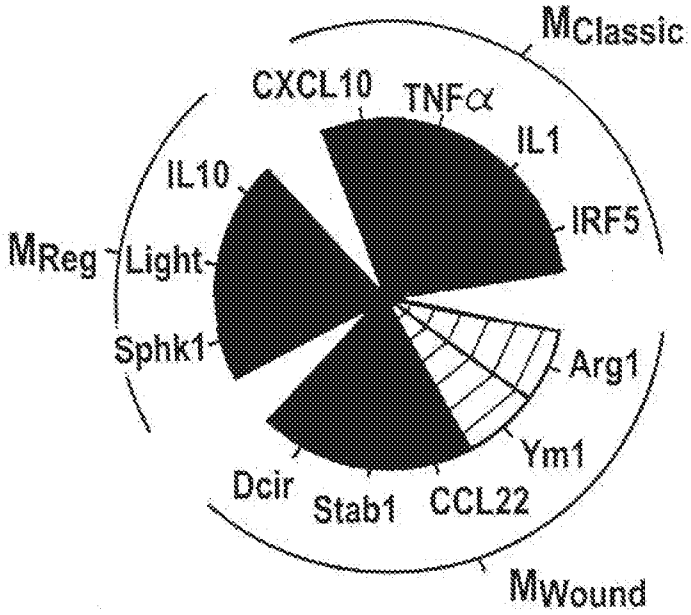

FIG. 21D

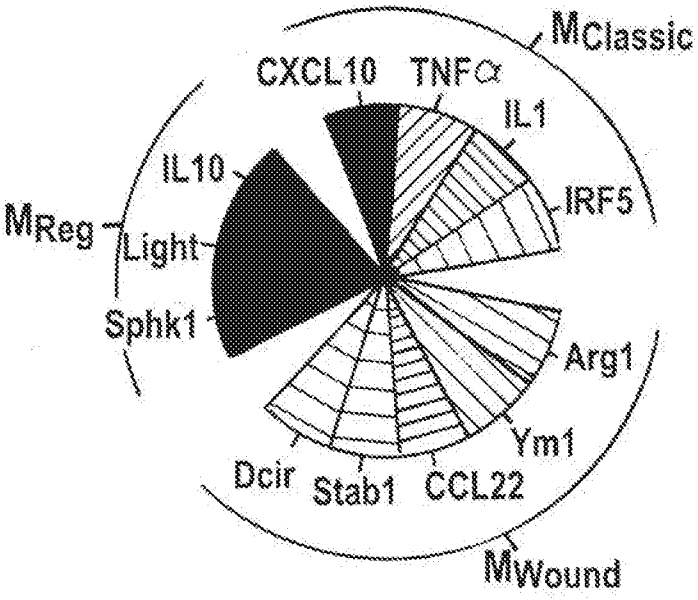

FIG. 21E

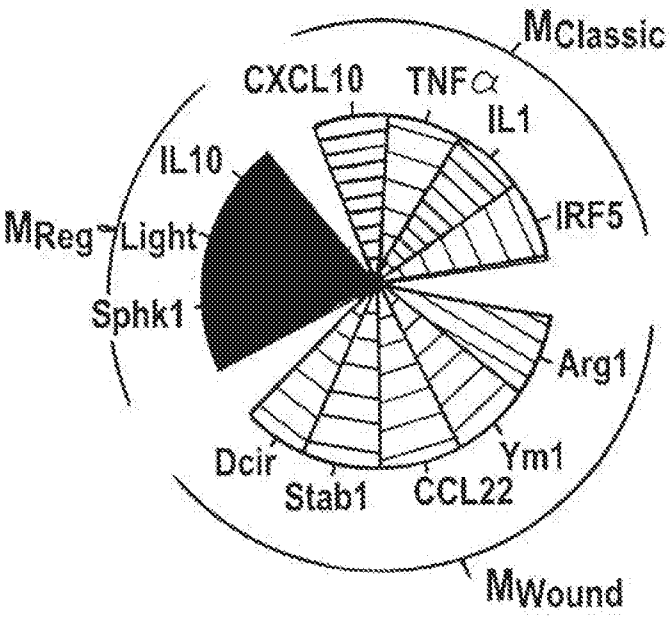

FIG. 21F

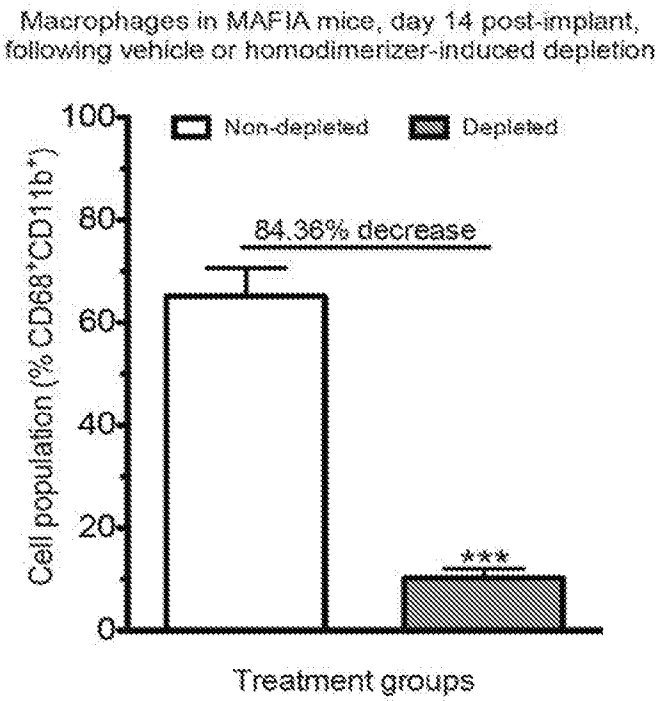
Macrophages in MAFIA mice, day 14 post-implant,
following vehicle or homodimerizer-induced depletion
Non-depleted
Depleted
84.36% decrease
***
Cell population (% CD68+CD11b+)
100
80
60
40
20
0
Treatment groups

FIG. 22

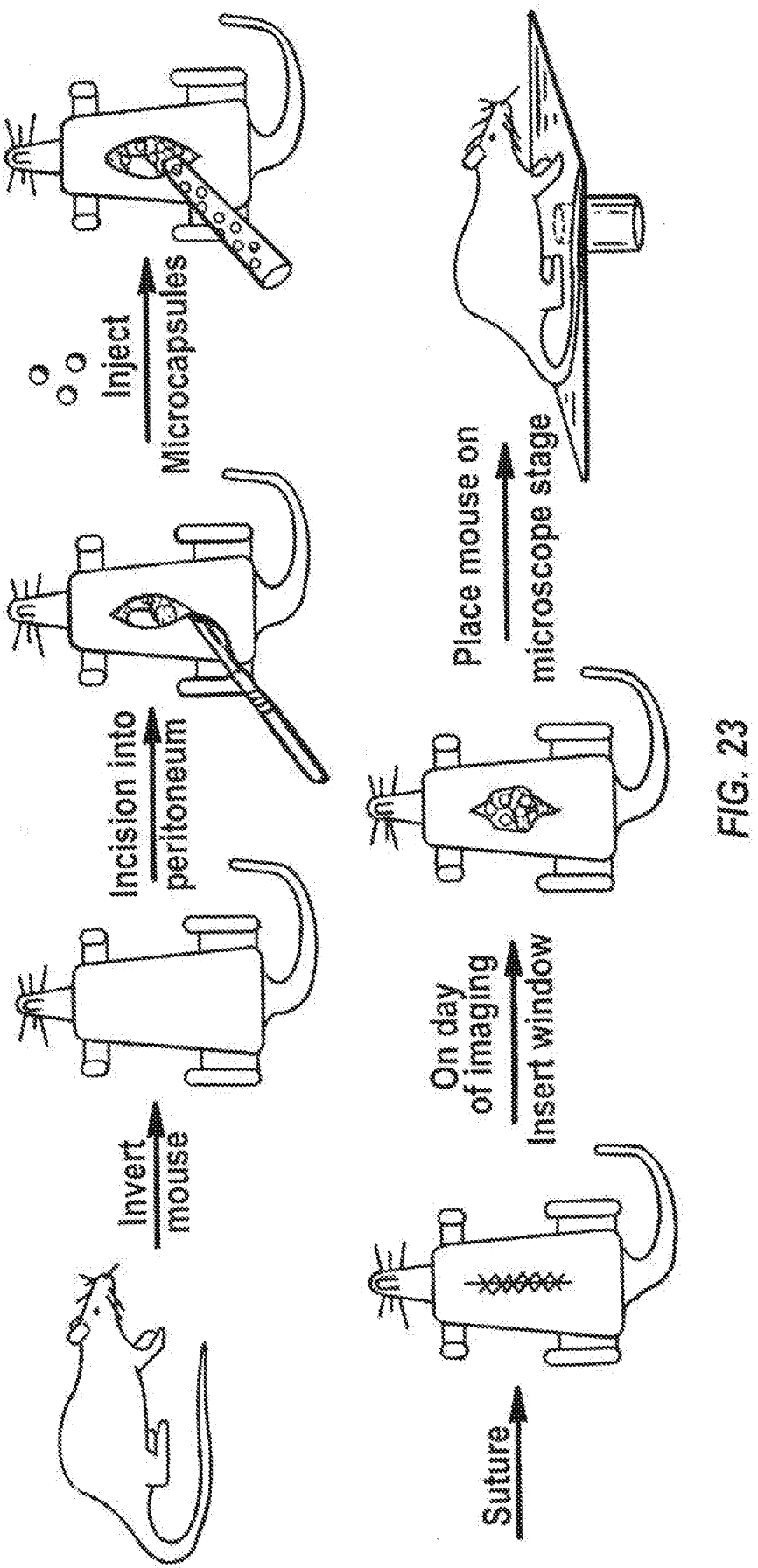
Suture
On day of imaging
Insert window
Place mouse on microscope stage
Invert mouse
Incision into peritoneum
Inject Microcapsules

FIG. 23

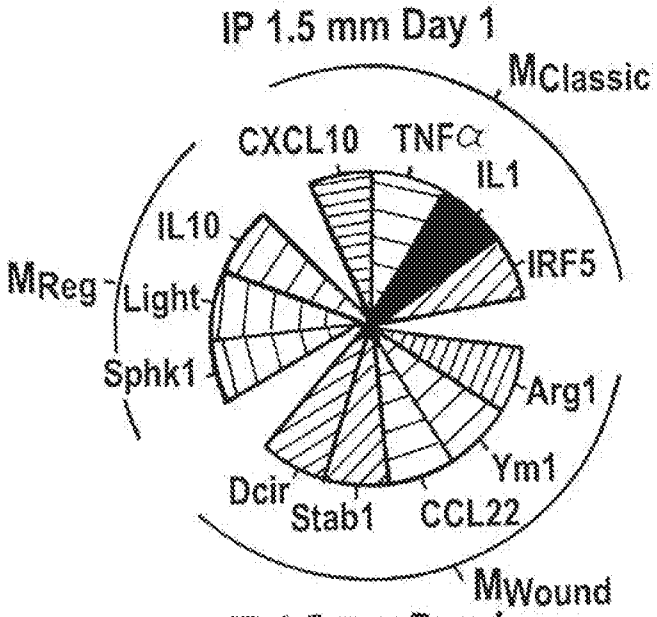

FIG. 24A

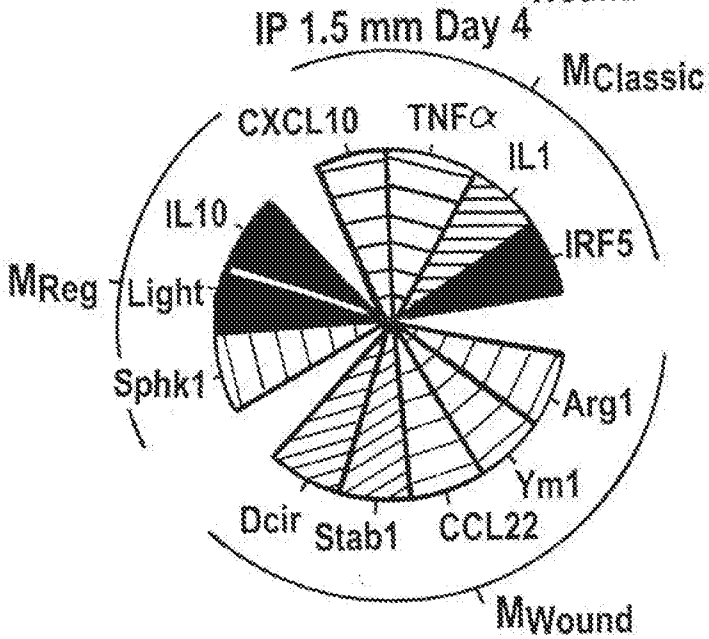

FIG. 24B

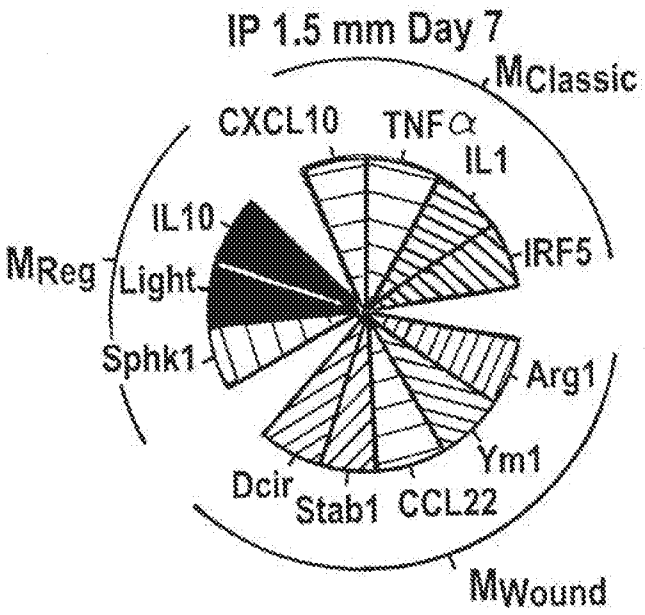

FIG. 24C

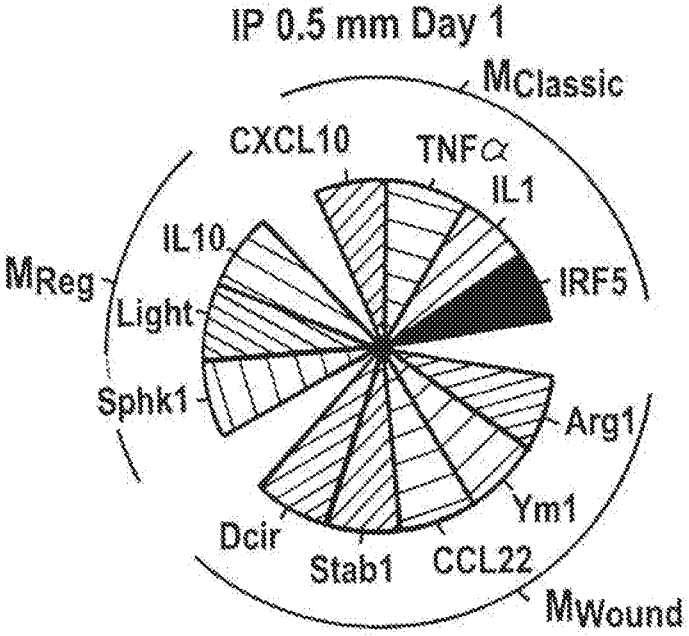

FIG. 24D

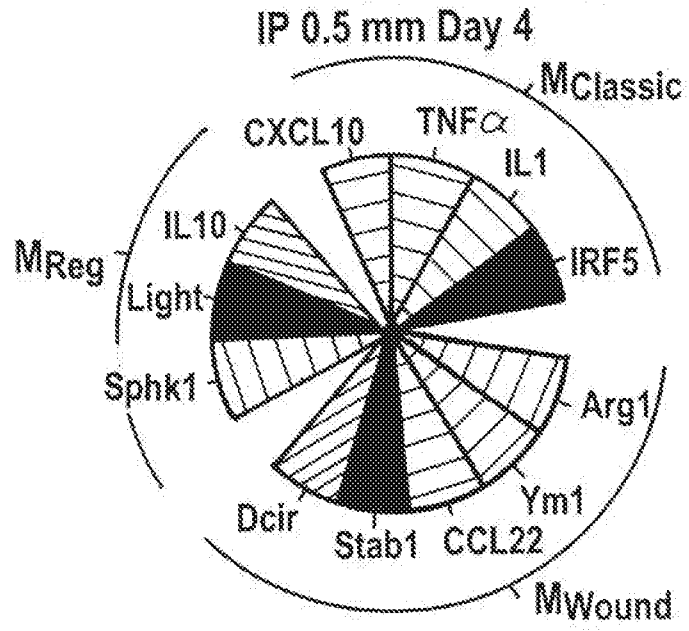

FIG. 24E

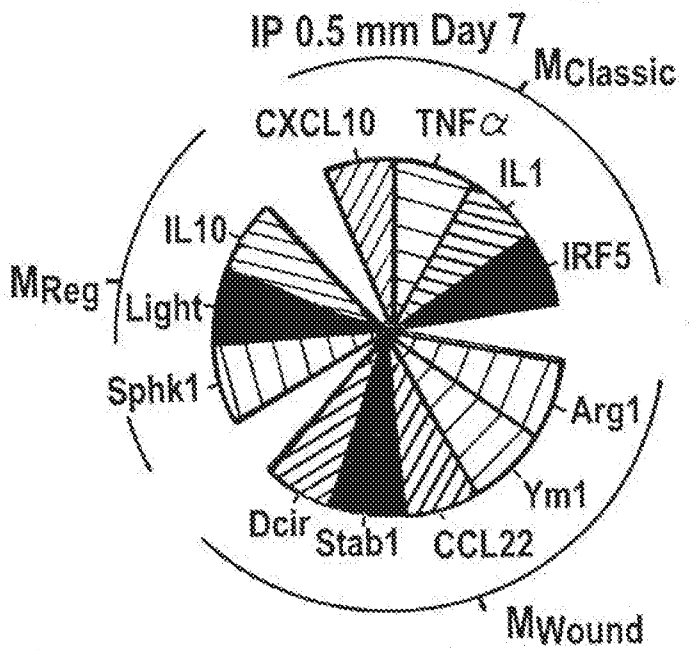

FIG. 24F

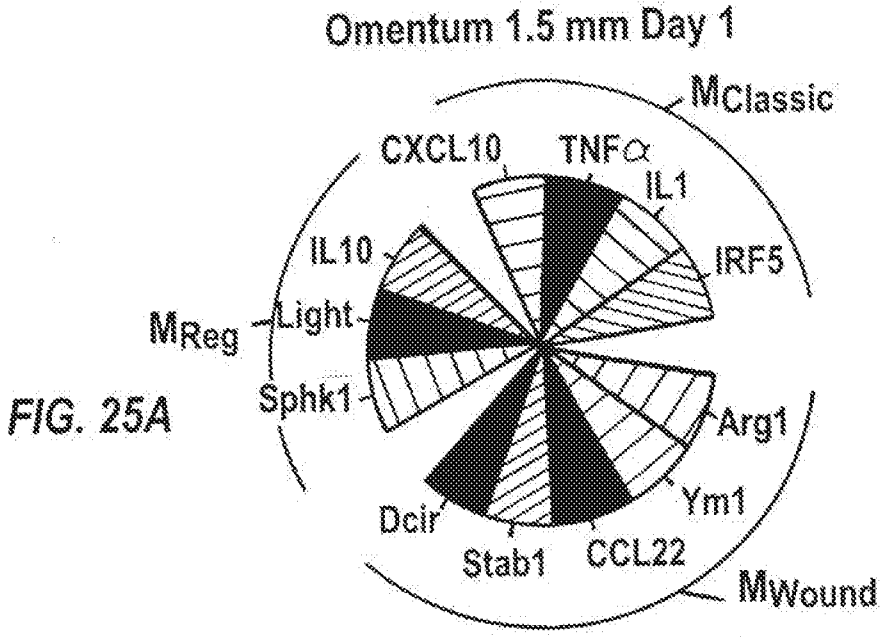

FIG. 25A

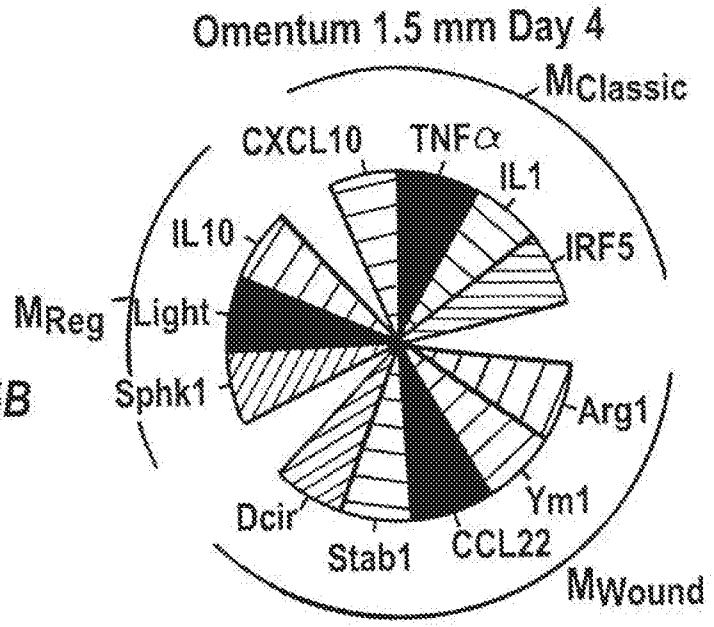

FIG. 25B

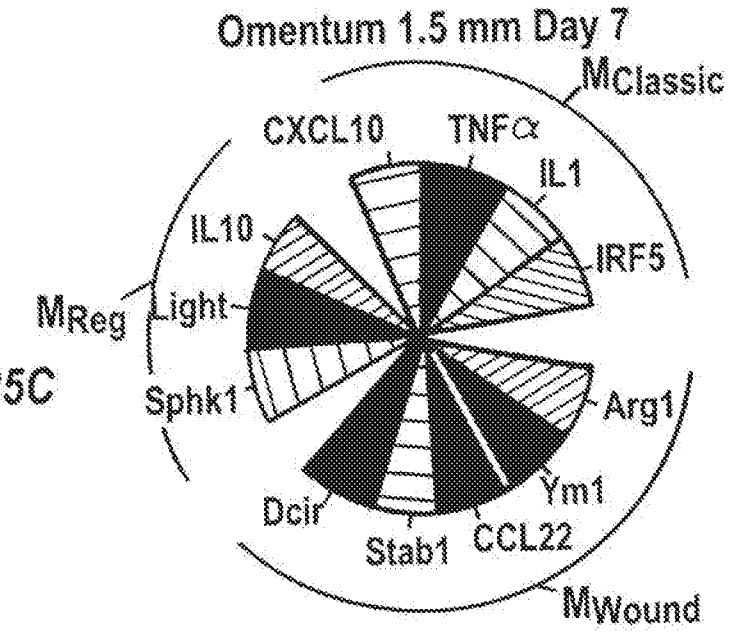

FIG. 25C

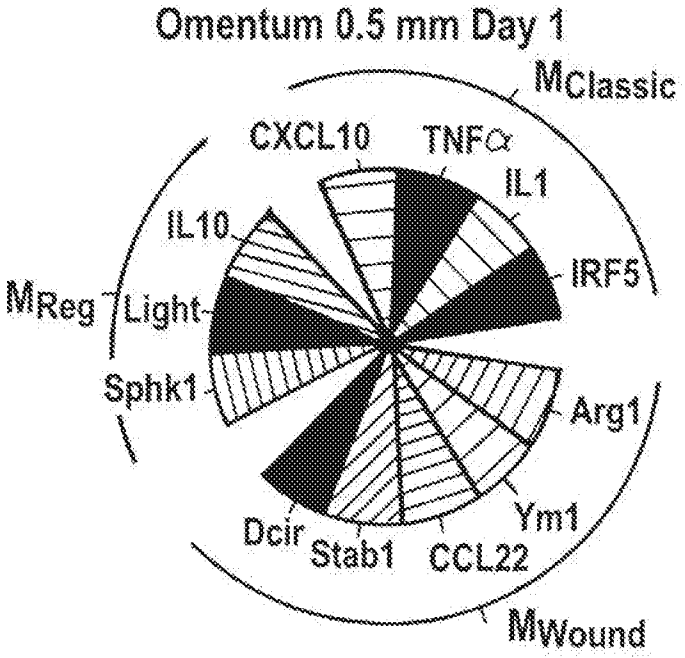

FIG. 25D

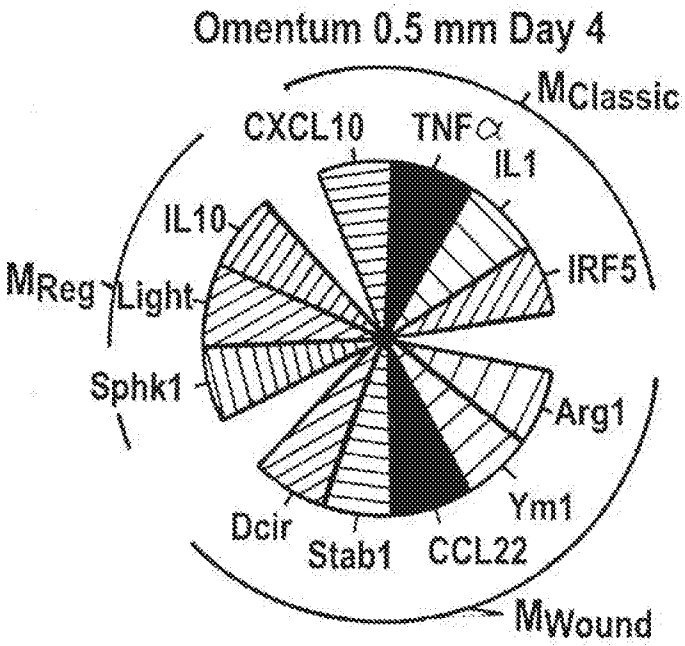

FIG. 25E

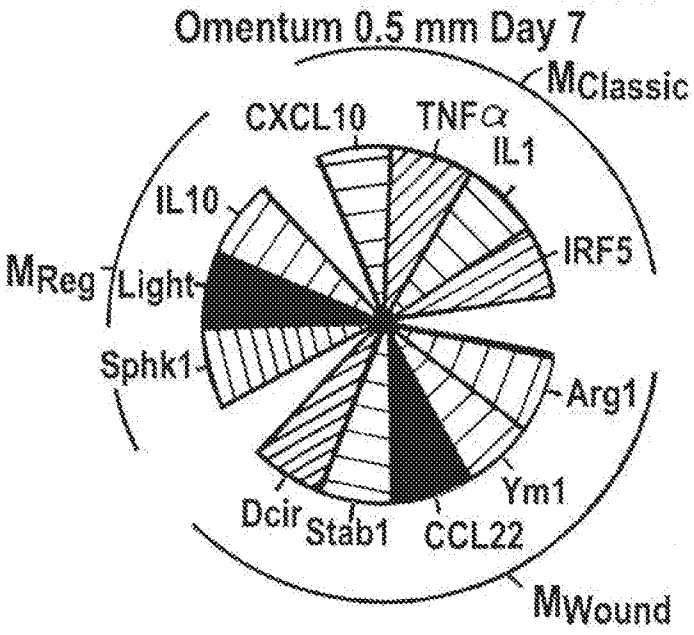

FIG. 25F

INTERNATIONAL SEARCH REPORT

International application No.
PCT/US2016/032920

Box No. I Nucleotide and/or amino acid sequence(s) (Continuation of item 1.c of the first sheet)

1. With regard to any nucleotide and/or amino acid sequence disclosed in the international application, the international search was carried out on the basis of a sequence listing:

   a. ☐ forming part of the international application as filed:

      ☐ in the form of an Annex C/ST.25 text file.

      ☐ on paper or in the form of an image file.

   b. ☐ furnished together with the international application under PCT Rule 13*ter*.1(a) for the purposes of international search only in the form of an Annex C/ST.25 text file.

   c. ☒ furnished subsequent to the international filing date for the purposes of international search only:

      ☒ in the form of an Annex C/ST.25 text file (Rule 13*ter*.1(a)).

      ☐ on paper or in the form of an image file (Rule 13*ter*.1(b) and Administrative Instructions, Section 713).

2. ☐ In addition, in the case that more than one version or copy of a sequence listing has been filed or furnished, the required statements that the information in the subsequent or additional copies is identical to that forming part of the application as filed or does not go beyond the application as filed, as appropriate, were furnished.

3. Additional comments:

INTERNATIONAL SEARCH REPORT

International application No.
PCT/US2016/032920

Box No. II Observations where certain claims were found unsearchable (Continuation of item 2 of first sheet)

This international search report has not been established in respect of certain claims under Article 17(2)(a) for the following reasons:

1. ☐ Claims Nos.:
because they relate to subject matter not required to be searched by this Authority, namely:

2. ☐ Claims Nos.:
because they relate to parts of the international application that do not comply with the prescribed requirements to such an extent that no meaningful international search can be carried out, specifically:

3. ☐ Claims Nos.:
because they are dependent claims and are not drafted in accordance with the second and third sentences of Rule 6.4(a).

Box No. III Observations where unity of invention is lacking (Continuation of item 3 of first sheet)

This International Searching Authority found multiple inventions in this international application, as follows:

see additional sheet

1. ☐ As all required additional search fees were timely paid by the applicant, this international search report covers all searchable claims.

2. ☐ As all searchable claims could be searched without effort justifying an additional fees, this Authority did not invite payment of additional fees.

3. ☐ As only some of the required additional search fees were timely paid by the applicant, this international search report covers only those claims for which fees were paid, specifically claims Nos.:

4. ☒ No required additional search fees were timely paid by the applicant. Consequently, this international search report is restricted to the invention first mentioned in the claims; it is covered by claims Nos.:

1-17, 46

Remark on Protest

☐ The additional search fees were accompanied by the applicant's protest and, where applicable, the payment of a protest fee.

☐ The additional search fees were accompanied by the applicant's protest but the applicable protest fee was not paid within the time limit specified in the invitation.

☐ No protest accompanied the payment of additional search fees.

FURTHER INFORMATION CONTINUED FROM PCT/ISA/ 210

This International Searching Authority found multiple (groups of) inventions in this international application, as follows:

1. claims: 1-17, 46

A preparation of biomedical devices, wherein at least 60 % of the devices of the preparation (i) have a sphere-like shape or a spheroid-like shape and (ii) have a diameter of at least X mm, but no more than Y mm, provided that Y is greater than X, X is 1.0,1.1, 1.2,1.3,1.4, 1.5,1.6,1.7, 1.8, 1.9, or 2.0, and Y is 2.0, 2.5, 3.0, 3.5, 4.0, 4.5, 5.0, 5.5, 6.0, 6.5, 7.0, 7.5, 8.0, 8.5, 9.0, 9.5, or 10.0, and
(a) no more than 20% of the devices of the preparation have other than a sphere-like shape or a spheroid-like shape;
(b) at least 50 % of the devices of the preparation comprise a live cell, or a plurality of live cells, or at least 1,000, 2,000 or 5,000 live cells/device;
(c) at least 50 % of the devices of the preparation having sphere-like shape or a spheroid-like shape comprise a live cell, or a plurality of live cells, or at least 1,000, 2,000 or 5,000 live cells;
(d) no more than 20% of the devices of the preparation have an edge;
(e) the cells in at least 50 % of the devices of the preparation are distributed essentially homogenously throughout the device;
(f) the cells in at least 50 % of the devices of the preparation having sphere-like shape or a spheroid-like shape are distributed essentially homogenously throughout the device;
(g) the cells in at least 50 % of the devices of the preparation are not distributed essentially homogenously throughout the device; and
(h) the cells in at least 50 % of the sphere-like shape or spheroid-like shape devices of the preparation are not distributed essentially homogenously throughout the device.
The first invention also covers the methods of treating a subject with a preparation of biomedical devices and a biomedical device for implantation.

---

2. claims: 18-45

Hydrogel capsules encaspulating cells, method of providing cells to an individual by administering hydrogel capsules, method of making the hydrogel capsules.

INTERNATIONAL SEARCH REPORT

International application No
PCT/US2016/032920

A. CLASSIFICATION OF SUBJECT MATTER
INV. A61L27/20 A61L27/38 A61L27/52 A61L27/54
ADD.

According to International Patent Classification (IPC) or to both national classification and IPC

B. FIELDS SEARCHED

Minimum documentation searched (classification system followed by classification symbols)
A61L

Documentation searched other than minimum documentation to the extent that such documents are included in the fields searched

Electronic data base consulted during the international search (name of data base and, where practicable, search terms used)
EPO-Internal, WPI Data

C. DOCUMENTS CONSIDERED TO BE RELEVANT

Category*	Citation of document, with indication, where appropriate, of the relevant passages	Relevant to claim No.
7 X	MINGLIN MA ET AL: "Core-shell hydrogel microcapsules for improved islets encapsulation", ADVANCED HEALTHCARE MATERIALS, WILEY - V C H VERLAG GMBH & CO. KGAA, DE, vol. 2, no. 5, 1 May 2013 (2013-05-01), pages 667-672, XP002724800, ISSN: 2192-2640, DOI: 10.1002/ADHM.201200341 [retrieved on 2011-12-03] the whole document -----	1-17,46
5 A	WO 2014/153126 A1 (MASSACHUSETTS INST TECHNOLOGY [US]) 25 September 2014 (2014-09-25) claims 1-29 -----	1-17,46

☐ Further documents are listed in the continuation of Box C.

☒ See patent family annex.

* Special categories of cited documents :

"A" document defining the general state of the art which is not considered to be of particular relevance

"E" earlier application or patent but published on or after the international filing date

"L" document which may throw doubts on priority claim(s) or which is cited to establish the publication date of another citation or other special reason (as specified)

"O" document referring to an oral disclosure, use, exhibition or other means

"P" document published prior to the international filing date but later than the priority date claimed

"T" later document published after the international filing date or priority date and not in conflict with the application but cited to understand the principle or theory underlying the invention

"X" document of particular relevance; the claimed invention cannot be considered novel or cannot be considered to involve an inventive step when the document is taken alone

"Y" document of particular relevance; the claimed invention cannot be considered to involve an inventive step when the document is combined with one or more other such documents, such combination being obvious to a person skilled in the art

"&" document member of the same patent family

Date of the actual completion of the international search	Date of mailing of the international search report
17 August 2016	14 -10- 2016

Name and mailing address of the ISA/	Authorized officer
2 European Patent Office, P.B. 5818 Patentlaan 2 NL - 2280 HV Rijswijk Tel. (+31-70) 340-2040, Fax: (+31-70) 340-3016	Schneider, Aurore

INTERNATIONAL SEARCH REPORT

Information on patent family members

International application No
PCT/US2016/032920

Patent document cited in search report	Publication date	Patent family member(s)	Publication date
WO 2014153126 A1	25-09-2014	AU 2014236296 A1	29-10-2015
		CA 2906174 A1	25-09-2014
		EP 2968115 A1	20-01-2016
		JP 2016519079 A	30-06-2016
		US 2014271843 A1	18-09-2014
		WO 2014153126 A1	25-09-2014